5-8-2015

Cannabinoid-mediated Epigenetic Regulation of Immune Functions

Jessica Margaret Sido
University of South Carolina - Columbia

Cannabinoid-mediated Epigenetic Regulation of Immune Functions

By

JESSICA MARGARET SIDO

Bachelor of Arts
Southern Illinois University at Edwardsville, 2006

Bachelor of Science
Southern Illinois University at Edwardsville, 2007

Submitted in Partial Fulfillment of the Requirements

For the Degree of Doctor of Philosophy in

Biomedical Science

School of Medicine

University of South Carolina

2015

Accepted by

Mitzi Nagarkatti, Major Professor

Prakash Nagarkatti, Chairman, Examining Committee

Carole Oskeritzian, Committee Member

Taixing Cui, Committee Member

Anindya Chanda, Committee Member

Lacy Ford, Vice Provost and Dean of Graduate Studies

DEDICATION

"The three great essentials to achieve anything worthwhile are, first, hard work; second, stick-to-itiveness; third, common sense."

— Thomas A. Edison

I dedicate this work to all the mentors, colleagues, friends, and family who have inspired and supported me while I strove to achieve that which was worthwhile.

ACKNOWLEDGEMENTS

I like to think of myself as a gracious person so I hope that all of the people I thank here will already know of my appreciation/gratitude. However, thank you can never be said enough, and so…

-Dr. Prakash and Dr. Mitzi thank you for allowing me into your lab. This opportunity has made my passion for research into a career, and for that, I can never be thankful enough.

-Dr. Carole thank you for being a never-ending source of positivity, I love knowing you are in my corner.

-Roshni because of you there was friendship, support, and hot chocolate to balance out the "other stuff". Thank you for setting the bar and then encouraging me to do better.

-Beth I thank you for all of your help, for believing in me, and pushing me to try harder.

-My committee members, Dr. Cui and Dr. Chanda, lab mates, faculty, rotating students, support staff, friends, and family whose numbers are too great to list thank you for all that you have done throughout the years.

-Steve, my fiancé, thank you for dealing with the stressed out, sleep deprived, short tempered version of me that always surfaced when I wrote, prepared for presentations, or fretted over deadlines. She is sorry that she yelled at you and hopes you forgive her, always.

-Mom, for taking me to the library whenever I wanted, helping me glue science projects to poster boards, and listening to me go on and on about [insert science topic here] thank you.

I did it all with hard work and a little luck. Thanks again.

This work was supported in part by National Institutes of Health grants P01AT003961, R01AT006888, R01ES019313, R01MH094755, and P20GM103641 as well as by Veterans Affairs Merit Award BX001357

ABSTRACT

The cannabinoid system consisting of exogenous and endogenous ligands as well as dedicated receptors has been proposed to play a regulatory role in immune functions. The exogenous cannabinoid Δ^9-tetrahydrocannabinol (THC), one of the most widely studied marijuana derivatives, has been associated with multiple anti-inflammatory properties over the years. The majority of THC research has centered on the shift from Th1 to Th2 responses however, the complexity of inflammation has since increased. Recent studies have revealed that epigenome, Th cell subsets, and immunoregulatory cell induction, are all known to impact inflammation. In the current research, we have attempted to look holistically at the impact of THC on inflammation, specifically addressing its effect on epigenome and regulatory cells such as myeloid derived suppressor cells (MDSCs). In regards to epigenetic regulation, we found that THC altered both DNA methylation profiles and microRNA (miRNA, miR) expression in immune cells. THC treatment decreased DNA methylation of key genes, STAT3 and arginase1 (Arg1), associated with the induction and suppressive capabilities of myeloid derived suppressor cells (MDSCs). Furthermore, THC treatment triggered alterations in miRNA expression in lymphocytes, decreasing the differentiation of Th1, via overexpression of miR-29b, and Th17, via reduced miR-21 expression. Moreover, we discovered that THC, a ligand for both CB1 and CB2 cannabinoid receptors, required a fully functional CB1 receptor for optimal induction of MDSCs. Additionally, functional

CB1 receptor was necessary for THC to inhibit the Th1 driven proinflammatory response associated with host versus graft disease (HvGD) leading to allogenic graft survival. In order to assess THC inhibition of inflammation, driven by Th1 and Th17, we also used delayed type hypersensitivity (DTH). In this model, THC was able to reduce both Th1 and Th17 associated cytokines and transcription factors. We have further highlighted the importance of the endocannabinoid (EC) system in immunoregulation through the therapeutic use of the endogenous cannabinoid receptor ligand 2-arachidonoyl glycerol (2-AG) and detection of 2-AG during an ongoing DTH response.

The impact of endogenous and exogenous cannabinoids and the CB receptors on expressed on immune cells on the regulation of immune response is an exciting area of research with potential implications in the prevention and treatment of inflammatory and autoimmune diseases. Taken together, our findings demonstrate for the first time how cannabinoids can regulate the immune response through alterations in the epigenetic and immunoregulatory pathways, thereby controlling inflammation driven by Th1 and Th17 cells. Our studies shed new light on how cannabinoid system can be targeted to therapeutically prevent and treat inflammatory and autoimmune diseases.

TABLE OF CONTENTS

LIST OF TABLES

LIST OF FIGURES

CHAPTER I: INTRODUCTION

1.1 THE ENDOCANNABINOID (EC) SYSTEM

The first use of cannabis as an alternative medicine is attributed to ancient China and Taiwan both of which used hemp seeds, derived from the *Cannabis sativa* or marijuana plant, as dietary additives (1). The most well studied cannabinoid extracted from marijuana is the aromatic terpenoid Δ^9-tetrahydrocannabinol (THC) (2). Once exogenous cannabinoids, such as THC, were discovered to act on the immune system, the search for possible receptors began in earnest. The search for cannabinoid receptors led to the discovery of the endogenous cannabinoid (endocannabinoid, EC) system (3). The EC system consists of cannabinoid receptors and their ligands.

After THC was isolated and synthesized, two receptors termed cannabinoid receptor 1 (CB1) and cannabinoid receptor 2 (CB2) were discovered, in 1990 and 1992 respectively, which could bind the exogenous cannabinoid (4); (5). While additional receptors have been found throughout the years, which can use cannabinoids as ligands, CB1 and CB2 remain the only dedicated CB receptors. All receptors associated with the EC system are G-protein coupled receptors (GPR) consisting of seven transmembrane helices, an extracellular N-terminus, and an intracellular C-terminus (3).

Somewhat controversial is the inclusion of the vanilloid and orphan GPR55 receptors to the EC system. The vanilloid receptor, which can be activated by voltage, protons, and vanilloid compounds (such as capsaicin), as well as cannabinoids, is found in the CNS and on immune cells (6); (7); (8). However, as many non-cannabinoid molecules can act as activators for this receptor, it cannot be considered exclusively as part of the EC system. GPR55 is present in numerous tissues, including the adrenals, gastrointestinal tract, and central nervous system, and also affects the G13 peptide (9); (10). The issue with including this receptor in the EC system is that while endocannabinoids have been found to activate the GPR55 in transformed human embryonic kidney cells (HEK293), these results are not always reproducible (10); (11).

The main cannabinoid receptors, CB1 and CB2, have been found to reside in various organ systems with CB1 having the highest rate of expression in the central nervous system and CB2, in the immune system (12); (13). However, CB1 receptors have also been found in the immune system, in particular on activated T cells, and CB2 receptors have been found in the CNS as well as other peripheral tissues (13); (14). While CB receptors interact with multiple ligands, specificity is maintained through structural and conformation requirements. CB1 receptor binding requires 20-22 carbon fatty acid chains, no less than three homoallylic double bonds, and at least five saturated carbons at the end of the acyl chain (15). Additionally, amino acid disparity in binding sites, due to single nucleotide polymorphisms, affects CB receptor affinity for individual ligands (16), (17), (18), (19), (20).

Not long after the discovery of the cannabinoid receptors, endogenous ligands, which act as lipid messengers derived from cellular membranes, were found (21). The

first EC discovered, N-arachidonyl ethanolamide (anandamide, AEA), was named anandamide from the Sanskrit for “internal bliss” (22). Anandamide was first found in the porcine brain in 1992 (3). In 1995, two independent groups isolated another endogenous cannabinoid, 2-arachidonoyl glycerol (2-AG), (23); (24). Maintenance of EC levels occurs through intercellular metabolism via the catabolic enzymes fatty acid amide hydrolysis (FAAH) and monoacylglyceride lipase (MAGL), for AEA and 2-AG respectively (25); (26); (27).

Endocannabinoids are synthesized locally as needed rather than being stored within vesicles (28). The synthesis of AEA can occur in two main ways: one is through N-arachidonoyl phosphatidylethanolaminephospholipase, which converts phosphatidylcholine and phosphatidylethanolamine to N-arachidonoyl phosphatidylethanolamine (NAPE), the anandamide precursor (29). The other accepted pathway is through phospholipase C hydrolysis of NAPE and phosphoanandamide, which is then dephosphorylated (30); (31); (32). However, 2-AG synthesis follows different pathways one of which involves 2-arachidonate-containing phosphoinositols, converted to diacylglycerols (DAGs), are finally hydrolyzed by DAG lipase (31); (32). Additionally, 2-AG can be formed from arachidonic acid-containing phosphatidylcholine via variable phospholipases and phosphatidic acid phosphatase (31). Upon synthesis these lipid messengers, due to the hydrophobic nature of the molecules, remain membrane bound till a high-affinity mechanism allows for cellular uptake to occur (33).

At first glance, the link between the EC system and immune regulation may appear tenuous or limited to neuroimmune disorders inasmuch as the CB1 receptor was initially understood to be CNS specific. However, in depth studies of the *Jurkat* T cell

line has shown that CB1 transcript expression is significantly increased, 29-fold, upon CD3/CD28 activation compared to non-stimulated cells (34). Even non-immortalized primary human T cells, isolated form peripheral blood, exhibit an 8-fold increase in CB1 transcript when activated (34). This is of great importance in the understanding of inflammatory diseases as T cells are a major component of the adaptive immune system and are direct mediators of a number of autoimmune diseases.

1.2 EPIGENETICS AND IMMUNITY

Epigenetic modifications are heritable changes to DNA which regulate gene expression (35); (36). The emerging field of epigenomics, including histone marks, DNA methylation, and microRNA expression, has been gaining attention as a way to fine tune the immune response (35); (36). Histone marks, such as acetylation and methylation, regulate gene expression through changes in chromatin remodeling altering DNA availability (37); (38). DNA methylation blocks transcription factor binding, causing inhibition of gene expression (39). Translation of mRNA is also regulated via microRNA (miR) target gene binding or degradation (40).

DNA methylation causes reversible gene silencing through the transfer of methyl groups to CpG clusters (41). DNA methylation can be inherited or created *de novo* by DNA methyl transferases (DNMTs) which transfer metyhyl groups from S-adenosyl-L-methionine (SAM) to the 5-position on cytosine residues found in CpG clusters within the DNA sequence (42). DNMTs can be broken into two groups those that maintain methylation patterns and those that alter methylation patterns through increased methyl transfers. DNMT1 is considered a maintenance DNMT as it binds preferentially to hemimethylated DNA (39). *De novo* metyhylation of CpG clusters occurs via the

DNMT3 family, 3a and 3b (41). It has been suggested that DNA methylation, at both a local and global level, is vital to proper cellular function (43); (44). Specifically, DNA methylation has been linked to immune function and immune cell differentiation (45); (46); (47).

microRNA (miRNA, miR) are short strands of RNA, around 20 nucleotides long, which originate from non-coding RNA (40). While non-coding RNA was initially considered useless, the role of miRNA as a gene expression regulator was discovered in the 1990's (48). miRNA most commonly inhibits gene expression through the binding of mRNA sequences; however miRs can also bind and degrade mRNA transcripts (40). Each miRNA has been predicted to bind numerous targets and therefore regulate the expression of various genes (40). An evolving role of miRNA in relation to immunity focuses on the regulation of T helper cell lineage-defining transcription factors and downstream targets (49); (50).

1.3 IMMUNE RESPONSE IN T HELPER CELL DRIVEN INFLAMMATION

T helper cells can differentiate into proinflammatory, anti-inflammatory, or regulatory cells based on lineage specific signals. Classically, T cell driven inflammation has been associated with the Th1 cell subset, and therefore elevated expression of IFN-γ, TNF-α, IL-12, and the transcription factor Tbx21 (Tbet) (51). Additionally, IL-17 producing cells, known as the Th17 cell subset, have been associated with progression of inflammatory disease (52). Hallmarks of Th17 cell driven inflammation include elevated levels of IL-6, IL-$17_{a/f}$, and the transcription factors TGFβ and IRF4 (51). While proinflammatory signals are necessary to maintain T cell activation and proliferation, immune regulatory or suppressive cell responses are also critical. Immune regulators

include T regulatory cells (Treg) and myeloid derived suppressor cells (MDSC), both of which are induced by proinflammatory microenvironments (53, 54); (55); (56). MDSCs, a subset of immature myeloid cells, which suppress T cell proliferation via L-arginine depletion, are often induced in both acute and chronic inflammatory models (57); (58).

Host versus graft disease (HvGD, transplant rejection) is primarily a Th1 driven inflammatory response initiated by the host against allogenic graft tissue. Acute HvGD is associated with elevated levels of IL-2, IFN-γ, and TNF-α indicative of cytotoxic and Th1 T cell activation (59). Interestingly, tolerance of allogenic graft cells/tissue has been found to be dependent on T cell subset regulators such as IL-6 levels and MDSC recruitment (59); (60). While success of allogenic transplants has increased significantly over the years, this is primarily due to severe immune suppression. The most common immune suppressive drugs; corticosteroids, calcineurin inhibitors, anti-proliferatives, and mammalian target of rapamycin (mTOR) inhibitors have increased graft survival (61); (62); (63); (64); (65). However, continued usage of these drugs causes side effects including immunotoxicity, leukopenia, susceptibility to cancer and/or infectious disease, and can even delay functionality of the graft (61); (66); (62); (67); (68); (63).

Type IV hypersensitivity commonly known as delayed type hypersensitivity (DTH, contact dermatitis) is a more complex model of inflammation resulting in combined Th1/Th17 activation (69); (52). The ability of DTH to induce both major proinflammatory T helper subsets stems from the activation of toll like receptors (TLR2 and TLR4) (70); (71, 72). It has been shown that activation of TLR2 and TLR4 causes secretion of IL-12 and IL-6, Th1 and Th17 differentiating cytokines respectively (70);

(71); (72). Type IV hypersensitivity is therefore associated with elevated IFN-γ and IL-$17_{a/f}$ expression (69); (52).

1.4 RATIONALE FOR USING CANNABINOID TREATMENTS

As mentioned earlier THC, AEA and 2-AG have all been shown to act through the CB1 receptor. The G-proteins that CB1 receptors activate include Gi, inhibitory proteins, which are known to modulate adenylate cyclase (73). Furthermore, the CB1 receptor upon activation has been found to increase ceramide, a bioactive lipid implicated in cellular differentiation, proliferation, and apoptosis (74). Additionally, recent findings show that AEA (mM) works in a CB1 dependent manner to induce myeloid derived suppressor cells (MDSCs), a regulatory cell type which has been shown to inhibit inflammatory responses to T cell activation (75). These data suggest that the EC system works through the CB1 receptor to elicit an anti-inflammatory response, upon activation of immune cells.

The anti-inflammatory properties of THC, including suppression of the antitumor response, have been well studied (76); (77); (78); (79); (79). THC has been shown to suppress inflammatory responses using various mechanisms such as apoptosis, altering the cytokine milieu, and through the induction of regulatory immune cells such as Tregs. THC exposure has been linked to cannabinoid receptor dependent apoptosis in splenic and thymic T cells, dendritic cells (DCs), and macrophages (80); (81); (82). In addition to apoptosis, THC can induce immunsupression by shifting the cytokine profile from proinflammatory (Th1 or Th17) to anti-inflammatory (Th2) (76); (83); (78). Cannabinoids have also been observed to decrease lymphocyte driven immune responses through the activation of regulatory cells such as Tregs and MDSCs (84); (85); (86); (75).

Furthermore, recent findings have shown that THC treatment can also affect epigenetic modifications including alteration of histone marks, DNA methylation profiles, and miRNA expression (38); (87); (88).

ECs have also been found to influence the immune response. Focusing first on 2-AG, it was found that its addition to anti-CD3 mAb activated T cells inhibited proliferation, but only at low cell density (89). Additionally, *in vitro* incubation with 2-AG was found to suppress IL-2 in activated *Jurkat* T cells at microMolar concentrations as well as in primary splenocytes (90); (91). Looking at the mitogen-induced proliferation of T cells, a dose-dependent inhibition was observed when AEA was added to *in vitro* cultures (92). In another *in vitro* experiment, it was found that when AEA was present at microMolar concentrations, prior to OVA stimulation, it caused decrease in IFN-γ production in ConA-stimulated splenocytes (93). Additionally, AEA treatment has also been shown to induce MDSCs in a CB1-dependent manner, and alter miR expression in DTH (75); (83).

1.5 STATEMENT OF HYPOTHESIS AND AIMS

There are over 80 autoimmune and inflammatory diseases in which there is no cure. Thus, the current treatment strategy includes use of immunosuppressive drugs that have significant toxicity and side effects. Moreover, chronic inflammation triggers a large number of clinical disorders including cardiovascular, neurodegenerative, cancer, obesity and the like. Thus, scientists are working towards understanding inflammatory pathways so that better targeted therapeutics can be developed to treat inflammation. In this context, cannabinoid receptor-ligand system which have been discovered on immune cells and system, offer novel approaches to regulate inflammation.

In the current research, we tested the central hypothesis that cannabinoids regulate inflammation through alterations in the epigenetic pathways, including DNA methylation and miRNA expression, leading to suppression of proinflammatory T cells and enhancement of regulatory T cell and MDSC pathways. To this end, we assessed the ability of THC to enact an anti-inflammatory tone in a wide array of inflammatory disease models such as HvGD, allograft rejection, and DTH response and we noted consistently, data supporting a role for epigenetic modifications involving DNA methylation and miRNA expression. Additionally, we set out to prove that THC treatment inhibits classical, Th1, as well as non-classical, Th17, T helper cell driven inflammation, while enhancing MDSCs. Finally, using the natural ligand for the cannabinoid receptors, 2-AG, we determined that the endocannabinoid system does play an integral role in regulating inflammatory responses.

CHAPTER II: Δ^9 Tetrahydrocannabinol-mediated Epigenetic Modifications Elicit Myeloid Derived Suppressor Cell Activation via STAT3/S100A8.

2.1 INTRODUCTION

Myeloid-derived suppressor cells (MDSCs), which were originally observed in cancer models, are anti-inflammatory mediators which can be helpful or harmful depending on the context. In cancer models MDSCs inhibit the T cell driven response against tumors allowing for cancer growth and metastasis (94); (95). However, in autoimmune diseases, MDSC induction is advantageous, working to reduce proliferative T cell inflammation (54); (53); (55); (56). It is therefore necessary to understand the mechanisms which lead to MDSC induction and activation in order to best utilize this duality. MDSCs can be categorized, in mice, into two major subsets granulocytic (Ly6G+Ly6C+GR1+CD11b+) or monocytic (Ly6G-Ly6C+GR1+CD11b+) (96). Additionally, MDSCs are defined by their ability to suppress T cell responses including proliferation (97); (98). The classic mechanism for MDSC suppression of T cell proliferation is L-arginine metabolism via either cytokine-induced nitric oxide synthases (iNOS or NOS2) or arginase1 (Arg1) (99).

As gene regulation is integral for cell function and development, interest in dynamic epigenetic modifications has become paramount. DNA methylation, one of the

most common forms of epigenetic regulation, controls gene expression by blocking transcription machinery causing reversible gene silencing . DNA methylation, both de novo and inherited, is dependent on DNA methyltransferases (DNMTs) (41). DNMTs transfer methyl groups from SAM (S-adenosyl-L-methionine) to the 5-position on cytosine residue found in CpG clusters within the DNA sequence (42). DNMT1, binds preferentially to hemimethylated DNA and is considered to be the maintenance DNMT, and the DNMT3 family, 3a and 3b, is deemed necessary for de novo methylation (41). Altered DNMT profiles are often seen in cancer patients suggesting that global methylation is vital to proper cellular function though no direct association between altered methylation profiles and MDSC induction has been highlighted in these studies (43); (44). Furthermore, DNA methylation has been linked to not only immune function, but also to immune cell differentiation (45); (46); (47); (100); (101); (102). Interestingly, MDSCs are not a terminally differentiated immune cell population. Rather MDSCs are considered a heterogeneous mixture of immature myeloid-origin cells which can differentiate into DCs or macrophages (103). It is the plasticity of immature cells which suggests that DNA methylation could be playing a role in both MDSC maintenance and activation. However, there is only one recent study indicating that HDAC11 may play a role as an epigenetic regulator in MDSC expansion and function (104).

Δ9-Tetrahydrocannabinol (THC), an exogenous cannabinoid derived from the Cannabis sativa plant, has long been known to act as an anti-inflammatory agent as well as suppress antitumor immune response (76); (77); (78); (79); (84). The immunosuppressive properties of THC, in cancer models, were shown to be, in part, due to the induction of Th2 anti-inflammatory cytokines (IL-4 and IL-10) and correlating

decrease of Th1 pro-inflammatory cytokines (IL-2 and IFN-γ) (76); (78). THC has also been shown to induce T regulatory cells (Tregs) (84); (85). Additionally, recent studies from our laboratory have suggested that administration of THC into mice can trigger large numbers of immunosuppressive MDSCs (86).

While it has been shown that THC can alter cytokines and transcription factors linked to MDSC differentiation or homing, its role in MDSC expansion and activation has not been clearly elucidated (86); (87); (75). Furthermore, the role of epigenetic pathways in the induction of MDSCs by THC has not been determined. In the current study, we investigated the effect of THC on methylation of several genes involved in the differentiation and activation of MDSCs, and our data demonstrate epigenetic regulation of several of the critical molecules involved in MDSC activation and functions including Arg1 and STAT3.

2.2 MATERIALS AND METHODS

Mice-

Female C57BL/6 (wild-type, BL6) mice, aged 6-8 weeks and at an average weight of 20 g, were obtained from the National Cancer Institute (Frederick, MD). All mice were housed in pathogen-free conditions and allowed ad libitum access to filtered water and Teklad rodent diet 8604 (normal chow) at the Animal Research Facility located at the University of South Carolina School of Medicine. All experiments were conducted under an approved Institutional Animal Care and Use Committee animal protocol.

Treatment with THC-

THC (NIDA-NIH) dissolved in ethanol was diluted in 1xPBS to a concentration of 20 mg/kg. THC was administered intraperitoneally (i.p.) into naïve mice. For depletion of S100A8, mice were given an i.p. injection of antiS100A8 (0.01 mg/mouse 8H150) 1 hour after THC treatment.

MDSC Isolation-

Sixteen hours after THC injection, mice were euthanized and the peritoneal exudate collected, three washes of 5 mL of ice cold 1xPBS were injected into the peritoneal cavity and after five minutes, with agitation, collected. The cells were resuspended in 1 mL then treated with Fc block for 10 minutes and labeled with PE conjugated anti-Gr1 Abs. The +EasySep positive PE selection kit procedure was followed to isolate Gr1 positive cells, as described (105). After isolation, cells were labeled with FITC-conjugated anti-CD11b and assessed for purity using flow cytometeric analysis, gating on live cells. To isolate Ly6G and Ly6C positive cells +EasySep positive PE and FITC selection kits were used respectively. Purity of the MDSC subset populations was assessed by using duel staining with Alexa Fluor 647-conjugated anti-CD11b.

Monoclonal Antibodies, Reagents, and Flow Cytometer-

Antibodies used for flow cytometric analysis (BioLegend) include: Fc block (93), PE conjugated anti-Gr1 (RB6-8C5), FITC conjugated anti-CD11b (M1/70), PE conjugated anti-Ly6G (1A8), FitC conjugated anti-Ly6C (HK1.4), and Alexa Fluor 647 conjugated anti-CD11b (ICRF44). Briefly, peritoneal lavage cells (10^6 cells) from BL/6 mice were incubated with Fc receptor antibodies (5-10 minutes) and incubated with conjugated

antibodies (20-30 minutes at 4°C). Next, cells were washed twice with 1xPBS/2% fetal bovine serum buffer. The stained cells were then assessed by flow cytometer (FC500; Beckman Coulter) and the resulting data analyzed by Cytomics CXP software (Beckman Coulter). Two-color flow cytometric analysis was completed for assessing presence of MDSCs in the bone marrow and peritoneal exudates. Three-color flow cytometric analysis was used to profile the MDSC subsets.

MeDIP-seq-

Purified genomic DNA was treated with dsDNA Shearase (Zymo Research, Irvine, CA). DNA fragments with size from 200bp to 400 bp were purified to construct sequencing library using Illumina Chip-seq library preparation kit. dsDNA was then denatured and immunoprecipitated with anti 5-methylcytosine antibody using a MeDIP kit from Diagenode (Denville, NJ). Precipitated DNA was purified and sequenced by HiSeq2500 (Tufts Genomic Core, Boston, MA). The sample before immunoprecipitation was also sequenced as input control.

MeDIP data Analysis-

MeDIP-seq libraries were sequenced with single-end reads of 50bp. Raw sequencing reads were mapped to mouse genome build mm9 using Bowtie software by allowing two mismatches in the read (106). The mapped reads were then filtered and only uniquely mapped reads were used for the downstream analysis. Mapped reads were analyzed with MEDIPS software (107), and visualized in IGB genome browser (http://bioviz.org/igb). The location of 3kb upstream and downstream of transcriptional start site (TSS) was generated using UCSC table browser. The DNA methylation signal of all genes within

this region was extracted. The correlations of overall DNA methylation across the whole genome and near the TSS site (3kb up and down stream) were analyzed by CEAS software (108).

Methylation specific (Msp) PCR-

Genomic DNA was isolated using the DNeasy kit (Qiagen) following the manufacture's protocol. Bisulfite conversion of CpG islands was completed using the Epitect Bisulfite kit (Qiagen). Msp PCR was run with PreMix F (Epicentre) and iTaq DNA polymerase (BioRad). Samples were assessed for expression of DNMT3a (Forward-5CAGCACCATTCCTGGTCATGCAAA3; Reverse-5TCAAGGTTTCCTGTCTGGTAGGCA3), and DNMT3b (Forward-5GCACAACCAATGACTCTGCTGCTT3; Reverse-5AGGACAAACAGCGGTCTTCCAGAT3) with an annealing temperature of 60°C. Additionally methylated (M) and un-methylated (UM) DNA primers were used for Arginase1, NOS2, and STAT3 (Table 2.I). Methylation index ([(M)/(M+UM)]*100) was used to assess DNA methylation. Universal methylated mouse DNA standard (Millipore S8000) was used as a control with all primers. Primers were generated using the Methyl Primer Express v1.0 software, and synthesized from IDT DNA technologies.

Effect of MDSCs on T cell proliferation-

To study the ability of MDSCs to suppress T cell proliferation, we used the following assay as described (75). Concanavalin A (ConA) activated (2.5 μg/mL) spleen cells, from naïve BL6 mice were cultured in triplicate (0.2 mL/well in a round bottom 96 well plate) with Mitomycin C inactivated MDSCs for 38-40 hours. Ratio of MDSCs to T cells

was 1:25 (Fig. 2.1 B only) or 1:2. Sixteen hours before collection and analysis, [^{3}H] thymidine (2 μCi/well) was added to the cell cultures. [^{3}H] thymidine incorporation was measured using a liquid scintillation counter (MicroBeta Trilux).

Western Blot Analysis-

Protein was isolated from purified MDSCs using radioimmunoprecipitation (RIPA) lysis buffer (Santa Cruz), as described (109). Five or 10 micrograms of protein was loaded and ran on a polyacrylamide gel (12%) at 60 V for 2.5 hours. Protein was then transferred to nitrocellulose at 100 V for 1 hour. Protein transfer was confirmed using 3 mL of Ponceau S staining solution. Nitrocellulose was then blocked in 5% nonfat dry milk in TBS. Nitrocellulose was then probed with antibodies to S100A8 (Calgranulin A [M-19] 1:2000), S100A9 (Calgranulin B [M-19] 1:1000), Arginase1 (V-20 1:1000), NOS2 (iNOS [M-19] 1:500), STAT3 (C-20 1:200), P-STA (9E12 1:200). HRP conjugated secondary antibodies were used at either 1:1000 or 1:2000 dilutions depending on the secondary required. For control protein bands γ-tubulin (Poly6209) or β-actin (Poly6221) were used at a dilution of 1:1000. ECL substrate (Thermo) was added for 1 minute, exposure time varied.

ImageJ-

Densitometry was performed on scanned western blot images as well as PCR gels using the ImageJ gel analysis tool (110). Scanned blots and gels were assessed for absolute density (AD), as determined by area under the curve, of each experimental and control band. Relative density (RD), for western blots, was determined by dividing the experimental band AD by the control band AD for both the protein of interest and a

structural protein. The normalized density ratio (NDR) was then calculated by dividing the protein of interest RD by the structural protein RD.

Cytokine Analysis in Cell Culture Supernatants-

ELISA MAX sandwich enzyme-linked immunosorbent assay (ELISA) kits (BioLegend) were used to assess the level of IL-6, IL-10, and IFN-γ cytokines. Sandwich ELISA kits (MyBioSource) were used to assess S100A8 and S100A9 levels. Isolated MDSCs from the bone marrow or peritoneal cavity ($2.5x10^6$ cells/mL) from naïve or THC treated mice were cultured in 0.2 mL aliquots in 96-well round bottom tissue culture plates for 16-20 hours. Cytokine production was quantified from cell supernatants (stored at -20°C). Absorbance was measured at 450 nm using a Victor2 1420 Multilable counter (Wallac).

qPCR-

Total RNA was isolated and purified using miRNeasy kit (Qiagen), following manufacturer's procedure. iScript cDNA synthesis kit (BioRad) was used according to manufacturer's specifications to reverse transcribe cDNA. qPCR was performed using Sso Advanced SYBR Green (BioRad) on a CFX Connect (BioRad). Samples were assessed for expression of βactin (Forward-5GGCTGTATTCCCCTCCATCG3; Reverse-5CCAGTTGGTAACAATGCCATGT3), IL-6 (Forward-5CAACGATGATGCACTTGCAGA3; Reverse-5GGTACTCCAGAAGACCAGAGG3), and IL-10 (Forward-5GCTCTTACTGACTGGCATGAG3; Reverse-5CGCAGCTCTAGGAGCATGTG3). Primers were synthesized from IDT DNA technologies with annealing temperatures of 60°C.

Cell Culture with conditioned media or recombinant S100A8 protein-

Isolated MDSCs were plated with ConA activated splenocytes at a ratio of 1:2 (MDSC:ConA splenocytes). Conditioned media was made by incubating isolated THC-induced MDSCs with phorbol 12-myristate 13-acetate (PMA) and calcium ionophore ionomycin (50 ng/mL and 10 μg/mL respectively) for five hours. Lyophilized S100A8 protein (MyBioSource mS100A8) was reconstituted in complete RPMI media (1% v/v penicillin/streptomycin, 1% v/v HEPES buffer, 10% v/v heat inactivated FBS, and 0.0002% v/v 2-mercaptoethanol). 2,000 ng of mS100A8 was added at 0 and 24 hours to cell culture wells.

Statistical Analysis-

Data are shown as mean ± S.E.M. Student's t Test was used to compare data between two groups. One-way ANOVA with Tukey post-hoc test was used to compare three or more groups. Experimental groups were compared to controls, $p < 0.05$ was considered significant.

2.3 RESULTS

T cell suppression is increased in THC-induced MDSCs.

The largest accumulation of resident MDSCs is located in the bone marrow (BM) (99). It has been shown that MDSCs migrate from this repository to sites of inflammation by following chemokine/cytokine signals (99). Our lab has shown that MDSCs will also migrate to the peritoneal cavity after a single THC injection (i.p.) (86). Knowing that the peripheral MDSCs are considered active, and therefore T cell

suppressive, we first determined if any differences existed between the resident BM MDSCs and the THC-induced MDSCs found in the peritoneal cavity. As such, naive C57BL/6 (wild-type, BL6) mice were given a single i.p. injection of THC to cause massive induction of MDSC to the peritoneal cavity, as earlier described (86). Sixteen hours after THC treatment, peritoneal lavage was used to collect peripheral THC-induced MDSCs. Resident BM MDSCs from naive BL6 mice were used as controls. MDSCs were purified (>95%) using positive selection magnetic beads. Flow cytometry was used to determine if any differences in MDSC and MDSCs subset populations existed. The naïve BM showed ~51% of Gr1+CD11b+ cells when compared to THC-induced peritoneal cells which contained ~83% Gr1+CD11b+ cells (Fig. 2.1A). Next, we sorted the Gr1+CD11b+ cells and stained them further for Ly6G and Ly6C to measure granulocytic (Ly6G+Ly6C+Gr1+CD11b+) and monocytic (Ly6G-Ly6C+Gr1+CD11b) MDSC subset proportions (Fig. 2.1D). In order to demonstrate that the THC-induced Gr1+CD11b+ cells were in fact T cell suppressive, we tested the levels of INF-γ secretion which decrease significantly upon addition of THC-induced MDSCs to activated T cells (Fig. 2.1B). We next assessed the suppressive capabilities of THC-induced MDSCs in comparison to resident BM MDSCs. We found that THC-induced MDSCs were significantly more suppressive of concanavalin A (ConA)-activated splenic T cells than the resident BM MDSCs (Fig. 2.1C). With literature suggesting that MDSC subsets can have differing levels of suppression we compared independently isolated Gr1+, Ly6G+, or Ly6C+ MDSC subsets, Ly6C+ subsets were isolated after positive selection of Ly6G+ cells using concurrent PE and FITC positive selection for Ly6G and Ly6C respectively (111); (112). The individually isolated pure MDSC subpopulations were then treated with

Mitomycin C and added to ConA activated spleen cells at MDSC to spleen cell ratio of 1:2, to study the ability of MDSCs to inhibit T cell proliferation (Fig. 2.1E). In all three isolation conditions, Gr1+, Ly6G+, or Ly6C+, THC-induced MDSCs showed significantly more suppression of T cell proliferation than resident BM MDSCs (Fig. 2.1E).

THC-induced MDSCs exhibit differential expression of functional proteins.

To explain how THC-induced MDSCs exhibited increased suppressive capabilities compared to resident BM MDSCs, we next looked at the expression of functional proteins. MDSCs ability to suppress T cell proliferation has been linked to elevated expression of L-arginine metabolizers Arg1 or NOS2 (113). The expression of Arg1 was greatly increased in THC-induced MDSCs compared to resident BM MDSCs (Fig. 2.2A). In order to ensure that Arg1 expression was specific to activated MDSCs, we looked at BM and splenic MDSCs from naïve mice as well as BM, splenic, and peritoneal MDSCs from THC-treated mice. We found no expression of Arg1 in naïve or BM resident MDSCs though peripheral MDSCs in THC-treated mice did exhibit Arg1 expression (Supp. Fig. 2.1A). However, NOS2 expression was reduced in THC-induced MDSCs isolated from the peritoneal cavity compared to naïve resident BM MDSCs (Fig. 2.2B). We also looked at the expression of the S100 proteins A8 and A9 due to the fact that while cancer studies have determined that secretion of S100A8 and S100A9 are associated with tumor induced MDSCs, no one has linked THC-mediated induction of MDSCs to the expression of these S100 proteins (114). Elevated levels of S100A8, but not S100A9, were observed in THC-induced MDSCs when compared to BM MDSCs (Fig. 2.2 C&D respectively). Because STAT3 plays a critical role in MDSC expansion,

activation and function we investigated the expression of phosphorylated STAT3 (P-STAT3) (115); (116); (117). Interestingly, THC-induced MDSCs showed an increased expression of P-STAT3/STAT3, when compared to resident BM MDSCs (Fig. 2.2E).

STAT3 associated cytokines are upregulated in THC-induced MDSCs.

It has recently been shown that Arg1 and S100A8 are downstream targets of STAT3 (118); (119); (87). As such, we looked at the spontaneous secretion of IL-10 and IL-6, known STAT3 activating cytokines, from MDSCs cultured overnight after isolation. Spontaneous secretion of IL-10 was low from both MDSC populations. However, THC-induced MDSCs secreted significantly more IL-10 than did resident BM MDSCs (Fig. 2.3A). This correlated with elevated expression of IL-10 message in THC-induced MDSCs (Fig. 2.3C). Spontaneous IL-6 secretion as well as the transcript was expressed at higher levels in THC-induced MDSCs when compared to resident BM MDSCs (Fig. 3B). This trend was supported by significantly increased IL-6 message in THC-induced MDSCs (Fig. 2.3D).

THC treatment increases S100A8 secretion.

Because STAT3 can regulate S100 proteins (119), we next determined the levels of S100 proteins A8 and A9. THC-induced MDSCs showed significantly increased S100A8, but not S100A9, secretion when compared to resident BM MDSCs (Fig. 2.3 E&F respectively). Also, we found that injection of THC systemically increased S100A8 levels when compared to naïve mice (Fig. 2.3G).

THC administration alters the methylation profile in MDSCs due to decreased DNA methyltransferases.

We next determined if THC induces MDSCs through epigenetic regulation. To that end, we first determined if THC could affect methylation by studying global changes in genomic DNA methylation patterns. We found that while overall methylation was unaffected by THC treatment, using CEAS software for correlational analysis, the methylation at promoter regions was altered when resident BM and THC-induced MDSCs were compared (Fig. 2.4 A&B respectively). Knowing that methylation changes could occur due to differential expression of DNA methyltransferases (DNMTs), specifically DNMT3a and DNMT3b, which are responsible for *de novo* methylation, both resident BM and THC-induced MDSCs were assessed for DNMT methylation and mRNA expression (120); (121). The methylation at the promoter region for both DNMT3a and DNMT3b was increased in THC-induced MDSCs (Fig. 2.4C). Additionally, THC-induced MDSCs had significantly reduced expression of DNTM3a and DNMT3b compared to resident BM MDSCs (Fig. 2.4D).

THC decreases the methylation of key MDSC functional genes.

We next investigated if the increase in Arg1, NOS2, and STAT3 seen in THC-induced MDSCs resulted from alterations in the methylation of these key genes associated with MDSC activation and function. Using Methyl Primer Express v1.0 software, individual gene methylation primers were developed for key genes associated with the suppressive function of MDSCs (Table 2.I). Furthermore, universally methylated mouse DNA (Methylated Standard-Millipore) was used as a baseline for comparisons between resident BM and THC-induced MDSC methylation. Using (CEAS software) we observed that promoter region methylation was decreased at Arg1 and STAT3 in THC-induced MDSCs (Fig. 2.5 A&B respectively). To support the findings

from the genomic DNA methylation analysis we used methylation specific PCR (Msp PCR). The methylation index showed that THC-induced MDSCs had deceased levels of methylation at Arg1 and STAT3, but not at iNOS, compared to naïve resident BM MDSCs (Fig. 2.5C). Methylation of the S100 proteins, S100A8 and S100A9, was not determined as there were no CpG islands found in the promoter regions of these genes. Together, these data demonstrated that THC induces immunosuppressive MDSCs through hypomethylation of critical genes that regulate MDSC functions.

S100A8 is important in maintaining a suppressive peripheral MDSC population.

In order to further elucidate the role S100A8 was playing in MDSC functionality, we first created a conditioned medium (CM). The conditioned medium contained both STAT3 activating cytokines, which could enhance Arg1 production, and soluble S100A8. CM was created by incubating THC-induced MDSCs in the presence of PMA (50 ng/mL) and calcium ionophore (10 μg/mL). Resident BM MDSCs, were then plated with or without CM, and ConA-activated splenocytes. Resident BM MDSCs caused just over 25% suppression of T cell proliferation in response to ConA compared to THC-induced MDSCs which caused 50% suppression (Fig. 2.6A). However, resident BM MDSCs in CM had significantly increased suppressive capabilities, reducing T cell proliferation by nearly 70%, compared to BM MDSCs without CM (Fig. 2.6A).

To further determine the role of S100A8 *in vivo*, we treated THC injected mice with a single dose of S100A8 antibody (8H150). The mice were then assessed for MDSC induction in the peritoneal cavity over 16 hours, via flow cytometric analysis of Gr1+CD11b+ cells. S100A8 Ab caused significant decrease in MDSC accumulation in

the peritoneal cavity at the 16 hour time point (Fig. 2.6B). Furthermore, looking at MDSC subsets, we found that upon blocking S100A8, significantly fewer granulocytic MDSCs were induced by THC, while no significant reduction was seen in monocytic MDSCs (Fig. 2.6 C&D respectively). Additionally, to ascertain the role of S100A8 in MDSC-induced suppression of T cell proliferation, recombinant protein (mS100A8) was added to plated resident BM MDSCs in the presence of ConA activated splenocytes. A significant increase in suppression was seen in resident BM MDSCs treated *in vitro* with mS100A8 compared to untreated resident BM MDSCs (Fig. 2.6E). Furthermore, mS100A8-treated resident BM MDSCs were able to suppress T cell proliferation to similar level as THC-induced MDSCs (Fig. 2.7C).

2.4 DISCUSSION

The mechanisms through which THC mediates immunosuppression include apoptosis, induction of T regulatory cells (Tregs), and the induction of a switch from Th1 to Th2 phenotype (80); (78); (77). Recently, our laboratory made an exciting finding that THC can induce massive numbers of MDSCs *in vivo* via activation of accessory immune cells such as mast cells (86); (75). MDSCs are a heterogeneous and immature cell population with an innate plasticity. Recently studies have highlighted this plasticity by showing that MDSC subsets can induce either TH17 or iTreg cells (122). It has also been found that MDSCs, which are generally considered beneficial in the tumor microenvironment, secrete soluble factors such as nitrous oxide, which can induce apoptosis in cancer cells (123). Together these findings highlight the need to understand what factors are associated with MDSC plasticity and it is likely that epigenetic modulation may be one of the contributing factors. As such, the focus of the current

study was to further elucidate the mechanisms through which THC induces and maintains a peripheral population of highly immunosuppressive MDSCs. Recently, it has been shown that THC treatment can alter gene specific methylation patterns in lymphocytes (38). Consequently we set out to determine the role of altered DNA methylation in the context of THC driven recruitment of MDSCs.

Research showing the involvement of THC in epigenetic modifications is limited. However, there is evidence suggesting that THC ingested through marijuana abuse can elicit both indirect and direct effects on gene expression (124); (125); (126); (127); (128); (87). Additionally, studies using SIV-infected (simian immunodeficiency virus) animals treated with THC found that up to 50% of all gene expression alterations were due to differential DNA methylation patterns (129). Furthermore, a CB1-dependent link with cannabinoid treatment was discovered in the regulation of keratinocyte differentiation by inducing DNA methylation (130). Such findings support the role of CB1 receptor agonists, such as THC, in altering DNMT activity resulting in changes in genomic DNA methylation patterns as seen in the current study.

Alteration of DNMT expression correlates directly with changes to gene loci specific DNA methylation pattern (131). Specifically, the changes in the methylation profile for transcription factors associated with MDSC activation or function, such as STAT3, was of paramount interest to us as elevated expression of STAT3 has been tied to increased MDSC-mediated immunosuppression (115); (116); (132); (87). We found that STAT3 levels were significantly increased in THC-induced MDSCs. It has been shown that that STAT3 activation, via IL-6 or G-CSF, is necessary for the expansion of functional MDSCs in part due to regulation of NADH oxidase (133). Consistent with

this, we also noted significant increase in IL-6 in THC-induced MDSCs. Additionally, it has been shown that the highly suppressive nature of activated MDSCs, via Arg1 expression, is STAT3 dependent (117). With STAT3 playing such an integral role in MDSC functionality, the differential expression we observed between resident BM and THC-induced MDSCs suggested that resident MDSCs may exist in a naïve or inactivated state.

One of the hallmarks of MDSC function is their ability to suppress T cell proliferation. MDSCs have been shown to inhibit T cell activation and proliferation via L-arginine metabolism, oxidative stress, Treg expansion, and cysteine depletion (134); (135); (58); (136); (137). Previously we showed that that THC-induced MDSCs have elevated levels of Arg1 expression thereby causing the suppression of T cell proliferation through L-arginine depletion (86). In the current study we also noted that THC-induced MDSCs had higher levels of Arg1 when compared to resident BM MDSCs. Furthermore, THC treatment has been associated with, a cannabinoid receptor dependent, loss of NOS2 activation due to cAMP signal inhibition (138); (139). This may explain why in the current study, why THC-induced MDSC did not exhibit an increase in NOS2. Additionally, the S100 proteins, S100A8 and S100A9, have been linked to MDSC expansion via the RAGE receptor, in cancer models (114). In conjunction with reported findings, the elevated expression of Arg1 and S100A8 we observed in the current study strengthen our claim that a single THC injection generates primed, or activated, peripheral MDSCs rather than just recruiting inactivated BM MDSCs to the periphery.

Although S100A8/A9 has been associated with MAPK and NF-κB signaling pathways, these S100 proteins can also be linked to the JAK/STAT pathway (140). For

instance, S100A8 has been associated with STAT3 activating cytokines including IL-10, in alveolar macrophages, and IL-6 induction, in PBMCs, creating an indirect association with the JAK/STAT signal pathway that we also observed in MDSCs (141); (142). More directly, P-STAT3 is known to have binding sites in the promoter region of S100A8 (119). This positive feedback interaction between STAT3 and S100A8 suggests that the S100 protein may play a vital role in MDSC function.

Hematopoietic progenitor cells (HPCs) maintain detectable levels of S100A8, for up to one week in culture, even upon differentiation at which point S100A9 expression is lost (119). The role that S100A8 plays in MDSC function, however, has not been reported. It has been shown that S100A8 is involved in granulocyte chemotaxis, and that S100A8/A9 secretion allows for MDSC accumulation (143); (114). A study by Hiroshima et al. observed a correlation between elevated S100A8 and Arg1 transcript levels, in alveolar macrophages (141). This finding supports our claim that increased S100A8 expression impacts MDSC function as an anti-inflammatory molecule similar to IL-10 (144); (145); (141); (146). TLR activation can also be positively influenced by the S100A8 protein (147). The current study, to the best of our knowledge, is the first one to report that elevated S100A8 levels in MDSCs regulate increased Arg1-driven T cell suppression.

A connection between increased S100A9 expression and the accumulation of tumor associated MDSCs, has been reported (119). Cheng et al. determined that CT-26, a tumor-cell conditioned media, was able to increase S100A9 expression, *in vitro*, in HPCs which correlated with a loss of DC differentiation (119). Additionally, Cheng et al. were able to show that the MDSCs accumulated via S100A9 overexpression were, in

fact, T cell suppressive (119). While inflammation has been shown to induce MDSC recruitment, THC treatment recruits active MDSCs without pro-inflammatory signals (86). Moreover, our studies showed that S100A9 was not induced by THC.

The ability of THC to alter gene expression via the upregulation of key microRNA has also been studied. A single THC treatment was found to induce miR-690 overexpression in conjunction with decreased CCAAT/enhancer binding protein (C/EBPα), a transcription factor associated with myeloid cell differentiation, in peripheral MDSCs (87). Specifically, over expression of C/EBPα, alone, was sufficient to increase the expression of the S100A9 protein, which is known to decrease in mature differentiated cells (148). As such it has been suggested that the attenuation of C/EBPα could play a role in maintaining an immature, and therefore functional, population of MDSCs upon THC induction (87). THC causing a reduction of C/EBPα levels, and therefore decreasing S100A9 expression, strengthens our claim that a S100A8 driven mechanism for THC-induced MDSC activation plays a critical role.

The mechanism of MDSC activation is one that remains elusive due the variety of environmental factors that are known to impact the generation, maintenance, and function of these regulatory cells. The current study attempted to highlight a mechanism by which THC caused the induction and activation of primed peripheral MDSCs, depicted in Fig. 2.7. After THC treatment, there is decreased methylation of STAT3 leading to an upregulation of the transcription factor, as well as STAT3 activating cytokines (IL-10 and IL-6), which together leads to increased P-STAT3. While low levels of IL-10 were secreted by THC-induced MDSCs, the ability of THC to activate additional IL-10 secreting cells such as Tregs further supports that THC plays a role in STAT3 activation

(88). P-STAT3, binds to the promoter region of S100A8 and Arg1, thereby increasing the expression of these proteins. Additionally, upon overexpression of S100A8 and Arg1, MDSCs became highly immunosuppressive. To the best of our knowledge this report is the first one to identify gene specific methylation profile of MDSCs following THC treatment, and how such epigenetic changes regulate the anti-inflammatory properties of MDSCs involving STAT3/S100A8 positive feedback loop.

Table 2.I. Primer sequences for the Msp PCR analysis of THC-induced and resident BM MDSCs.

Gene	Primer	Sequence (5'-3')	Annealing Temp
Arg1	ARGMF	CGG GTT AAA TTC GGG TTA TC	55°C
	ARGMR	CGA ACT ACC GCG ATT CTA ATC	
	ARGUF	CCA AAC TAC CAC AAT TCT AAT CTA	
	ARGUR	TTT TGG GTT AAA TTT GGG TTA TT	
NOS2	NOS2MF	TAT ATA AAC GAG GTA TTC GCG C	55°C
	NOS2MR	CTT TAA CGC TAT CCC TTT ATC G	
	NOS2UF	GAA TAT ATA AAT GAG GTA TTT GTG T	
	NOS2UR	TCT TTA ACA CTA TCC CTT TAT CAC C	
STAT3	STATMF	GAG GTA TAA TTT TGT TTG GTG TT	60°C
	STATMR	AAA CCC AAC TAA CCA ACC TA	
	STATUF	GGT ATA ATT TCG TTC GGT GTC	
	STATUR	AAC CCG ACT AAC CGA CCT	

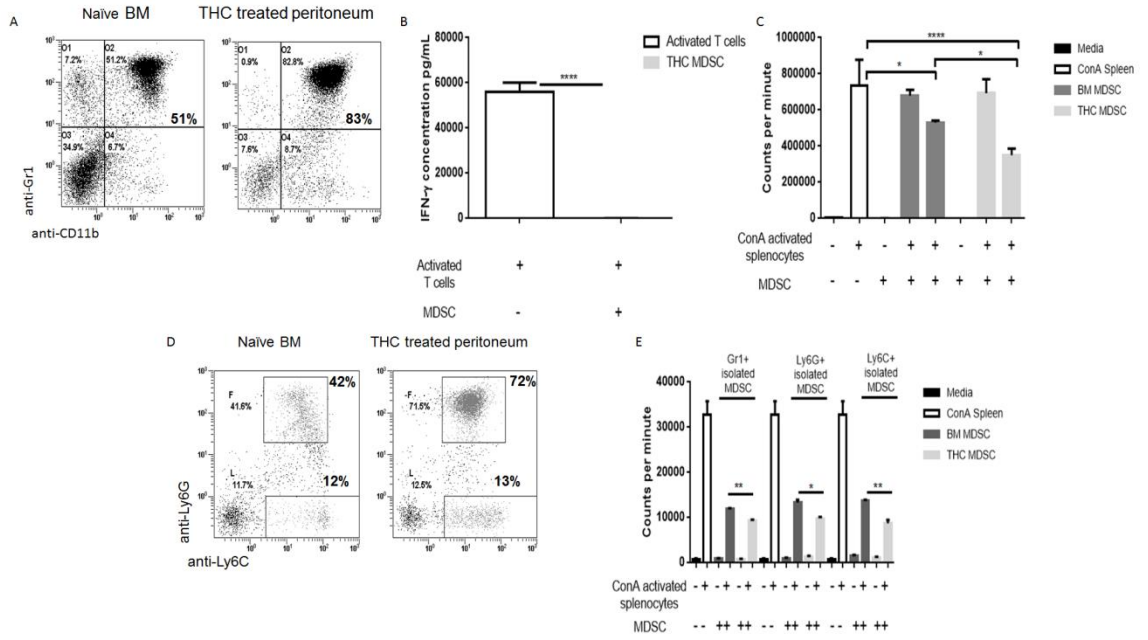

Figure 2.1: THC-induced MDSCS differ from resident BM MDSCs in subset proportion and suppressive functionality.

MDSCs were isolated from peritoneal exudates, at 16 hours after THC injection, and naïve BM using positive selection magnetic beads for αGr1, αLy6G, or αLy6C. MDSCs were Mitomycin C treated prior to plating with BL6 spleen cells activated with ConA (MDSC:T cell ratios 1:25 and 1:2). IFN-γ was assessed, in cell supernatants using sandwich ELISA kits (Biolegend) after co-culture. Proliferation of spleen cells was assessed 40 hours after stimulation using [^{3}H] thymidine (co-cultured for 16 hrs). A) Flow cytometric analysis for MDSC proportion (dot plots gated only on live cells), double stained for GR1+CD11b+ cells in naïve BM (left panel) and THC treated peritoneal exudate (right panel). B) Levels of IFN-γ secreted by activated T cells with and without MDSC co-culture. C) Ability of MDSCs to suppress proliferation of T cells. MDSCs from naïve BM, or THC-treated peritoneal exudate MDSCs were co-cultured with ConA activated splenic T-cells. D) Flow cytometric analysis of MDSCs from naïve BM (left panel), or THC-treated peritoneal exudate (right panel) MDSCs following triple-staining with CD11b+, Ly6G+, and Ly6C+ cells (dot plots gated on CD11b positive cells). E) Suppression of T cell proliferation by Gr1+, Ly6G+, Ly6C+ cells isolated from naïve BM and THC-treated peritoneal exudate co-cultured with ConA activated splenic T-cells. Representative data from replicate experiments (mean±S.E.M) * $p < 0.05$, ** $p < 0.01$, *** $p < 0.005$, **** $p < 0.0001$ ANOVA/Tukey.

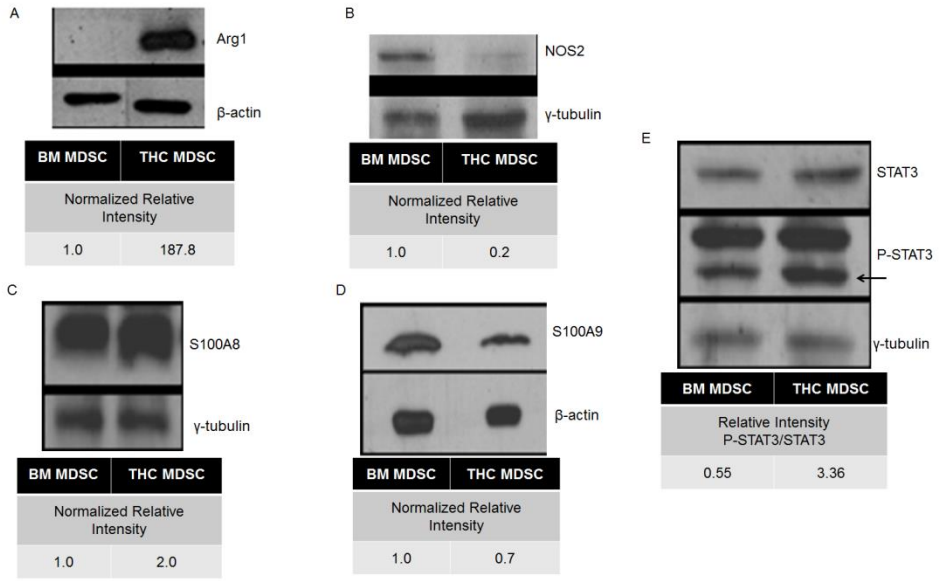

Figure 2.2: THC-induced MDSCs have differential expression of MDSC associated proteins compared to resident naïve BM MDSCs.
Western blot followed by densitometric analysis via ImageJ with beta actin or gamma tubulin used for normalization. MDSC-associated proteins including, A) Arginase1, B) NOS2, C) S100A8, D) S100A9, and E) STAT3 (P-STAT3), in MDSCs derived from naïve resident BM and THC-induced peritoneal exudate. Representative data from triplicate experiments (mean±S.E.M) * $p < 0.05$, ** $p < 0.01$, *** $p < 0.005$, **** $p < 0.0001$.

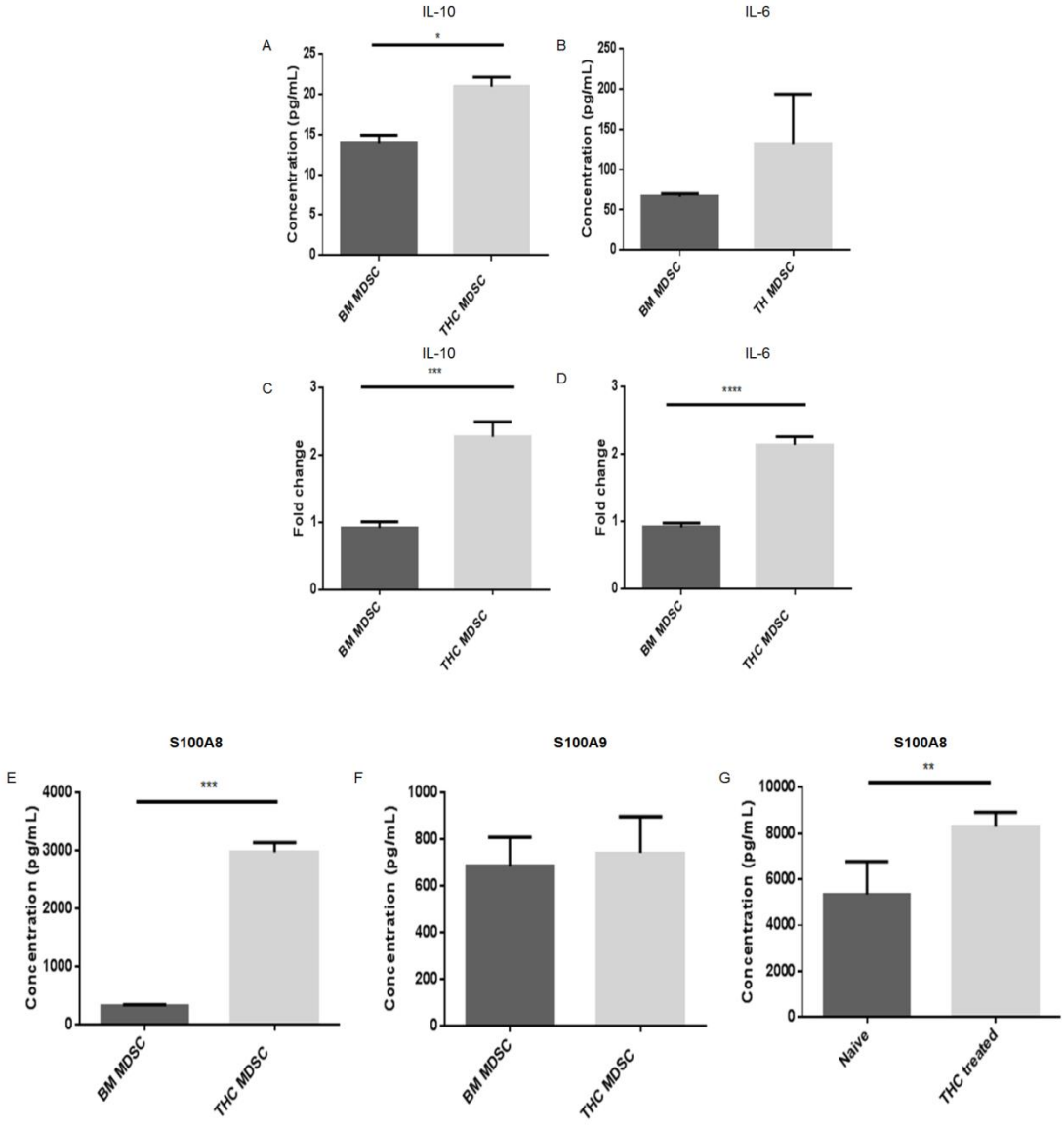

Figure 2.3: THC-induced MDSCs exhibit elevated levels of cytokines associated with STAT3 activation.

THC-induced MDSCs and resident naïve BM MDSCs were cultured overnight and cell supernatants collected for cytokine analysis using sandwich ELISA kits: A) IL-10, B) IL-6. cDNA was isolated from MDSCs for real time (q) PCR analysis: C) IL-10 mRNA, D) IL-6 mRNA. Spontaneous secretion from THC-induced and resident naïve BM MDSC culture supernatants: E) S100A8 F) S100A9. Serum from THC-treated or naïve mice were analyzed for S100: G) S100A8 levels. Representative data from replicate experiments (mean±S.E.M) * $p < 0.05$, ** $p < 0.01$, *** $p < 0.005$, **** $p < 0.0001$ Student's T-Test.

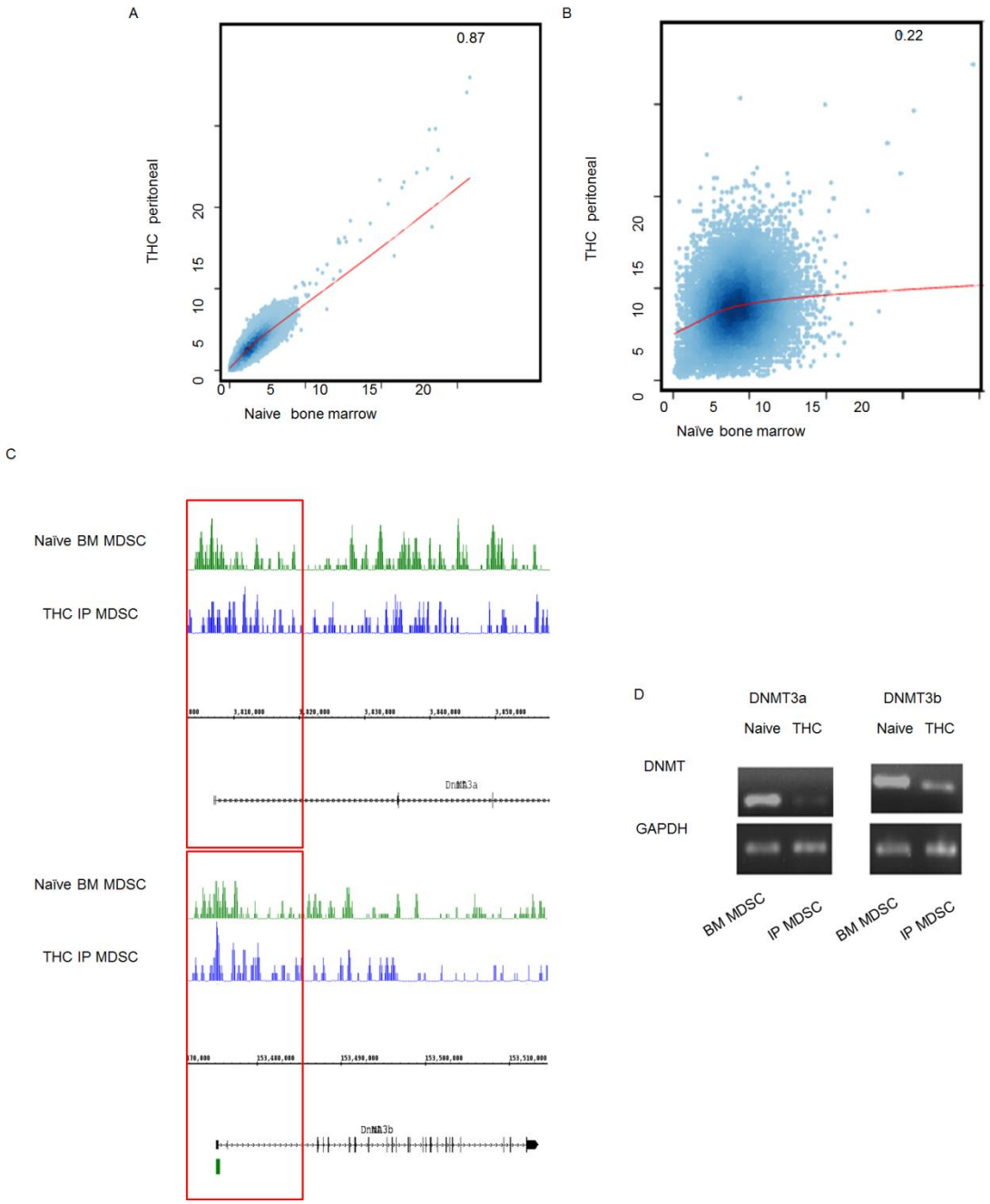

Figure 2.4: THC alters the methylation profile of MDSCs.
Genomic DNA from THC-induced MDSCs (n=5 mice) and naïve resident BM MDSCs (n=5 mice) was assessed for genomic methylation via MeDIP-seq. A) Correlations of genome-wide DNA methylation signal (CEAS software) in THC-induced and resident BM MDSCs. B) Correlations of DNA methylation within 3kb up and down stream of transcriptional start site (TSS) in THC-induced and resident BM MDSCs. C) DNA methylation near the TSS of DNMT3a and 3B (upper and lower panels respectively). D) PCR for DNMT3a and 3b message in THC-induced and resident BM MDSCs. Representative data from replicate experiments.

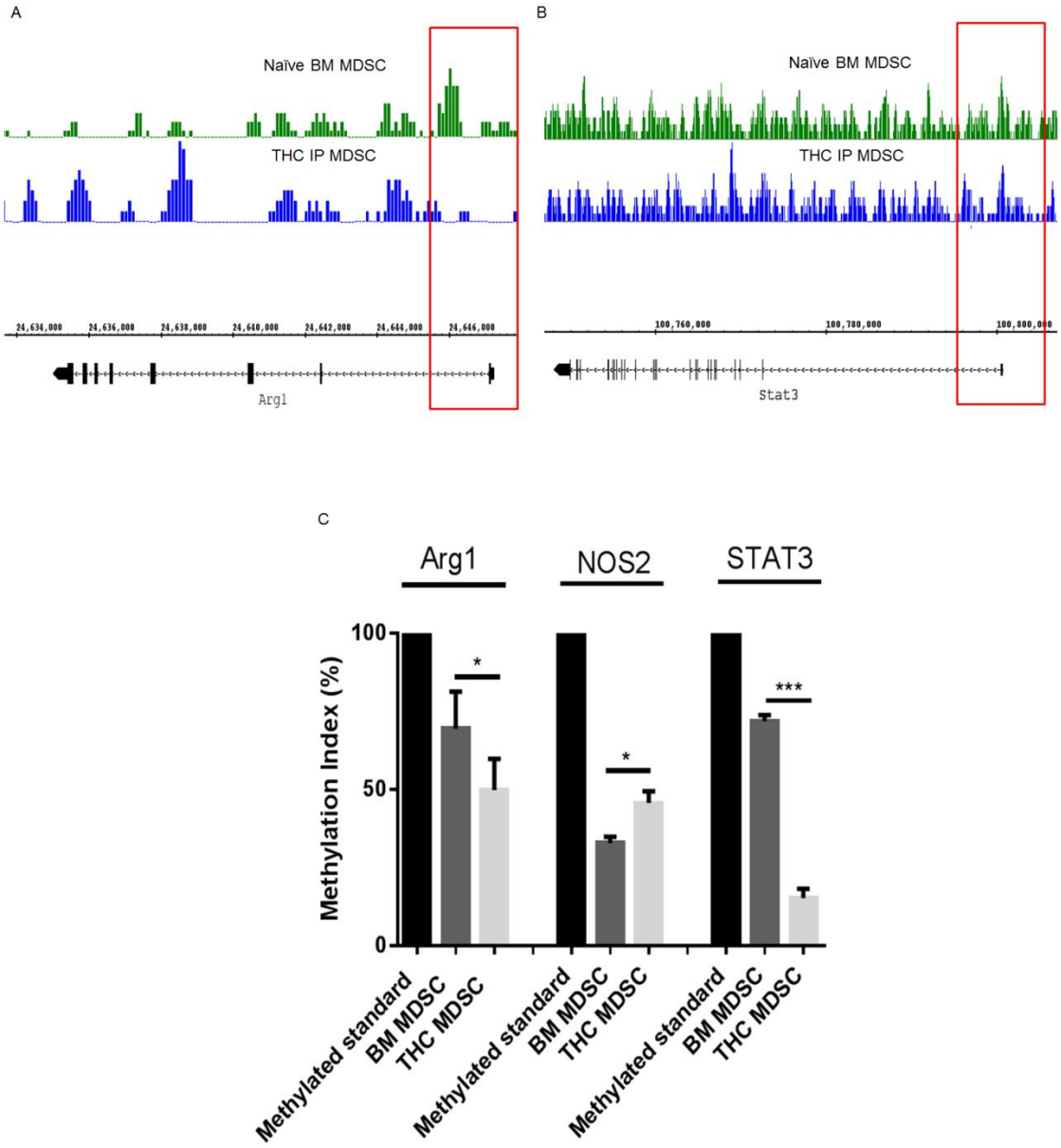

Figure 2.5: THC- induced MDSCs differ from resident BM MDSCs in promoter region methylation.

Bisulfite converted genomic DNA was assessed for promoter region associated methylation in THC-induced and naïve BM MDSCs. A) DNA methylation near the TSS of Arg1 in THC-induced and resident BM MDSCs. B) DNA methylation near the TSS of Stat3 in THC-induced and resident BM MDSCs. Methylation specific (Msp) PCR products were ran on agarose gel (2%) and densitometry assessed using ImageJ. A) Methylation index for Arg1, NOS2, and STAT3 in THC-induced and resident BM MDSCs (fully methylated mouse DNA was used as a control). Data from replicate experiments (mean±S.E.M) * $p < 0.05$, ** $p < 0.01$, *** $p < 0.005$, **** $p< 0.0001$ Student's T-Test.

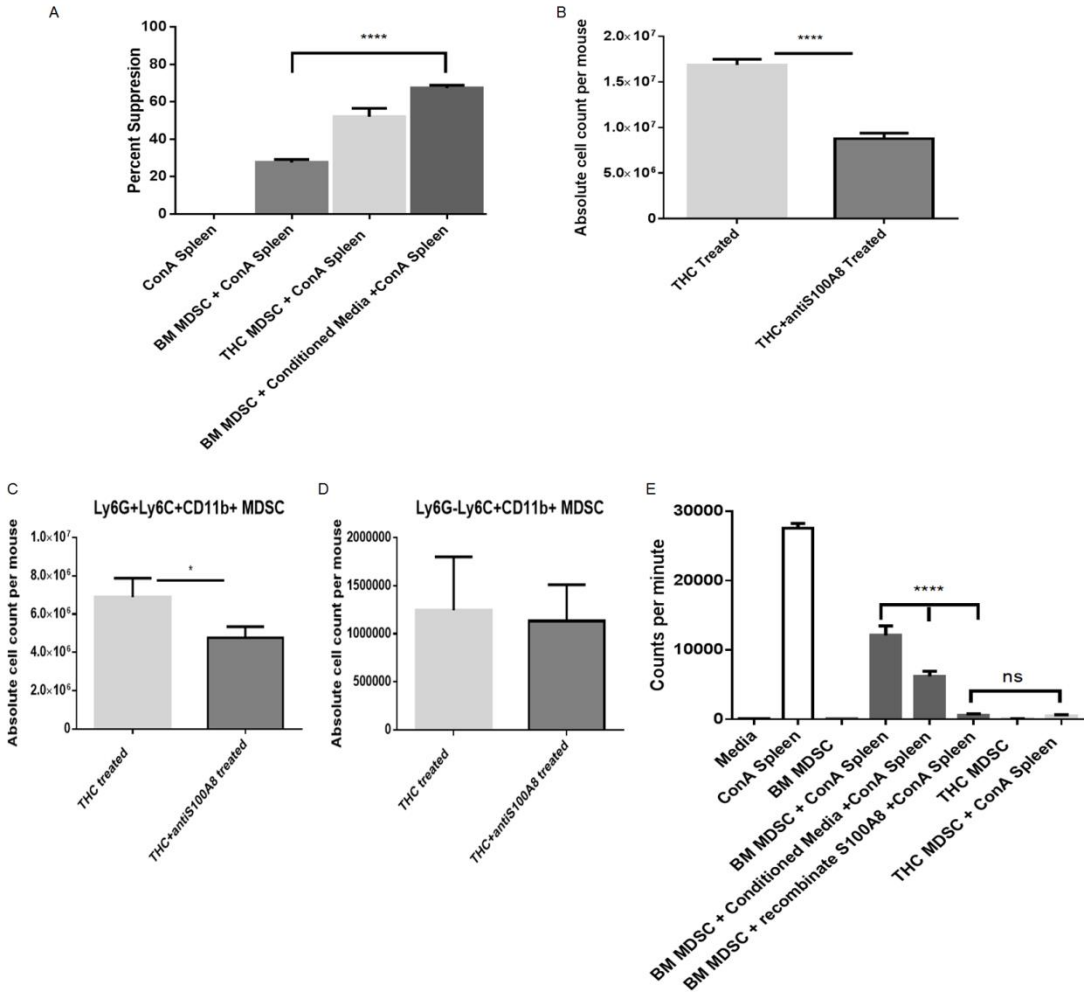

Figure 2.6: S100A8 protein impacts both MDSC induction and activation. Conditioned medium (CM) was obtained from THC-induced MDSCs cultured for 5 hours in the presence of PMA and calcium ionophore, and then assessed for suppressive capabilities. A) Ability of CM to enhance MDSCs or CM as indicated. Thymidine incorporation was used to detect T cell proliferation and percent suppression when compared to controls was plotted. B-D) Effect of anti-S100A8 Abs on THC-induced MDSCs in the peritoneal cavity. Antibody (8H150) against S100A8 was administered 1 hour after THC treatment, and assessed for MDSC accumulation. Data indicate absolute cell counts of B) Gr1+CD11b+, C) granulocytic MDSCs (Ly6G+LyC+CD11b+), D) monocytic MDSCs (Ly6G-Ly6C+CD11b+) cells in the peritoneal cavity. E) Effect of addition of recombinant S100A8 protein (mS100A8) on ability of MDSCs to suppress T cell proliferation. T cell proliferation was studied by activation using ConA as described above. The cultures received conditioned medium or mS100A8 as indicated. Representative data from replicate experiments (mean±S.E.M) * $p < 0.05$, ** $p < 0.01$, *** $p < 0.005$, **** $p < 0.0001$ Student's T-Test or ANOVA/Tukey.

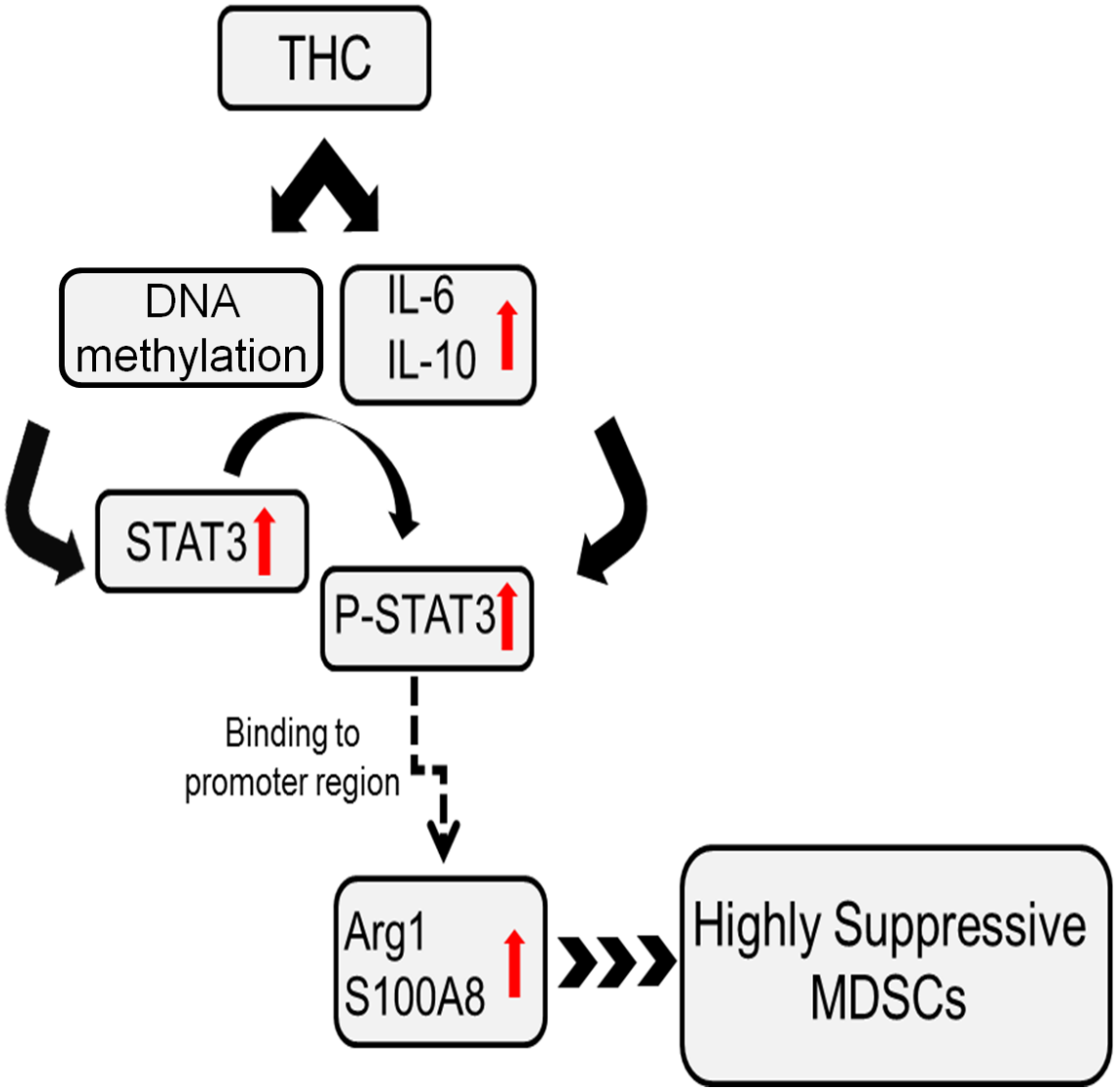

Figure 2.7: Proposed working model for the mechanism of MDSC induction and activation by THC

THC treatment causes hypomethylation of genes associated with MDSC function, such as STAT3, allowing for reduced gene silencing. Additionally, THC treatment increases the STAT3 activating cytokines IL-6 and IL-10. Phosphorylated STAT3 is then able to bind the promoter region of S100A8 and Arg1 increasing the suppressive capability of the THC-induce MDSCs.

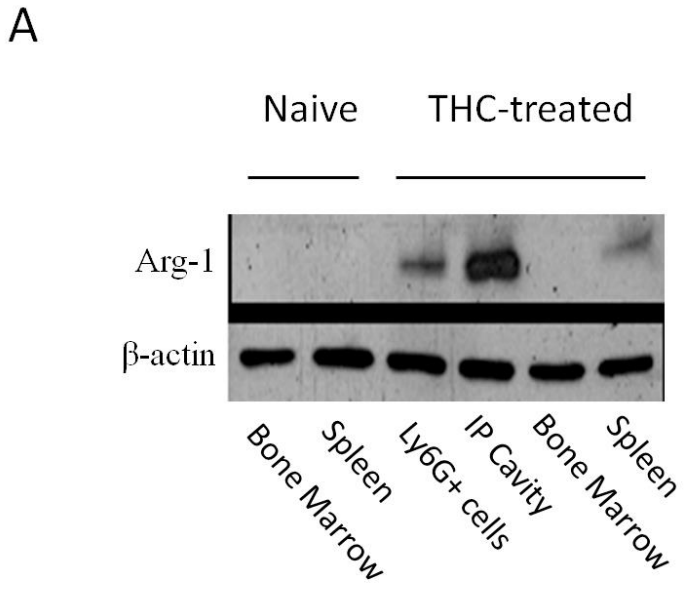

Supplemental Figure 2.1: Arginase1 expression specific to peripheral MDSCs in THC treated mice.

Western blot with beta actin used for normalization. MDSC-associated protein A) Arginase1 in MDSCs derived from naïve resident BM and spleen (n=5) and THC treated mouse peritoneal exudate, BM, and spleen (n=5)

CHAPTER III: Δ^9-Tetrahydrocannabinol attenuates allogeneic host-versus-graft response via cannabinoid receptor 1 mediated induction of MDSCs.

3.1 INTRODUCTION

Host versus graft disease (HvGD), perhaps better known as transplant rejection, is primarily a T cell driven process involving recognition of alloantigens that leads to rejection of allograft cells or tissue. Through the use of immunosuppressive drugs, the success rate of allogeneic transplants has steadily increased over the years. However, the chronic use of these drugs often results in major complications in the graft recipient. The four major categories of immunosuppressive drugs used today include corticosteroids, calcineurin inhibitors, anti-proliferatives, and mammalian target of rapamycin (mTOR) inhibitors. These anti-rejection treatments focus largely on halting the alloreactive T cell activation or proliferation in the host. By causing global inhibition of T cells, the host's innate immune system becomes severely impaired (61); (62); (63); (64); (65). For instance, cyclosporine, a calcineurin inhibitor, can cause immunotoxicity through the destruction of liver tissue (61); (66). Additionally, anti-proliferatives, such as mycophenolate (MMF) and mTOR inhibitors, cause leukopenia and can delay functionality of the graft (62); (63).

Furthermore, use of any severe immune suppressive drug is associated with increased risk of infection, bacterial or viral, and cancer. Specifically, treatment of allograft rejection, with current drug options, can result in lymphomas as well as

accelerated hepatitis infections (67); (68). Such severe drug related issues has necessitated the continued search for an HvGD treatment which has a better cost to benefit ratio.

Δ^9-Tetrahydrocannabinol (THC) is one of many cannabinoids derived from the *Cannabis sativa* plant, which was first described in a 1964 paper by Gaoni and Mechoulam (149);. THC is a known ligand for cannabinoid receptors 1 and 2 (CB1 and CB2) which were discovered in the 1990's (4, 150). CB1 and CB2 are G-protein coupled receptors which have been shown to be expressed both in the central nervous system (CNS) and the periphery, including the immune system (3); (12); (13); (14). Upon activation, CB1 and CB2 receptors are known to modulate adenylate cyclase, both calcium and potassium channels, reduce T cell proliferation, and have been associated with regulation of the cytokines leading to a shift from a pro-inflammatory Th1 to an anti-inflammatory Th2 response (151); (152); (153); (154). The anti-inflammatory properties of THC have been very well characterized by our laboratory and others (77); (155); (156). Recently, we made an exciting observation that administration of THC results in massive induction of myeloid derived suppressor cells (MDSCs) (86). MDSCs are innate regulatory cells which are known to reduce T cell driven inflammatory responses in cancer models (57). In mice, MDSCs are positive for the cell surface markers CD11b and Gr1 (57). The heterogeneous population of progenitor and immature cells, which make up MDSCs, reduce inflammation by producing arginase-1 (Arg-1) and/or iNOS (58).

Currently THC, under the brand name Marinol, has been approved for medicinal use. Marinol has been used to alleviate pain and nausea associated with cancer

treatments, stimulate appetite in those with wasting diseases such as HIV/AIDS, and for spasticity in multiple sclerosis patients (157). Furthermore, our lab recently found that THC treatment significantly reduces symptomology associated with graft versus host disease (GvHD), where the immune cells from the allograft attack recipient tissue, in a cannabinoid receptor dependent manor (78). Based on such studies, we hypothesized that cannabinoids may have the potential to be used in transplantation (158). To the best of our knowledge, THC has not been directly tested against allograft rejection *in vivo*. Due to the fact that immune cells express cannabinoid receptors and produce endocannabinoids, studies focused on addressing the role of cannabinoid receptor-ligand system may offer novel insights into their mechanism of action in enhancing the survival of an allograft.

In the current study, we found that THC treatment reduces inflammation associated with HvGD and causes significant increase in the survival of allogeneic skin allograft. These effects of THC were primarily mediated by its ability to induce immunosuppressive MDSCs. The current study suggests a role for the cannabinoid system in the regulation of transplantation immunity and treatment.

3.2 MATERIALS AND METHODS

Mice-

Female C57BL/6 (H-2^b wild-type, BL6) mice, aged 6-8 weeks and at an average weight of 20 g, were obtained from the National Cancer Institute (Frederick, MD) and used as recipients. Female C_3H/HeJ (H-2^k, C_3H) mice, from The Jackson Laboratory, were used as donors. CB1 KO (-/-) mice (H-2^b C57BL/6 background) were a gift from Dr. James

Pickel, National Institute of Mental Health Transgenic Core Facility. CB2 KO (-/-) mice (H-2^b C57BL/6 background) were obtained from The Jackson Laboratory. The CB1 and CB2 KO mice were used at 6 weeks of age and averaged 20 g. B6D2F1/J (F1 H-$2^{d/b}$) mice aged at least 8 weeks with an average weight of 20 g, obtained from The Jackson Laboratory, were also used as recipient mice. All mice were housed in pathogen-free conditions and allowed ad libitum access to filtered water and Teklad rodent diet 8604 (normal chow) at the AAALAC-accredited Animal Research Facility located at the University of South Carolina School of Medicine. All experiments were conducted under an approved Institutional Animal Care and Use Committee animal protocol.

Treatment with THC and Induction of Acute HvGD-

THC (procured from NIDA-NIH) dissolved in ethanol was diluted in 1xPBS to a concentration of 20 mg/kg. THC or vehicle (ethanol diluted in 1xPBS) was administered intraperitoneally (i.p.) at a volume of 0.1mL/mouse, 2 hours prior to allogeneic cell injection. To induce HvGD we used a modified localized HvGD model developed by Shevach et al. (159), which has also been used in other studies (160); (161); (162). Briefly, acute HvGD was induced by injecting $2.2x10^7$ C_3H spleen cells subcutaneously (SubQ). These cells were split with half injected into the right and left hind flanks, of BL6 recipient mice. The inguinal draining lymph nodes (IngLN) were harvested daily for 5 days to study the localized HvGD, following MLR kinetics (163). THC treatment was continued daily until the termination of the study (day 5). Similarly, cannabinoid receptor antagonist SR141716 (5-(4-Chlorophenyl)-1-(2,4-dichloro-phenyl)-4-methyl-N-(piperidin-1-yl)-1H-pyrazole-3-carboxamide; CB1 antagonist), SR144528 (N-[(1S)-endo-1,3,3-trimethylbicyclo [2.2.1]heptan2-yl]-5-(4-chloro-3-methylphenyl)-1-[(4-

methylphenyl)methyl]-1H-pyrazole-3-carboxamide; CB2 antagonist), and AM-630 (6-Iodo-2-methyl-1-[2-(4-morpholinyl)ethyl]-1H-indol-3-yl](4-methoxyphenyl)methanone; CB2 antagonist) were dissolved in dimethyl sulfoxide (DMSO) containing 20 µL Tween-80 (Sigma-Aldrich) and then diluted in 1xPBS to a concentration of 20 mg/kg, cannabinoid receptor antagonist vehicle consisted of DMSO with 20 µL Tween-80 diluted in 1xPBS. Receptor antagonists were administered via i.p. injection at a volume of 0.1 mL/mouse 1 hour prior to each THC treatment. Vehicle control groups received ethanol (EtOH) or DMSO diluted in 1xPBS to a similar concentration as treatment groups.

Monoclonal Antibodies, Reagents, and Flow Cytometer-

Antibodies used for flow cytometric analysis (BioLegend) included: Fc block (93), FITC conjugated anti-H-2^b (KH95), PE conjugated anti-H-2^k (15-5-5), Alexa Fluor 488 conjugated anti-CD3e (145-2C11), PE/Cy7 conjugated anti-CD4 (GK1.5), PE conjugated anti-CD8a (53-6.7), PE/Cy7 conjugated anti-CD25 (PC61), PE/Cy5 conjugated anti-CD28 (37.51), PE/Cy5 conjugated anti-CD44 (IM7), PE conjugated anti-CD69 (H1.2F3), PE conjugated anti-Gr1 (RB6-8C5), and FITC conjugated anti-CD11b (M1/70). HvGD IngLN and peritoneal exudates were assessed by flow cytometric analysis. Briefly, IngLN cells (10^6 cells in 25 µL) from BL6 recipient mice were incubated with Fc receptor antibodies (5-10 minutes) and incubated with conjugated antibodies (20-30 minutes at 4°C). After incubation with conjugated antibodies cells were washed twice with 1xPBS/2% fetal bovine serum buffer. The stained cells were then assessed by flow cytometer (FC500; Beckman Coulter) and the resulting data analyzed by Cytomics CXP software (Beckman Coulter). All flow cytometer plots were gated on live cells only.

Two-color flow cytometric analysis was performed for assessing persistence of donor H-2^k cells in the recipient IngLN, spleen, and peritoneal exudates. Three-color flow cytometric analysis was used to profile the IngLN response to disease and treatment. Two-color flow cytometric analysis was used to look for myeloid derived suppressor cell (MDSC) populations in the peritoneal exudate.

Cytokine and Chemokine Analysis-

ELISA MAX sandwich enzyme-linked immunosorbent assay (ELISA) kits (BioLegend) were used to assess the level of IFN-γ, TNF-α, MCP-1, IL-2, and IL-6 cytokines. Sandwich ELISA kit for G-CSF (Abcam) was also used. Cells from the inguinal lymph nodes (IngLN, $5x10^6$ cells/mL) from HvGD mice were cultured in 0.2 mL aliquots in 96-well round bottom tissue culture plates for 16-20 hours. To assess MCP-1 and G-CSF levels in the peritoneal exudate, a 1 mL of 1xPBS lavage was collected as described previously (164). Cytokine production was quantified from cell supernatants (stored at -20°C). Absorbance was measured at 450 nm using a Victor2 1420 Multilable counter (Wallac).

Thymidine Analysis of Ex Vivo Proliferation due to Allograft Restimulation-

Lymph node cells from HvGD BL6 mice collected 10 days after treatment with THC injection, were cultured in triplicate (0.2 mL/well in a round bottom 96 well plate) with mitomycin C-inactivated C_3H spleen cells, for 4 days. Sixteen hours before collection and analysis [^{3}H] thymidine (2 µCi/well) was added to the cell cultures. The radioactivity was measured using a liquid scintillation counter (MicroBeta Trilux).

MDSC Isolation-

Sixteen hours after THC injection, mice were euthanized and the peritoneal exudate collected (86). Briefly, the peritoneal cavity was washed 3x with ice cold 1xPBS (5 mL per wash) for 5 minutes with agitation to recover cells. The cells were resuspended in 1 mL then treated with Fc block for 10 minutes and labeled with PE-conjugated anti-Gr1. The +EasySep positive PE selection kit procedure was followed to isolate Gr1 positive cells, as described previously (105). After isolation cells were labeled with FITC conjugated anti-CD11b and assessed for purity using flow cytometeric analysis.

MDSC Depletion Assay-

MDSCs were depleted by the i.p. injection of Ly-6G/Ly-6C purified antibody (RB6-8C5), as described (165). Depletion antibody was given three hours after every other THC treatment in doses of 0.1 and 0.05 mg/mouse. Control mice received isotype matched control Abs. Mice were euthanized at the end of the 5 day model as outlined previously. Peritoneal exudates were assessed for the presence of MDSCs and H-2^k cells and IngLN were assessed for cellularity and T cell activation.

MDSC Adoptive Transfer-

Isolated THC induced MDSCs ($5x10^6$), greater than 95% pure as described earlier (56), were transferred into BL6 HvGD mice via an i.p. injection 30 minutes after subcutaneous injection of graft cells. Mice were euthanized 18 or 90 hours after graft injection. Peritoneal exudates were assessed for the presence of MDSCs and MDSC chemokines, MCP-1 and G-CSF, and IngLNs were assessed for cellularity and T cell populations.

Dual Skin Allograft Transplant-

We performed dual skin grafts on each recipient mouse; one allograft (right graft bed) and one autograft (left graft bed). First, graft skin was obtained from the tail of a C_3H donor mouse and transferred into the recipient mice, either BL6 or F1. Secondly, tail skin grafts from autologous donor mice were transplanted on to the recipient mice, either BL6 donor to BL6 recipient or F1 donor to F1 recipient. Recipient mice were treated with THC, or vehicle, 2 hours prior to the skin graft procedure. Mice were kept in protective casts for 9 days following the graft procedure (166). Grafts were assessed for rejection starting on day 9 after graft placement. Treatment of either THC or vehicle was given i.p. every other day for 14 days, and after this point, all treatments were stopped. For assessment of CB1 receptor involvement, the pharmacological antagonist SR141716A was given (20 mg/kg) i.p one hour prior to each THC treatment. Mice were scored as +/+ accepted graft, +/- partially rejected graft (less than 50% scabbed over or less than a halving in graft size), or -/- fully rejected graft. For depicting graft survival +/+ and +/- skin grafts were considered viable and -/- skin grafts were nonviable.

Statistical Analysis-

HvGD experiments ($n \geq 4$ mice per treatment group) were repeated 2 or more times to ensure repeatability. Skin graft experiments were run in triplicate ($n > 7$ mice was used for statistical analysis). Data are shown as mean ± S.E.M. Student's t Test was used to compare data between two groups. One-way ANOVA with Tukey post-hoc test was used to compare three or more groups. Log-rank (Mantel-Cox) test was used to determine

significance of survival curves. Experimental groups were compared to vehicle, $p < 0.05$ was considered significant.

3.3 RESULTS

THC treatment reduces lymphocyte proliferation in inguinal lymph nodes.

To determine if THC could have a therapeutic role in allograft rejection, we modified a mouse model of acute HvGD; with a strong and rapid host immune response to the graft (159). As such, the recipient mice (BL6 haplotype H-2^b) were given a bolus ($2.2x10^7$ cells) of graft (C_3H haplotype H-2^k) splenocytes subcutaneously two hours after THC (20 mg/kg body weight) or vehicle treatment (ethanol diluted in 1xPBS). Treatment was administered i.p. daily (Fig. 3.1A). Mice were assessed for symptomology of HvGD 4 days after graft injection, with T cell proliferation and Th1 associated cytokine secretion being used as markers of disease induction. The draining lymph nodes (inguinal, IngLN) were collected and assessed for T cell proliferation. The data showed that total cellularity in the IngLN in HvGD mice was significantly decreased with THC treatment from the greater than fivefold increase observed in vehicle treated HvGD mice (Fig. 3.1B). Flow cytometric analysis revealed that T cell subset (CD3+CD4+ and CD3+CD8+) proportions, were increased in vehicle treated HvGD mice compared to naive mice (Fig. 3.1 C&D). However, HvGD mice given THC treatment showed a significant reduction in both T cell populations bringing these T cell numbers back to naïve levels (Fig. 3.1 C&D).

THC treatment suppresses secretion of pro-inflammatory cytokines.

Previously our lab group has shown that THC treatment can reduce cytokines and

chemokines associated with inflammatory disease models (76, 84). As HvGD is known to be accompanied by increases in Th1 associated cytokines, the impact of THC treatment on the pro-inflammatory environment in the IngLN of HvGD mice was assessed. Cytokines well known for their involvement in transplant rejection include IFN-γ and IL-2, which are typically expressed at high levels early after receipt of the graft, TNF-α, which increases as HvGD progresses, and IL-6, which plays a role in graft tolerance by skewing the Th1/Th2 balance (59). To this end, the IngLN from THC or vehicle treated (ethanol diluted in 1xPBS) HvGD mice were collected, 4 days after the injection of graft cells, and cultured for 24 hours to assess spontaneous cytokine secretion in the draining lymph node microenvironment . IL-2, a cytokine known to increase T cell proliferation and IFN-γ, which is associated with cytotoxic T lymphocyte (CTL) killing, were elevated in vehicle treated mice with HvGD but reduced by nearly 50% upon THC treatment (Fig. 3.1E left). Additionally, TNF-α and IL-6 (Fig. 1E) were over-expressed in vehicle treated HvGD mice; however, a significant reduction was seen in THC treated mice. To ensure that THC treatment was in fact targeting the HvGD T cell response rather than ablating naïve T cell function, mice were treated with THC alone, as a control. Cell counts in the IngLN (Fig. 3.1B), absolute numbers of CD3+CD4+ and CD3+CD8+ cells in the IngLN (Fig. 3.1 C&D), as well as cytokines (Fig. 3.1E) in mice treated with THC alone were not changed significantly when compared to naïve mice. Thus, in subsequent experiments, we primarily compared HvGD+Veh versus HvGD+THC groups.

Inguinal lymph node activation is decreased by THC administration.

One hallmark of HvGD is that a second transplant with the same haplotype

disparity will be rejected by the host more rapidly than the initial graft. To determine if THC could favorably impact this outcome of allograft rejection, HvGD mouse IngLN were restimulated *ex vivo*. HvGD mice treated with either vehicle (ethanol diluted in 1xPBS) or THC were rested for 10 days, from the time of the last treatment injection, and then restimulated with C_3H splenocytes. Proliferation due to restimulation was assessed using [^{3}H] thymidine incorporation. Mice given vehicle treatment showed significantly increased rates of proliferation compared to THC treated mice (Fig. 3.2A). Having found that *ex vivo* restimulation was decreased in THC treated HvGD mice, we next looked at the number of FasL expressing cells in the IngLN. We found that significantly fewer cells expressed FasL (Fig 3.2B upper) and that the number of active T cells expressing the Fas receptor (Fas) was also significantly reduced (Fig. 3.2B lower) in THC treated HvGD mice. Additionally, T cell activation markers were analyzed to ascertain how THC affects proliferation rates after treatment. To this end, IngLN were collected 4 days after graft cell injection from both vehicle and THC treated mice, and evaluated for cells positively expressing activation markers. Expression of CD25, which is found on memory T cells and is part of the IL-2 receptor, CD28, a necessary co-stimulatory molecule that interacts with CD80/86 on APCs, and CD69, an early activation marker, were assessed in HvGD IngLN by flow cytometry. HvGD mice treated with THC had significantly fewer CD25+, CD28+, and CD69+ cells in the IngLN than did the vehicle treated mice (Fig. 3.2C).

THC decreases the inflammatory response allowing for H-2^k graft cell persistence.

In HvGD, the final step in graft rejection is apoptosis of the graft cells caused by CTLs and natural killer (NK) cells (167). Since THC treatment caused a reduction in the

number and proportion of CD3+CD8+ cells and FasL expression, H-2^k positive cells were evaluated to determine if treatment extended the life of the graft cells. The draining IngLN, spleen, and peritoneal cavity were selected as possible sites of graft cell persistence. While no cells positive for H-2^k were found in vehicle treated (ethanol diluted in 1xPBS) HvGD mice (Fig. 3.2D) allograft cells were detected in the peritoneal cavity of THC treated HvGD mice (Fig. 3.2D). The H-2^k+ cells were measurable in the peritoneal cavity as early as 16 hours after injection of the graft (Fig. 3.2D). To analyze whether daily THC treatments are sufficiently immunosuppressive to allow for continued persistence of the graft cells, the peritoneal exudate was monitored at 24 hour intervals. Interestingly, H-2^k+ cells persisted for the entire 90 hour duration of THC treatment (Fig. 3.2E).

THC treatment induces suppressive MDSCs in HvGD mice.

Our laboratory has shown that high levels of Gr1+CD11b+ MDSCs are induced by a single injection of THC i.p. into mice and that such cells are highly immunosuppressive (86). To test if THC injection in the current HvGD model also triggers Gr1+CD11b+ MDSCs, we harvested the cells from the peritoneal cavity, 18 hours after graft injection, and stained them for Gr1+CD11b+ expression. While HvGD+Veh (ethanol diluted in 1xPBS) treated mice showed less than 3% MDSCs, equivalent to an absolute count around $0.04x10^6$ cells and similar to naïve mice, HvGD+THC treated mice showed marked increase in Gr1+CD11b+ MDSC, the proportion of which increased to 75%, or $3.2x10^6$ cells, at 18 hours and dropped to 46%, or $2.4x10^6$ cells, at 90 hours (Fig. 3.3A). As many immature myeloid cells express the cell surface markers Gr1 and CD11b we looked at the T cell suppressive property of

these double-positive cells to ensure that they were indeed MDSCs (97); (98). Next, the Gr1+CD11b+ MDSCs from the peritoneum of THC treated HvGD mice, isolated at 18 hours, were purified (greater than 95% purity Gr1+CD11b+ cells) using positive selection based on expression of Gr1, as described earlier (56). Isolated MDSCs were co-cultured, at various concentrations, in a mixed leukocyte reaction (MLR) with BL6 IngLN as responders and C_3H spleen cells treated with mitomycin C, as stimulators (1:8 ratio). Proliferation of the BL6 IngLN cells was measured using thymidine incorporation. Gr1+CD11b+ MDSCs (from here on denoted as MDSCs) significantly reduced T cell proliferation in a dose-dependent manner (Fig. 3.3B).

Due to the fact that MDSC induction has been associated with inflammatory disease, we next set out to show that THC treatment, and not the disease model, was driving MDSC recruitment (168); (169); (170). Previous studies from our lab demonstrated that cannabinoid receptor ligand treatment increases the level of MCP-1 (CCL2), which has also been associated with an increase in MDSCs at the tumor site (75); (171). Additionally, we looked at G-CSF which in our lab has previously been shown to be elevated in THC-mediated MDSC induction (86). To this end, the peritoneum exudate was collected, with a single lavage of 1 mL 1xPBS, and assessed for cytokine and chemokine levels. We found MCP-1 and G-CSF were elevated only in THC treated HvGD mice (Fig. 3.3 C&D respectively).

THC induced MDSCs play an integral role in in the amelioration of HvGD.

To determine the importance of MDSCs in reducing overall HvGD symptomology, we used the anti-Ly-6G/Ly-6C purified antibody (RB6-8C5) to deplete

Gr1+ MDSCs. The depletion antibody was given 3 hours after every other THC treatment in decreasing doses of 0.1 and 0.05 mg/mouse. The IngLN cellularity for CD3+CD4+ (Fig. 4A) and CD3+CD8+ (Fig. 3.4B) T cells was significantly increased in HvGD mice, which was decreased following treatment with THC and control Ab. Interestingly, HvGD+THC mice that received anti-Ly-6G/Ly-6C Ab showed reversal of THC effect resulting in increased numbers of T cells (Fig. 3.4 A& B). Additionally, the impact of MDSC depletion on T cell activation markers including CD25, CD28, and CD44 was assessed. Upon treatment with anti-Ly-6G/Ly-6C Ab, we saw a significant increase in cells positive for the CD25, CD28, and CD44 activation markers (Fig. 3.4C). To ensure that RB6-8C5 depleted the MDSCs, Gr1+CD11b+ cells in the peritoneal cavity were analyzed. RB6-8C5 caused a stark decrease in MDSC proportion in THC treated HvGD mice from 67% to about 11% (Fig. 3.4D). Finally, RB6-8C5 administration along with THC treatment resulted in a significant decrease in the number of H-2^k+ cells in the RB6-8C5 group consistent with a decrease in allograft persistence (Fig. 3.4E).

Because MDSC depletion decreased the efficacy of THC treatment in HvGD mice, we tested if adoptive transfer of THC-induced MDSCs into allograft recipient mice would suppress HvGD. MDSCs were isolated from THC treated mice 18 hours after treatment as outlined previously. Isolated THC-induced MDSCs ($5x10^6$), at greater than 95% purity, were then transferred into BL6 HvGD mice via an i.p. injection 30 minutes after subcutaneous injection of graft cells. Adoptively transferred mice were assessed for IngLN cellularity and T cell populations four days after the injection of graft cells. We noted that transfer of MDSCs suppressed the HvGD as indicated by the total number of cells (Fig 3.5A) as well as CD3+CD4+ and CD3+CD8+ T cell subsets (Fig 3.5B),

although to a lesser extent than THC. Additionally, we looked at the peritoneal exudate for MDSC persistence as well as MDSC homing cytokine levels (18 hours after graft cell injection). When the peritoneal exudate was enumerated for Gr1+CD11b+ cells in MDSC transferred HvGD mice, we found that there were significantly reduced numbers of MDSCs in the peritoneal cavity compared to the THC treated group (Fig. 3.5C). In corroboration with reduced overall cellularity within the peritoneum, the proportion of persisting H-2^k+ cells was reduced by 50% in MDSC treated compared to THC treated HvGD mice (data not shown). In addition, MCP-1 and G-CSF were undetectable in mice adoptively transferred with MDSCs when compared to those exposed to THC which showed very high levels (Fig 3.5 D&E). These data showed that adoptively transferred MDSC may be less effective because they may not be able to survive or home.

THC-mediated reduction of HvGD occurs in a CB1 dependent manner.

Immune cells express both CB1 and CB2 receptors, as such specific antagonists were used *in vivo* to ascertain whether THC was working preferentially through activation of CB1, CB2, or both receptors (13); (78); (28); (75). BL6 mice were treated with CB1 or CB2 receptor antagonist (SR141716 or SR144528 respectively at 20 mg/kg i.p.) one hour prior to each THC treatment. As seen earlier, HvGD+THC mice showed decreased absolute cellularity of the IngLN when compared to HvGD+Veh (DMSO+20 µL Tween-80 diluted in 1xPBS) mice. Interestingly, HvGD+THC+CB1 antagonist treated mice but not HvGD+THC+CB2 antagonist treated mice showed a reversal in IngLN cellularity when compared to HvGD+THC mice, thereby suggesting that THC was acting through CB1 but not CB2 receptors (Fig. 3.6A). To further corroborate that the CB2 receptor was not involved, we used another CB2 receptor antagonist (AM630)

(14), and found that this antagonist was also not able to reverse the effect of THC on HvGD (Fig. 3.6B). As confirmation that THC was working through the CB1 receptor, CB1 KO mice were incorporated into the HvGD model as recipients. Thus, we induced HvGD in BL6 wild-type and CB1 receptor KO mice and treated them with THC. The data indicated that THC treatment did not reduce IngLN cellularity in HvGD mice with a nonfunctional CB1 receptor compared to THC treated wild-type HvGD mice (Fig. 3.6C). Next, we studied MDSC induction in wild-type, CB1 KO, or CB2 KO allograft recipient mice and found that the proportion of MDSCs in the peritoneal exudate was 84%, in wild type BL6 mice, while CB1 KO mice had 25%, and CB2 KO mice had 63% (Fig. 3.6D). Looking not only at MDSC proportion but also absolute cell counts we also noted a significant reduction from CB1 but not CB2 KO mice, $8.6x10^6$ and $17.1x10^6$ cells respectively, when compared to wild-type mice which averaged $16.2x10^6$ peritoneal exudate MDSCs (Fig. 3.6E).

THC significantly extends life of allogenic skin grafts.

While all of the data shown above indicated that THC can suppress HvGD, we next tested directly whether THC treatment could reduce rejection of complete haplotype mismatched skin allografts. To this end, tail skin from donor C_3H mice, kept in place on the recipient mouse using a compression cast in lieu of sutures, acted as a complete mismatch allograft (166). The cast was removed after nine days. Allograft rejection was assessed daily starting on day 9 after transplant, 1 hour after cast removal. Mice were treated with either THC or vehicle (ethanol diluted in 1xPBS) every other day for 14 days via i.p injection as described earlier. The data showed that the skin allograft survival curve for THC treated BL6 recipient mice, mean survival >12 days, was significantly

extended compared to vehicle-treated mice, mean survival <10 days (Fig. 3.7A). Axillary and brachial LNs, from the skin transplant mice, were restimulated with mitomycin C treated C_3H splenocytes, *ex vivo*, and proliferation analyzed using thymidine incorporation. THC treated skin graft recipient mice showed significantly less proliferation than did vehicle treated graft mice (Fig. 3.7B). In order to show that the protective effects of THC on the skin allograft were not specific towards one MHC haplotype, we moved our dual graft model into B6D2F1/J mice which have a different haplotype disparity H-$2^{d/b}$ than BL6 mice when compared to the H-2^{k} allograft. We again found that THC treatment was able to significantly extend the skin allograft survival curve, mean survival =12 days, compared to vehicle treatment, mean survival <10 days (Fig. 3.7C). Furthermore, having shown that CB1 receptor function was integral in reducing the inflammatory response to allograft cells we used the antagonist (SR141716A) along with THC treatment in the BL6 skin graft model. A significant reduction in the life of the skin graft was observed upon pharmacologically blocking the CB1 receptor, mean survival <11 days, compared to THC treatment without CB1 receptor antagonist, mean survival =14 days (Fig. 3.7D).

3.4 DISCUSSION

While the immunosuppressive properties of THC have been well elucidated, whether THC can be used to prevent allograft rejection has not been previously studied (172). Recently, we suggested that activation of cannabinoid receptors may provide a novel approach to prevent transplant rejection (158). THC has been found to affect nearly every aspect of cellular immunity including T cells, natural killer cells, macrophages, neutrophils, mast cells, and B-cells (as reviewed throughout the years

(155); (173); (174); (175); (77); (3, 155). It has also been established that THC can impact the biasing of T cell differentiation from Th1 to Th2 (154); (176); (177); (88)). Moreover, THC can also induce immunosuppressive cells such as MDSCs and Tregs (86); (88); (78)). Thus, it is worth investigating if THC can suppress allograft rejection.

In the current study, we found that THC-induced MDSCs may play a critical role in suppressing allograft rejection. This was evident from experiments using the antibody, RB6-8C5, which depleted the MDSC *in vivo* and caused a reversal of the ability of THC to ameliorate HvGD. THC-induced MDSCs suppressed the T cell proliferation against the allogeneic cells *in vitro*. Furthermore, adoptive transfer of THC-induced MDSCs into HvGD mice caused significant suppression of HvGD response. Together, these data provided strong support to the fact that THC may suppress allograft rejection through induction of MDSCs. Our laboratory has shown previously that THC treatment triggers rapid and massive induction of MDSCs in naïve mice after a single dose (86). While MDSCs were first associated with cancer as part of the tumor microenvironment which decreased T cell based anti-tumor immunity and increased tumor progression, recent studies have indicated that MDSCs may also be induced at sites of inflammation (57, 178); (179). The suppressive functionality of MDSCs is most commonly attributed to the release of Arg-1 or iNOS (58). THC-induced MDSCs have been shown to be suppressive to T cell proliferation in response to both polyclonal and antigen-specific stimuli (86). The importance of MDSCs in creating tolerance in grafts was shown recently through the adoptive transfer of LPS-induced MDSCs i.v. (60). The transfer of MDSCs delayed the rejection of minor antigen disparity, HY, skin grafts (60). MDSCs were also present in

tolerated grafts including MHC-mismatched kidney transplants in rats (98). Additionally, the suppressive function of MDSCs was deemed vital, as MDSCs unable to produce Arg-1 via IL-13 treatment were less effective, in ameliorating GvHD in lethally irradiated BALB/c mice (180). However, adoptive transfer of MDSCs was not sufficient to cause graft persistence in fully mismatched antigen disparity (60). In the current study, we found that the adoptive transfer of THC-induced MDSCs, suppressed the immune response in the LN of mice with HvGD and reduced the total numbers of cells, including CD3+CD4+ T cells and CD3+CD8+ T cells, although this was not as effective as administration of THC alone. These data suggested that MDSCs, at least in part, play a role in THC-mediated suppression of allogeneic response in the recipient. THC may be more effective *in vivo* because immunosuppression can be induced through additional mechanisms such as induction of Tregs, switch from Th1 to Th2 , apoptosis in activated T cells , and suppression of cytokines (88); (78); (154); (176); (80); (181); (84). Alternatively, treatment with MDSCs may not be as effective because the cells may not be able to maintain an immature, and therefore suppressive, phenotype after adoptive transfer or may not migrate to the grafted site to mediate suppression unlike those MDSCs directly induced by THC. We concluded this was due to lack of MDSC homing cytokines, such as MCP-1 and G-CSF, which are necessary for MDSC migration and retention of suppressive capabilities (182). The findings of De Wilde et al., which show that MDSCs are directly involved in tolerance lend credence to our findings that THC, a known MDSC inducer, reduces HvGD symptomology, attenuating acute transplant rejection (60).

In the current study, we noted that THC-mediated effect on allograft response was

regulated through CB1 rather than CB2 receptors. Recently, a study looking at Mixed Lymphocyte Reaction (MLR) *in vitro* found that the CB2 receptor was necessary for THC induced T cell suppression (183). The findings of Robinson et al showed a CB2 dependent decrease in IL-2 production however the role of MDSCs was not assessed in the study (183). We found that THC was able to significantly reduce the *in vivo* proinflammatory response, including T cell activation and proliferation, to allograft in wildtype BL6 mice with functional CB1 and CB2 receptors. However, when the functionality of the CB1 receptor was compromised, either by genetic knock out or pharmacological blockade, THC was less effective in inhibiting the proinflammmatory response including T cell proliferation. In contrast, a loss of CB2 receptor function had little to no impact on THC mediated immunosuppression. The observation that CB1 activation was necessary for HvGD amelioration was explained in part when the role of cannabinoid receptors in MDSC induction was observed. We showed that THC mediated induction of MDSCs, in this model, was dependent on a functional CB1 receptor. Additionally, THC-mediated shift in T cell differentiation from Th1 to Th2 has recently been found to involve both the CB1 and CB2 receptors (154). Newton et al. found that the shift was due to the CB1-dependent decrease in IL-12Rβ1 binding and a CB2-dependent increase in GATA-3 expression (154). Together, CB1 and CB2 activation creates a simultaneous drop in IFN-γ and rise in IL-4. The role of CB1 in T cell differentiation brings to light the often overlooked involvement of this receptor with peripheral immune cells. While CB2 is expressed at higher levels in naïve immune cells, CB1 expression has been found to be elevated upon activation, specifically in T cells (34, 184). Furthermore, THC treatment of T cell lines, in lieu of activation, resulted in

elevated CB1 levels (185). Together these findings support our claim that THC is working in a CB1 receptor dependent manner.

In the current study, we found that THC treatment in HvGD mice led to significant suppression of proinflammatory cytokines. In particular THC significantly reduced the secretion of IL-2, IL-6, and IFN-γ which are associated with the loss of graft function and ultimately lead to allograft destruction. Our lab has reported that THC treatment in an autoimmune hepatitis model can reduce both TNF-α and IL-6 levels in serum (76). Furthermore, THC treatment led to reduced IL-2 and IFN-γ secretion in ConA activated splenic T cells (186). In addition to reducing proinflammatory cytokines, necessary for T cell proliferation, THC can also reduce the expression of receptors necessary for T cell activation. We found that THC was able to significantly reduce the number of cells expressing CD25, CD28, CD69, and CD44 co-stimulatory and activation markers in HvGD mice. Additionally, THC treatment brought the expression of these T cell activation receptors to levels not significantly different from naïve mice. It has been shown that the co-stimulator ICOS, expression and transcription, can be down regulated via THC treatment of anti-CD3/CD28 stimulated CD4+ splenic T cells (187). Cannabinoid receptor binding has also been found to inhibit T cell activation through co-stimulator interference. Focusing on the role of APCs in T cell activation, a recent study found that heat-stable antigen expression was decreased on macrophages upon THC treatment resulting in extended T cell unresponsiveness (103). Furthermore, CD28 blockade is known to play a major role in tolerance, though not sufficient to prevent graft rejection. While there has been no direct evidence which ties THC to the depletion of the co-stimulatory molecule CD28, it is known that THC treatment inhibits pathways

associated with CD28 binding (139). CD28 activation is involved in PI3K/AKT and NF-κB proliferative pathways. Binding of CD28 to PI3K, PKC-θ, or Grb2 have all been suggested as NF-κB activation regulating pathways (188). NF-κB activation is important in graft rejection as recent literature shows that impaired NF-κB activation can be correlated to skin graft tolerance (189). The fact that PI3K subunit p110δ is upregulated in transplanted HY-mismatched heart graft tissue suggests that the CD28/PI3K/NF-κB pathway could be integral in rejection (190). It has been known for some time that THC treatment inhibits NF-κB DNA binding, and that high levels of IL-10 can suppress PI3K binding of CD28 (139); (191). The research reported here acts as a bridge to these concepts. Additionally, reduced CD28 co-stimulation, as well as THC treatment, has been implicated in the development of anergy in mouse lymphocytes (192); (193). As such, we suggest that THC treatment; induces an increase in Th2 cytokines which inhibit CD28 binding thereby reducing NF-κB and allowing for graft tolerance.

Together, the current study shows for the first time that cannabinoid receptor-ligand system may play a critical role in allograft rejection. THC treatment reduced the T cell response in the host by dampening the secretion of pro-inflammatory cytokines and expression of T cell activation markers. Additionally, THC treatment resulted in delayed graft destruction even in a major histocompatibility complex disparity model of allogenic skin transplant. Induction of highly immunosuppressive MDSCs following THC treatment proved to be necessary, at least in part, for THC-mediated attenuation of allograft rejection. We also noted that this effect of THC was dependent on activation of CB1 rather than CB2 receptors. The current study sets the stage for additional studies on the cannabinoid system in regulating transplant rejection involving potential

manipulation of endocannabinoids, receptors, as well as use of cannabinoid receptor select agonists that are not psychoactive.

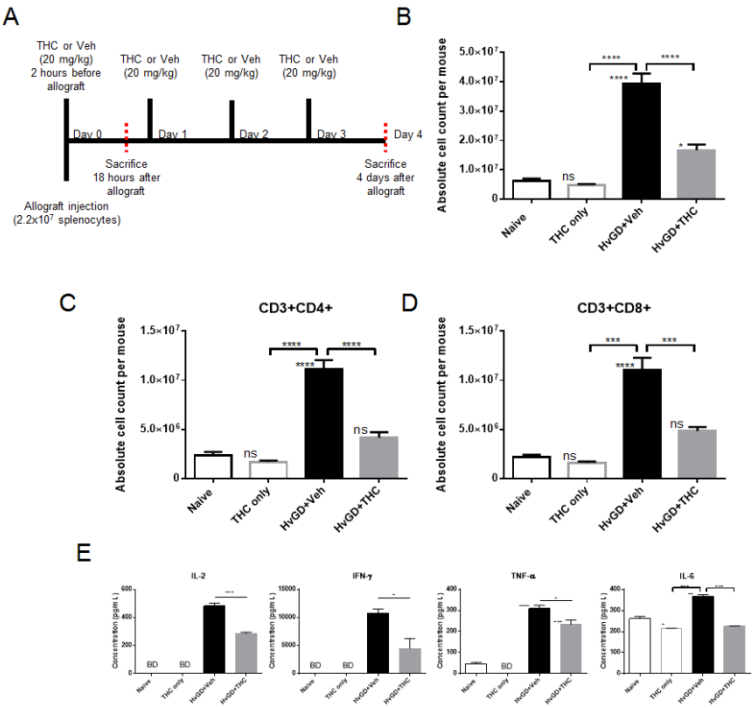

Figure 3.1: THC treatment ameliorates HvGD.

C57BL/6 (BL6) mice were given THC or vehicle, ethanol diluted in 1xPBS, (n=5 mice per group) 2 hours prior to graft cells (C_3H $2.2x10^7$ subcutaneously) and daily after graft injection until sacrifice. On day 4 after allograft injection, T cell populations were assessed by harvesting draining inguinal lymph nodes (IngLN) and then triple-staining the cells with fluorochrome-labelled antibodies against CD3, CD4, and CD8 antigens. IngLN cells, collected on day 4 after allograft injection, were also cultured for 24 hours and supernatants harvested to assay the spontaneously produced Th1 cytokines. (A) Schematic of procedure and treatment regimen. (B) Absolute cell count in the IngLN. (C-D) Absolute number of CD3+CD4+ (C) and CD3+CD8+ (D) cells in the IngLN. (E) Spontaneous secretion of IL-2, IFN-γ, TNF-α, and IL-6. Representative data of 3 experiments shown (mean ± S.E.M). * $p < 0.05$, ** $p < 0.01$, *** $p < 0.005$, **** $p < 0.0001$ Student's t test.

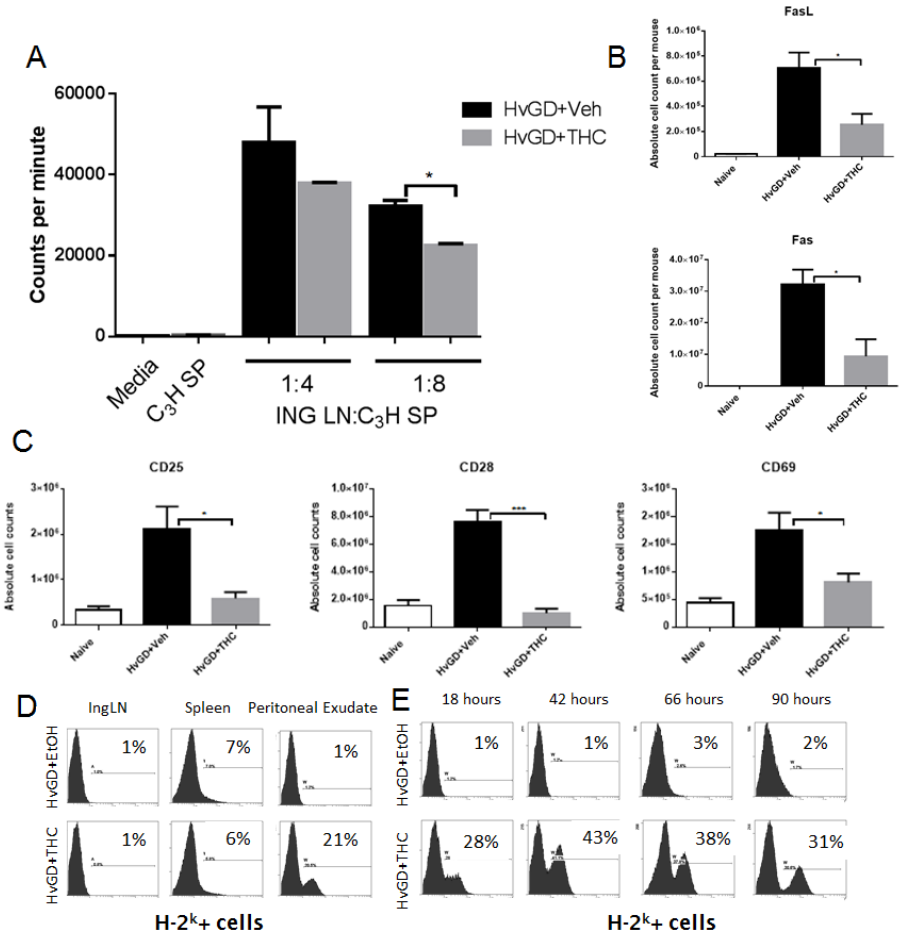

Figure 3.2: THC treatment reduces lymphocyte activation in the recipient mice and allows for allograft persistence.

IngLNs were harvested from BL6 HvGD mice (n=5 mice per group) 10 days after final THC treatment, day 14 after allograft injection. Next, IngLNs were harvested and *restimulated in vitro* with donor C_3H spleen cells (mitomycin C inactivated). Proliferation of IngLN cells was assessed 4 days after *in vitro* restimulation using [^{3}H] thymidine. IngLN activation status was determined 4 days after allograft injection by individually staining the cells for antibodies against CD25, CD28, and CD69 antigens. (A) C_3H restimulation in vehicle, ethanol diluted in 1xPBS, and THC-treated HvGD mice (data shown as mean ± S.E.M). (B) T cell activation marker expression, CD25, CD28, and CD69 on IngLN cells (similar results seen in two replicate experiments). (C) H-2^k cell persistence in recipient mice. (D) H-2^k cell persistence in the peritoneal cavity throughout the five days (similar results seen in replicate experiments). * $p < 0.05$, ** $p < 0.01$, *** $p < 0.005$, **** $p < 0.0001$ Student's t test.

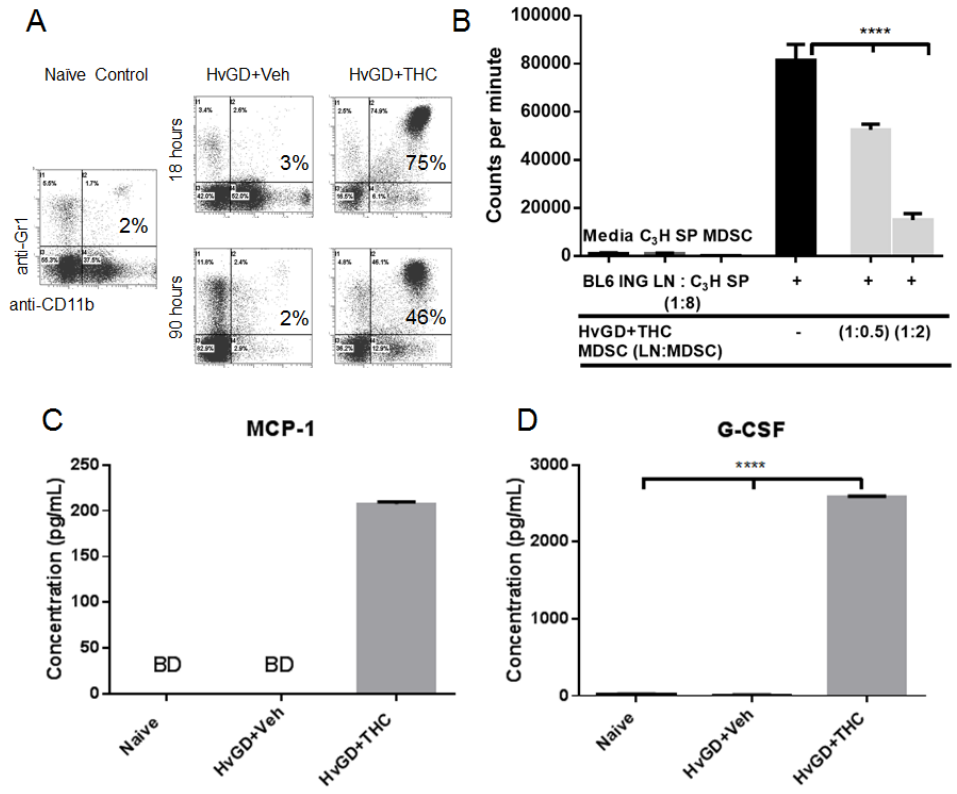

Figure 3.3: THC treatment induces immunosuppressive MDSCs.

Cells were isolated from peritoneal exudates (n=5 mice per group) either18 or 90 hours after graft injection, and stained for Gr-1 and CD11b stained to identify MDSCs, MDSCs were also isolated using positive selection PE-magnetic beads for Gr1. C_3H cells and MDSCs were mitomycin C inactivated prior to plating with BL6 IngLN cells. Proliferation of IngLN cells was assessed 4 days after MLR stimulation using thymidine. (A) Gr1+CD11b+ MDSCs in the peritoneal cavity, at 18 and 90 hours after graft cell injection, (similar results seen in replicate experiments). (B) MDSC suppression of MLR against C_3H cells ($p<0.01$, one-way ANOVA and Tukey HSD post-hoc test). (C, D) Peritoneal exudates were collected 18 hours after graft injecion (1 mL ice cold 1xPBS) and assessed for MDSC homing cytokines, MCP-1 (CCL2) and G-CSF. Representative data of replicate experiments shown (mean ± S.E.M). * $p < 0.05$, ** $p < 0.01$, *** $p < 0.005$, **** $p< 0.0001$ ANOVA/Tukey.

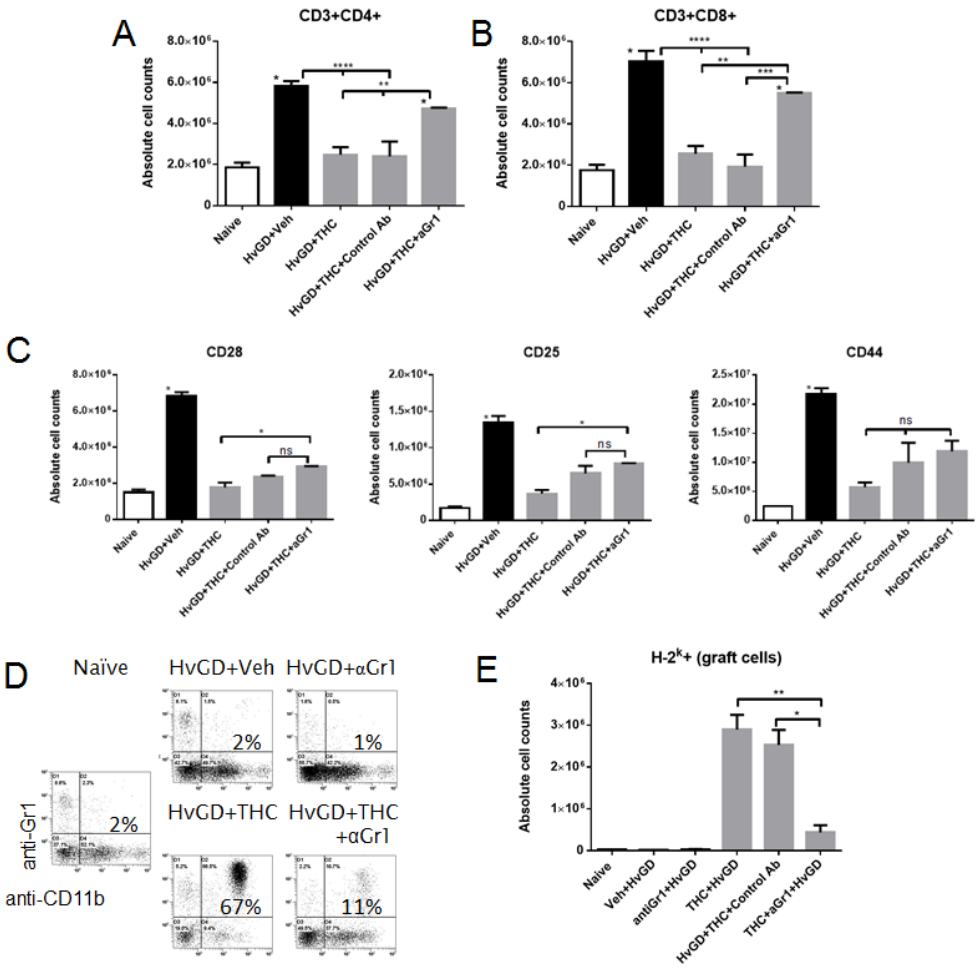

Figure 3.4: Role of MDSCs in HvGD modulation as determined via MDSC depletion.

MDSCs were depleted by i.p. injection of Ly-6G/Ly-6C purified Ab (RB6-8C5) or isotype matched control Ab (n=5 mice per group). Depletion Ab was given three hours after every other THC treatment in decreasing doses of 0.1 and 0.05 mg/mouse. Peritoneal exudates were assessed for the presence of MDSCs and donor H-2^k cells, and IngLN were assessed for cellularity and T cell activation, day 4 after graft injection. (A) Absolute cell count of CD3+CD4+ T cells in IngLN. (B) Absolute cell count of CD3+CD8+ T cells in IngLN. (C) T cell activation marker expression, CD25, CD28, and CD44 (right), on IngLN cells. (D) Proportion of MDSCs in the peritoneal cavity. (E) Allograft cell persistence at the conclusion of the five day experiment. Representative data of 3 experiments shown (mean ± S.E.M). * $p < 0.05$, ** $p < 0.01$, *** $p < 0.005$, **** $p< 0.0001$ Student's T test or ANOVA/Tukey.

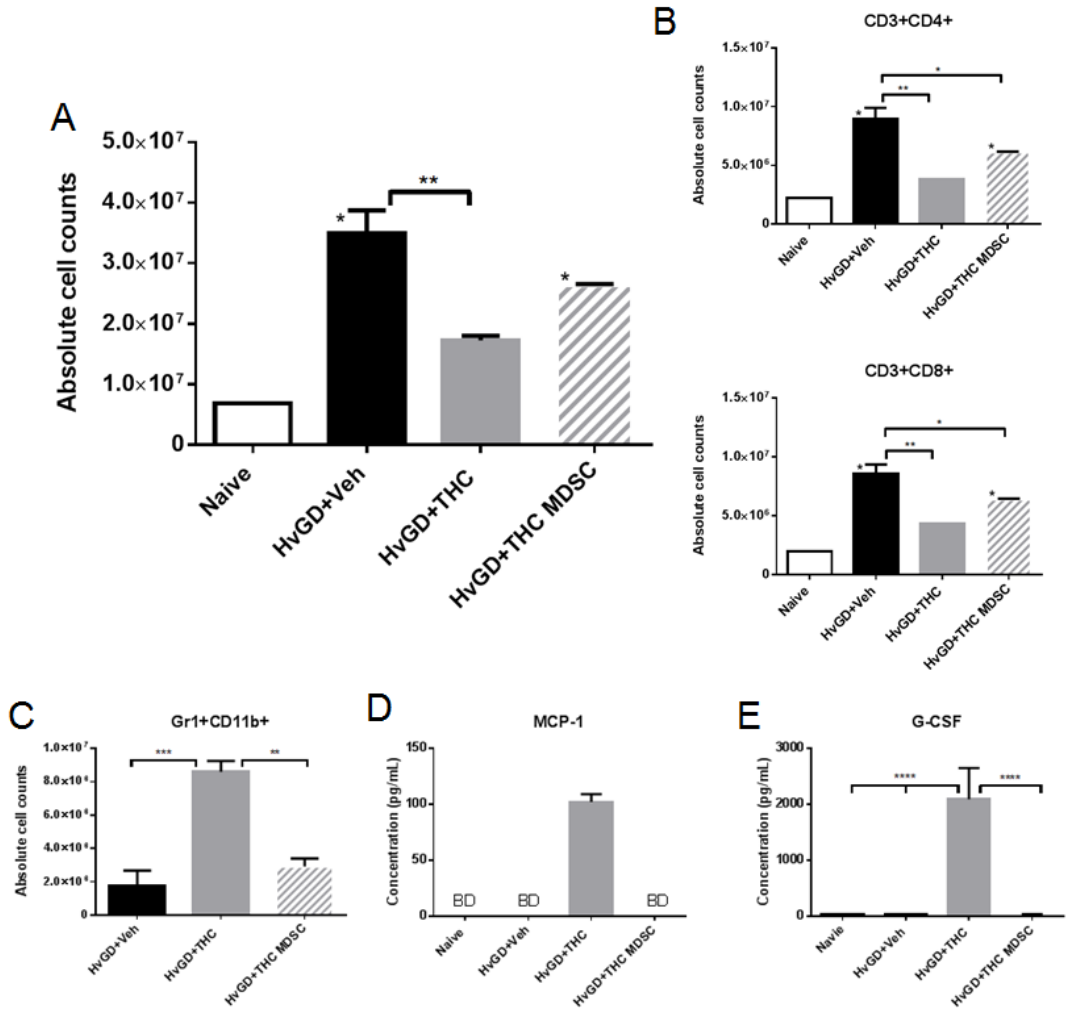

Figure 3.5: Role of MDSCs in HvGD modulation as determined via adoptive transfer.

Isolated THC induced MDSCs ($5x10^6$), greater than 95% pure, were transferred into BL6 HvGD mice (n=5 per group) via an i.p. injection 30 min after subcutaneous injection of graft cells. Mice were euthanized at two time points day 4, for IngLN analysis, and 18 hours, for peritoneal lavage analysis, after graft injection. Peritoneal exudates were assessed for the presence of MDSCs and the MDSC homing chemokines. (A) Cellularity in the IngLN. (B) T cell populations, CD3+CD4+ (top) and CD3+CD8+ (bottom), in IngLN. (C) Overall MDSC cellularity of the peritoneal cavity. (D) MCP-1 levels in the peritoneal exudate. (E) G-CSF levels in the peritoneal exudate. Similar results seen in replicate experiments (mean ± S.E.M). * $p < 0.05$, ** $p < 0.01$, *** $p < 0.005$, **** $p< 0.0001$ ANOVA/Tukey.

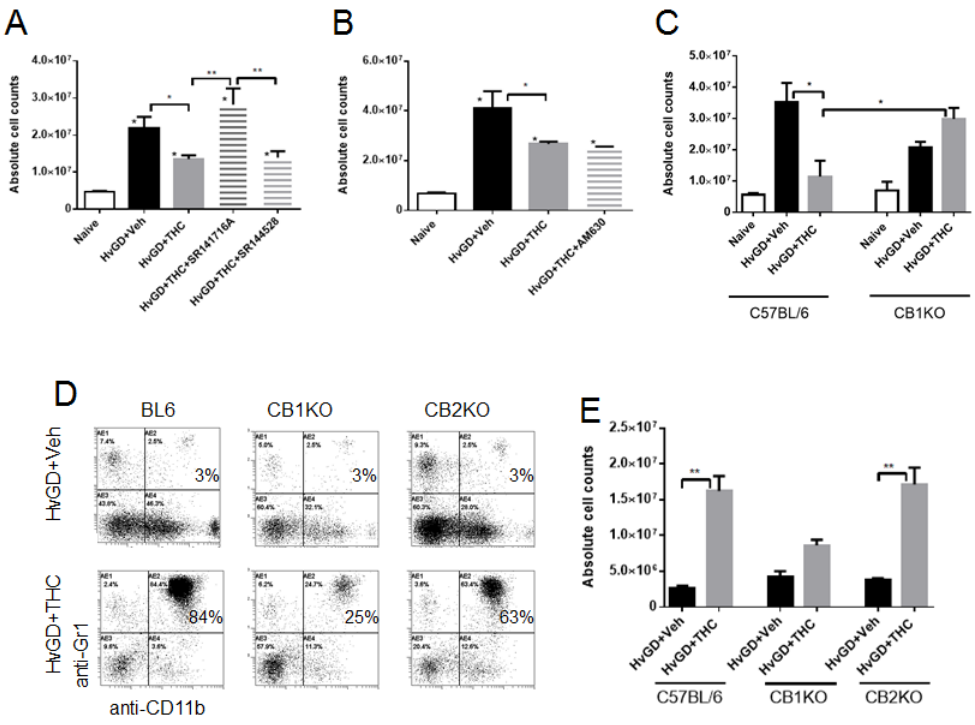

Figure 3.6: THC works through the CB1 receptor to ameliorate HvGD.

BL6 mice (n=5 per group) were given either CB1 or CB2 receptor antagonist 1 hour prior to treatment with THC or vehicle, DMSO+20 µL Tween-80 diluted in 1xPBS. (A) Absolute cellularity in IngLN, day 4 after graft injection, using CB2 and CB1 receptor antagonists, SR144528 and SR141716A respectively (data shown as mean ± S.E.M). (B) Absolute cellularity in IngLNs, day 4 after graft injection, using CB2 receptor antagonist AM630 (data shown as mean ± S.E.M). (C) Cellularity on IngLn in BL6 and CB1 KO HvGD mice, day 4 after graft injection. (D) THC induction of peritoneal MDSCs in BL6, CB1 KO, and CB2 KO HvGD mice, 18 hours after graft injection (mean ± S.E.M). (E) Absolute cell counts of peritoneal MDSCs in BL6, CB1 KO, and CB2 KO HvGD mice. * $p < 0.05$, ** $p < 0.01$, *** $p < 0.005$, **** $p < 0.0001$ Student's T test or ANOVA/Tukey.

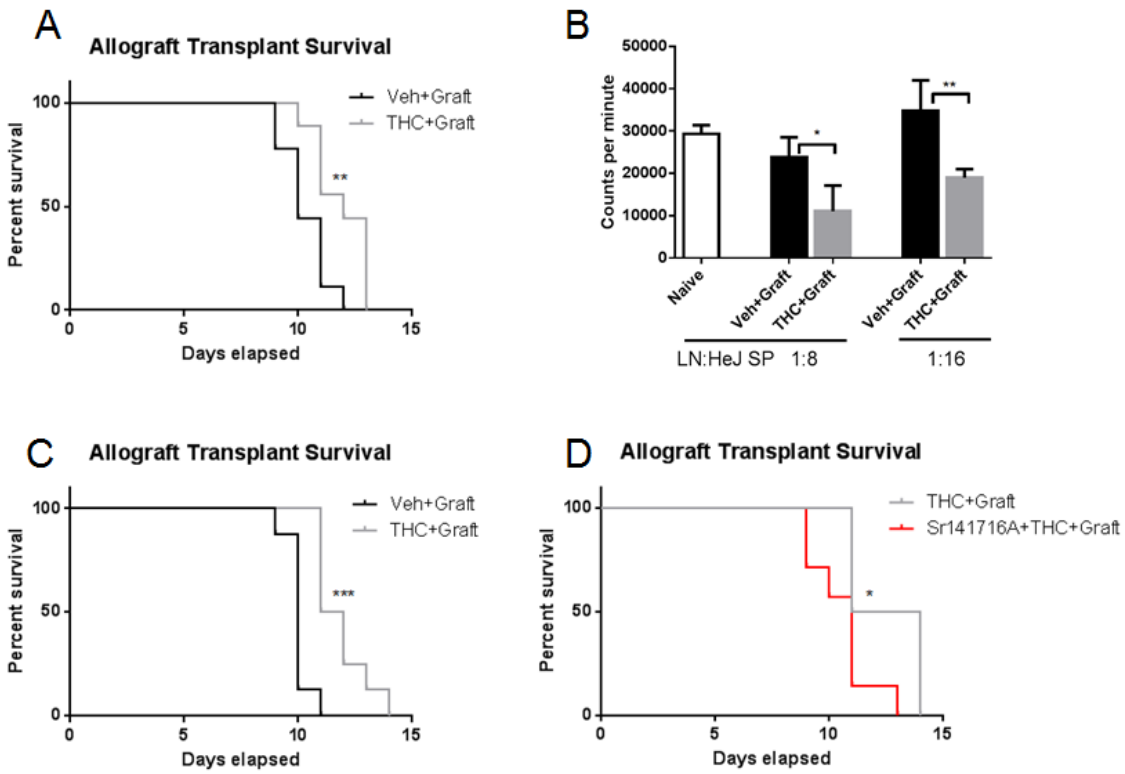

Figure 3.7: THC treatment significantly extends survival of allogenic skin grafts.

The dual skin graft method was used to include a technical control (all autograft skin transplants survived). THC treatment was given every other day for two weeks. (A) C_3H allograft on BL6 recipient mice: survival of allograft in THC and vehicle (ethanol diluted in 1xPBS)-treated mice (mean ± S.D. n=9 vehicle treated mice and an n=9 THC treated mice). (B) Skin graft rejection mice from panel A were rested ten days (from the last treatment) and then the axillary and brachial lymph nodes were restimulated *ex vivo* with C_3H splenocytes. Thymidine assay was used to determine proliferation. (C) C_3H allograft on B6DF1/J (F1) recipient mice: survival of allograft in THC and vehicle-treated mice (mean ± S.D. n=8 vehicle treated mice and an n=9 THC treated mice). (D) C_3H allograft on BL6 recipient mice survival of allograft in THC or SR141716A+THC-treated mice (mean ± S.D. n=6 SR141716A+THC treated mice; and an n=4 THC treated mice). Log-rank test (survival curves) and ANVOA/Tukey * $p < 0.05$, ** $p < 0.01$, *** $p < 0.005$, **** $p < 0.0001$.

CHAPTER IV: Δ^9-Tetrahydrocannabinol attenuates delayed type hypersensitivity via microRNA regulation of Th1 and Th17 differentiation.

4.1 INTRODUCTION

T helper cell differentiation, has classically, represented distinct T cell lineages impacted by cytokine milieu, Th1 (IL-12), Th2 (IL-4), Th17 (IL-6 and TGFβ), and T regulatory cells (Tregs- TGFβ), leading to terminally differentiated T cell subsets (51). Over the years, it has been shown that interaction between T helper cell subsets, such as Th1 and Th2, can regulate the differentiation of other T cell lineages (194); (195). While the Th1, proinflammatory, versus Th2, anti-inflammatory, responses have been clearly defined (as reviewed though the years (196); (197); (198); (199); (200) the discovery of additional proinflammatory T helper cell populations, such as Th17, has complicated our understanding of T cell interactions. Recent evidence has shown that Th1 secreted cytokines, IFN-γ and IL-2, can inhibit Th17 differentiation and that while IL-17a/f expression cannot directly inhibit the Th1 responses, elevated levels of TGFβ associated with active Th17 cells can (201); (202); (203); (204). Further muddling these proinflammatory cell interactions is the fact that Th17 and Th1 lineages may have some overlap due to immune cell plasticity and the emergence of proposed Th17/Th1 and "non-classic" Th1 lymphocytes (205); (206); (207); (208); (209).

Heritable genetic modifications, known as epigenetics, have arisen recently as the explanation for selective gene expression (35); (36). Epigenomics broadly encompasses

DNA methylation, histone acetylation and methylation, as well as microRNA (miRNA or miR) expression. Evidence now exists which highlights the influence of epigenetic modifications on immune cell differentiation and activation (38); (210); (211); (212); (88); (213). miRNA, ~20 nucleotide long strands of RNA, most commonly inhibit gene expression through the binding of mRNA sequences (40). Each miR can bind numerous targets and therefore regulate the expression of multiple genes (40). Interestingly, lineage-defining transcription factors and the downstream targets associated with T helper cell subsets have become a major focus for epigenetic modification such as miRNA binding (49); (50).

Inflammation seen in delayed type hypersensitivity (DTH), plays a critical protective role against intracellular pathogens. However, such inflammation, is often seen against innocuous non-pathogenic antigens leading to sever damage to the tissue as seen during contact dermatitis against nickel or poison ivy. Classically, DTH was considered to be a Th1 driven inflammatory disease; however treatment with anti-IFN-γ showed that such mice continue to exhibit signs of DTH (69). More recently, the importance of Th17 cells in DTH disease progression was highlighted in IL-17 knockout mice which showed significantly reduced ear swelling in an allergenic contact dermatitis model (52). Thus, depending on the antigen, it is likely that both Th1 and Th17 cells play an effector cell role.

Immune cells are well established to express cannabinoid receptors, while their precise role in the regulation of immune response remains unclear. Δ^9-Tetrahydrocannabinol (THC), one of the most well studied bioactive cannabinoids derived from the *Cannabis sativa* plant, has long been shown to reduce T cell driven

inflammation via; apoptosis, induction of immuneoregulatory cells, regulation of T helper cell cytokines, and even epigenetic modifications (79); (84); (76); (86); (154); (87); (88); (38); (214). Majority of THC research, in regards to inflammation and autoimmunity, has centered on the Th1/Th2 axis. Specifically, we and others, have found that THC treatment increases anti-inflammatory cytokines, causing a subsequent drop in proinflammatory cytokines such as IL-12, IFN-γ, and TNF-α, and reduced T cell activation (154); (186); (79); (84). THC treatment has also been found to induce Tregs which are known to inhibit both Th1 and Th17 lineage differentiation (76); (88); (215). Furthermore, THC has been found to significantly reduce cytokines associated with Th17 differentiation such as IL-6 and IL-17_a (216). Recently, our lab has found that the ability of THC to shift the immune response from proinflammatory to anti-inflammatory involves, in part, miRNA regulation (87); (88).

While cannabinoid receptor agonists can attenuate DTH, the role of THC in regulation of epigenetic modifications has not been assessed (217); (218); (83). Furthermore, the ability of THC treatment to inhibit both Th1 and Th17 differentiation within a hypersensitivity model has not been reported. With this in mind, we set out to determine if THC treatment could inhibit both Th1 and Th17 T cell lineages, in a methylated BSA (mBSA) sensitization/rechallenge model of DTH, via miRNA regulation. Our results suggest that THC can attenuate DTH response to mBSA by inhibiting both Th1 and Th17 cells through reversal of the miRNA alterations brought about during the DTH response.

4.2 MATERIALS AND METHODS

Mice-

Female C57BL/6 (BL6) mice, aged 6-8 weeks and at an average weight of 20 g, were obtained from Harlan Laboratories. All mice were housed in pathogen-free conditions and allowed ad libitum access to filtered water and Teklad rodent diet 8604 (normal chow) at the Animal Research Facility located at the University of South Carolina School of Medicine. All experiments were conducted under an approved Institutional Animal Care and Use Committee animal protocol.

Induction of delayed type hypersensitivity (DTH) and THC treatment-

DTH was induced in C57BL/6 mice using a sensitization/rechallenge method (83). Briefly, mice (n=5 per experimental group) were sensitized with a subcutaneous injection (100 µL/hind flank) of 1.5 mg/mL methylated BSA (mBSA- Sigma Aldrich) emulsified in complete Freunds adjuvant (CFA- Sigma Aldrich). Six days later, the mice were rechallenged with a footpad injection (20 µL/footpad) of 10 mg/mL mBSA in 1xPBS. Δ^{9}-Tetrahydrocannabinol (THC- NIDA-NIH) dissolved in ethanol was diluted in 1xPBS to a concentration of 20 mg/kg. THC or vehicle (ethanol diluted in 1xPBS) was administered intraperitoneally (i.p.) at a volume of 0.1 mL/mouse into DTH mice daily starting on Day 3. Percent swelling was measured as [(Thickness(mBSA rechallenged footpad) - Thickness(1xPBS rechallenged footpad)) / Thickness(1xPBS rechallenged footpad)] * 100.

Monoclonal antibodies, reagents, and flow cytometer-

Antibodies used for flow cytometric analysis (BioLegend) included: Fc block (93), PE Cy7 conjugated anti-CD3 (145-2C11), PE conjugated anti-CD19 (6D5), FitC conjugated anti-CD69 (H1.2F3), FitC conjugated anti-$IL17_a$ (TC11-18H10.1), and PE conjugated anti-CD4 (GK1.5). In short, popliteal lymph node cells (PopLN- 10^6 cells in 25 µL) from rechallenged BL6 mice were incubated with FC receptor antibodies (5-10 minutes) and incubated with conjugated antibodies (20-30 minutes at 4°C). After incubation with conjugated antibodies cells were washed twice with 1xPBS/2% fetal bovine serum buffer. The stained cells were then assessed by flow cytometer (FC500; Beckman Coulter) and the resulting data analyzed by Cytomics CXP software (Beckman Coulter). Intracellular Cytokine Staining Kit (BD biosciences) was used for IL-17a staining per manufacturer's specifications. Briefly, cells were first stained for cell surface CD4 receptor and then fixed/permeablized. Fixed/permeabolized cells were then stained for $IL\text{-}17_a$. Three-color flow cytometric analysis was used to profile the lymphocyte activation. Two-color flow cytometric analysis was used to look for Th17 cell differentiation.

Thymidine analysis of lymph node proliferation-

Draining lymph node cells from mBSA sensitized mice (1.5 mg/mL *in vivo*) were co-cultured in triplicate (0.2 mL/well in a round bottom 96 well plate) with mBSA (40 mg/mL) for 48 hours. Sixteen hours before collection and analysis [^{3}H]thymidine (2 µCi/well) was added to the cell cultures. The radioactivity was measured using a liquid scintillation counter (MicroBeta Trilux).

Histological assessment of rechallenged footpad-

Footpads from THC- or vehicle-treated DTH mice were isolated for histological examination. Rechallenged feet were cut distal to the ankle and decalcified/fixed in Cal-Rite (Fisher scientific). The footpad was then embedded in paraffin and sectioned into 6µm sections and stained for Hematoxylin and Eosin (H&E) for assessment of edema and immune cell infiltration (83).

Cytokine analysis in cell culture supernatants-

ELISA MAX sandwich enzyme-linked immunosorbent assay (ELISA) kits (BioLegend) were used to assess the level of IL-$17_{a/f}$, IFN-γ, and TNF-α cytokines. Cells were isolated from spleen and draining lymph nodes of DTH mice, plated at $1x10^6$ cells/well, cultured overnight (18-20 hours) for spontaneous cytokine secretion in complete RPMI media (1% v/v penicillin/streptomycin, 1% v/v HEPES buffer, 10% v/v heat inactivated FBS, and 0.0002% v/v 2-mercaptoethanol). Cytokine production was quantified from cell supernatants (stored at -20°C). Absorbance was measured at 450 nm using a Victor2 1420 Multilable counter (Wallac).

qPCR analysis of gene expression-

Total RNA was isolated and purified using miRNeasy kit (Qiagen), following manufacturer's procedure. iScript cDNA synthesis kit (BioRad) was used according to manufacturer's specifications to reverse transcribe cDNA. qPCR was performed using Sso Advanced SYBR Green (BioRad) on a CFX Connect (BioRad). Samples were assessed for expression of β actin, Tbx21 (Tbet), RORγT, IRF4, Pten, NFκB, IFN-γ, and SMAD7. Primers, as found on PrimerBank (Harvard Medical School), were synthesized from IDT DNA technologies with annealing temperatures of 60°C (Table I).

microRNA (miRNA or miR) array and array analysis-

Affymetrix miRNA array version 4, which integrates all mature miRNA sequences in miRBase Release 20 (miRBase v20), was used to profile miR expression in the PopLN 24 hours after mBSA rechallenge in DTH mice. The array identified over 3,000 unique mouse miRs as identified in miRBase v20 using the FlashTag biotin HSR hybridization technique, as previously described (87). In brief, log transformation of fluorescent intensities obtained from the hybridization was used to generate heat maps. Hierarchical clustering, using Ward's method, and similarities were measured using half square Euclidean distance. Fold changes in miR expression were obtained from the raw array data, and only those miRs with greater than 2.0-fold change were considered for further analysis. miR predicted targets, alignments, and miR SVR scores were determined using online databases (TargetScan, microRNA.org, and miRWalk). Determination of miR interaction and pathway analysis was completed using Ingenuity Pathway Analysis (IPA-Ingenuity Systems). Venn diagram construction was done using LucidChart Venn diagram maker (https://www.lucidchart.com/pages/examples/venn_diagram_maker).

miR validation in PopLN cells-

miR levels were validated using miScript II RT kit (Qiagen), following manufacturer's specifications for 5x miScript HiSpec Buffer. qPCR was performed using miScript SYBR Green (Qiagen) on CFX Connect (BioRad). Samples were assessed for expression of SNORD96A, miR-21a-5p, miR-223-3p, miR-29b-3p, miR-125a-5p, and miR-142-5p (Qiagen).

miR transfection of primary cells-

Transfection of primary cells was completed using the HiPerFect Transfection kit (Qiagen) following the manufacturer's protocol. Briefly, DTH draining lymph node cells were plated ($4x10^5$ cells/well) in complete RPMI media. Transfection, 6 hours at 37°C, with mimic (40 ng/well), inhibitor (100ng/well), and negative mimic (Negative Control siRNA- 40 ng/well) was done in serum free RPMI media (1% v/v penicillin/streptomycin, 1% v/v HEPES buffer, and 0.0002% v/v 2-mercaptoethanol) with 6µL HiPerFect transfection reagent. Transfection complex was added one drop at a time into cell culture. Transfection mimic, inhibitor, and negative mimic were purchased from Qiagen. Twenty-four hours from initial incubation cells were collected, total RNA isolated (miRNeasy kit- Qiagen), and cDNA reverse transcribed (miScript II RT kit- Qiagen) for miR validation and target gene expression analysis.

Statistical analysis-

Data is shown as mean ± S.E.M. Student's t-test was used to compare data between two groups. One-way ANOVA with Tukey post-hoc test was used to compare three or more groups. Experimental groups were compared to controls, $p < 0.05$ was considered significant.

4.3 RESULTS

Hypersensitivity is decreased in THC treated DTH mice

Delayed type hypersensitivity (DTH) is a T cell driven response to antigens, mediated primarily by Th1 and Th17 cells. In the current study, we used methylated

BSA (mBSA) as an antigen to induce DTH in the mouse footpads as described previously (83). Briefly, mice were sensitized by injecting mBSA (1.5mg/mL in CFA) into the footpads on day 0 followed by rechallenge with mBSA on day 6 (10mg/mL in 1xPBS) (Fig. 4.1A). These mice received 20 mg/kg THC or vehicle (ethanol diluted in 1xPBS) on days 4, 5 and 6 after initial sensitization (Fig. 4.1A). We used relative percent swelling of footpad as the primary indicator of DTH response 24 hours after rechallenge with mBSA. THC treatment of DTH mice significantly reduced swelling in the hind footpad compared to vehicle treatment (Fig. 4.1B) as well as draining lymph node (popliteal lymph node, PopLN) cellularity (Fig. 4.1 C). Additionally, we looked at lymphocyte proliferation, due to *ex vivo* rechallenge (40 mg/mL mBSA) of sensitivzed draining lymph nodes, via [^{3}H]thymidine incorporation. We found that THC treatment was able to significantly decrease mBSA induced lymphocyte proliferation compared to vehicle treated DTH mice (Fig. 4.1D). Moreover, histological analysis showed reduced swelling in THC-treated mice correlated with a significant decrease in lymphocyte infiltration in the rechallenged footpad (Fig. 4.1 E-H).

THC treatment reduced lymphocyte activation

Furthermore, assessment of lymphocyte activation, using the early lymphocyte activation marker CD69, in the PopLN showed significant decrease in THC-treated DTH mice compared to vehicle (Fig. 4.2A). As CD69 can be used as an early activation marker for both T and B cells we next looked at both CD3+CD69+ T cell and CD19+CD69+ B cell populations. THC treated DTH mice showed a decrease in both proportion (Fig. 4.2 B&D) and absolute cell counts (Fig. 4.2 C&E). We next studied Th17 cells by double-staining for IL-17 and CD4. The gating of such cells revealed that

IL-17_a producing T cells also showed significant decrease in the proportion and absolute numbers in DTH+THC treated mice compared to DTH+Veh mice (Fig. 4.2 F&G).

THC treatment reduces expression of proinflammatory transcription factors

To show that THC treatment was inhibiting T helper cell driven inflammation we next looked at proinflammatory cytokines which have been linked to DTH including IL-$17_{a/f}$, IFN-γ, and TNF-α (219). We observed significant decreases in spontaneous secretion of IL-17, IFN-γ and TNF-α in DTH+THC treated mice when compared to DTH+Veh treated mice (Fig. 4.3A). Having seen a decrease in Th1 and Th17 proinflammatory cytokines, IFN-γ and IL-$17_{a/f}$ respectively, we next looked at lineage-dependent transcription factors Tbx21 (Tbet for Th1), and RORγT and IRF4 (for Th17) in the PopLN cells (220); (221); (222). THC treatment significantly decreased the expression of both Th1 and Th17 lineage specific transcription factors, compared to vehicle treated DTH mice, (Fig. 4.3B). Finally, we looked at markers of overall inflammation including Pten, the PIK_3/Akt inhibitor, and NFκB, a transcription factor critical for expanding proinflammatory cytokine expression (223); (224). Interestingly, THC treatment of DTH mice caused a significant increase in Pten levels (Fig. 4.3C) and a correlative drop in NFκB expression (Fig. 4.3D) when compared to DTH+Veh mice, indicative of a reduced inflammatory response.

Induction of DTH in mice causes miRNA dysregulation

The importance of miRNA in hypersensitivity was recently highlighted by the observance of similarly elevated miRNA expression in both human and mouse allergic contact dermatitis skin samples (225). Using Affymetrix miRNA array version 4 (JHMI

deep sequencing & microarray core) we assessed the expression of over 3,000 miRNA in the PopLN from naïve and DTH mice. In order to visualize the miRNA dysregulation caused by DTH a heat map was constructed using log transformation of fluorescent intensities obtained from the FlashTag biotin HSR hybridization (Fig. 4.4A). One thousand five hundred and twenty-nine miRs were up/down regulated in DTH mice compared to naïve; however the expression of only 70 miRNA were altered at greater than 2.0 fold change, 51 upregulated and 19 downregulated (Fig. 4.4B). miR-21 and -223 were selected from the top upregulated miRNA (Fig. 4.4B) as potential inflammatory markers associated with DTH response and validated by qPCR (Fig. 4.4C). Also, of interest, for possible therapeutic targets, were the top downregulated miRs (Fig. 4.4C) of which miR-29b, -125a, and -142 were selected and validated by qPCR (Fig. 4.4E).

THC treatment reverses DTH mediated miRNA dysregulation

Having validated two upregulated miRs, and three down-regulated miRs as markers potentially associated with DTH response, we next set out to determine what impact, if any, THC treatment in DTH mice would have on these miRNA expression. Interestingly, DTH+THC mice showed a significant reversal of the DTH dysregulated miRNA (Fig. 4.5 A&B). Thus, THC treatment caused down-regulation of miR-21 and -223 and up-regulation of miR-29b and -142, while having no significant effect on miR-125a. Next, we selected 20 miRs, evenly distributed, from the top up- and down-regulated miRs and using Ingenuity pathway analysis (IPA) tried to connect these miRs of interest to Th1 and Th17 differentiation. In this analysis, we were able to identify 2 miRs namely, miR-21 that was downregulated, and miR-29b that was upregulated in

DTH+THC mice, were connected to the proinflammatory T helper cell activation pathway (Fig. 4.5C).

THC-mediated regulation of miR-21 and -29b inhibits Th1 and Th17 differentiation

As implicated by the pathway analysis, IFN-γ is a target of miR-29b as indicated by the miR SVR score (miRWalk- Fig. 4.6A) and alignment (miRNA.org- Fig. 4.6B). Thus THC-mediated upregulation of miR-29b may have contributed to decreased IFN-γ induction. Additionally, SMAD7, a negative regulator of TGFβ signaling, is a strong target of miR-21 as indicated by the miR SVR score (miRWalk- Fig. 4.6A) and alignment (miRNA.org- Fig. 4.6D) (226). Thus, THC-mediated down-regulation of miR-21 may have contributed to increased SMAD7. Next, we tried to confirm the expression of these molecules in the PopLN cells using qPCR. The data indicated that THC treatment of DTH mice was able to decrease IFN-γ (Fig. 4.6C) and increase SMAD7 expression in PopLN cells (Fig. 4.6E) when compared to DTH+Veh mice.

THC treatment alters microRNA specific target gene expression

In order to confirm that the reduced proinflammatory T helper cell differentiation was due to the miRNA regulation, we next looked at primary cell transfections with miR-21 and -29b. Draining lymph node cells from DTH mice were transfected (HiPerFect-Qiagen) with either miRNA mimics or inhibitors (Qiagen) for six hours with target gene expression assessed at 24 hours after transfection. The transfection was performed as detailed in our previous publications (212); (87); (227). We found that miR-29b inhibitor significantly increased IFN-γ levels compared to miR-29b overexpression (Fig. 4.6F).

Additionally, SMAD7 levels were significantly elevated with miR-21 inhibition compared to miR-21 overexpression (Fig. 4.6G).

4.4 DISCUSSION

While cannabinoid receptor agonists have been shown to reduce type IV hypersensitivity associated with DTH the role of THC as an epigenetic regulator of proinflammatory T helper cell differentiation has not yet been fully elucidated in this model (217); (218); (83). To this end, we investigated the effect of THC on mBSA-induced DTH response which is mediated primarily by Th17 and Th1 cells, specifically addressing how THC may downregulate the transcription factors and cytokines that promote such T cell activation. Furthermore, we also investigated how THC can induce miR expression so as to alter the expression of some key regulatory pathways that impact Th17 and Th1 differentiation.

The natural compound THC found in marijuana is well known for its immunoregulatory properties. Specifically, in regards to T cell activation, THC treatment has been shown to reduce secretion of proinflammatory cytokines, including IFN-γ and TNF-α, and suppress proliferation of T cells via apoptosis and/or induction of regulatory immune cells such as Tregs and MDSCs (79); (84); (76); (86); (154). As such, THC has been shown to be highly effective therapeutically in numerous models of T cell driven inflammatory disease including inflammatory lung injury, autoimmune hepatitis, and allogenic hematopoietic cell transplantation (88); (76); (78). To this end, we studied the effect of THC on type IV hypersensitivity in mice. This hypersensitivity is involved in

inducing contact dermatitis against a wide range of antigens such as those found in poison ivy and metals such as nickel.

DTH as type IV inflammatory reaction against antigens plays a critical role in protection against infections with intracellular pathogens. However, chronic DTH response can also trigger significant tissue damage. Moreover, contact with non-infectious antigens such as nickel or poison ivy can also trigger a robust DTH response leading tissue damage. In such instances, there is need for the use of anti-inflammatory and immunosuppressive drugs to attenuate T cell activation. Understanding that DTH response is complicated by the fact that both Th1 and Th17 cell subsets have been shown to contribute to the overall pathogenesis associated with disease progression is necessary for developing therapeutics (228). The ability of THC to act as an inhibitor of Th1-driven inflammation, which we saw in the current study, has been well documented in other models such as cancer and autoimmunity (229); (84). However, the role of THC as a Th17 inhibitor has been more indirect focusing, instead, on THC-mediated Treg induction as the main modulator of Th17 regulation (76); (88). Nonetheless, in the current study we show a direct inhibition of Th17 differentiation via a derepression of SMAD7, a known inhibitor of the Th17 lineage, which occurs upon THC treatment of DTH mice (226). Although there is no direct evidence to show that THC can inhibit Th1 and Th17 differentiation simultaneously, recently cannabinoid receptor agonists were shown to reduce concurrent Th1/Th17 cell differentiation (230). This corroborates our findings that THC treatment of mBSA-induced DTH response reduces the secretion of Th1/Th17 activating cytokines, IFN-γ and IL-$17_{a/f}$, and lineage specific transcription factors, Tbet and RORgT.

Epigenetic modifications, including miRNA expression, have been linked to fundamental biological processes including, but not limited to, cellular differentiation and proliferation (225); (231). As such, dysregulation of miRNA seen in disease models, including psoriasis, multiple sclerosis, and rheumatoid arthritis, has become a topic of major interest for possible therapeutic targets (232); (233); (234). In the current study, we identified two miRNA and two target genes as possible therapeutic modalities: miR-21 with its target SMAD7 and miR-29b with its target IFN-γ. miR-21 has been identified to play a critical role in multiple inflammatory models, including allergic contact dermatitis, rheumatoid arthritis, and experimental autoimmune encephalomyelitis, for the regulatory role it plays in Th17 differentiation (225); (235); (226). As suggested by Vennegaard et al. who saw elevated levels of miR-21 in the skin of mice with allergic contact dermatitis, we observed greater than 2.0 fold increase in miR-21 expression in mice with DTH response, when compared to naïve controls. Furthermore, miR-29b has been shown to be necessary in the regulation of Th1differentiation in mice, and implicated in various inflammation models (236); (237); (238); (239). We observed a downregulation of miR-29b greater than 2.0 fold in mice with DTH when compared to naïve controls, indicating a loss of restriction in the Th1 cell lineage and therefore promoting their differentiation.

We suggest in this study that the ability of THC to impact T helper cell differentiation stems from its ability to act as an epigenetic regulator. While only limited research exists on the role THC plays in the regulation of epigenetic modifications, this research base is growing. THC treatment has been found to alter DNA methylation patterns in diseases which elicit inflammatory response such as, simian

immunodeficiency virus (SIV), and even in regulatory immune cells, including myeloid derived suppressor cells (MDSC) (129); (214). The role of THC in histone mark regulation, both acetylation and methylation has only recently been studied by Yang et al. in T helper cell subsets (38). Additionally, research centered on THC-mediated alterations of miRNA profiles is severely limited (88); (240); (87). Thus, to more fully understand what role THC treatment is playing in T helper cell differentiation, we looked at the ability of THC to alter miRNA expression changes seen due to DTH. Interestingly, we saw a complete reversal of DTH-induced upregulation of miR-21 and -223 as well as downregulation of miR-29b, -125a, and -142. Having shown that THC treatment reduced Th1 and Th17 specific cytokines and transcription factors, we focused in on miR-21 and -29b, and using transfection of primary cells proved direct targeting of SMAD7 and IFN-γ messages, respectively.

In conclusion, the current study suggests that the elevated levels of IFN-γ seen in mice with DTH potentially caused by an increase in miR-21 expression and subsequent decrease in SMAD7, may induce increased Th17 differentiation (Fig. 4.7). However, with THC treatment, miR-29b, an inhibitor of IFN-γ, was overexpressed indirectly downregulating miR-21, and thereby derepressing SMAD7 (Fig. 4.7). In short, THC treatment was able to effectively inhibit Th1 and Th17 lineages in the DTH model of hypersensitivity. Together these findings suggest that THC can be used therapeutically in type IV hypersensitivity as well as autoimmune models where Th1 and Th17 cells have been implicated in disease progression. Furthermore, our findings that THC regulates T helper cell differentiation via altered miRNA expression are vital to fully elucidating the role cannabinoid receptor agonists play in adaptive immunity.

Table 4.I. Primer sequences for qPCR analysis of gene expression in popliteal lymph node cells.

Gene	Primer	Sequence (5'-3')	Annealing Temp
β actin	Forward	GGC TGT ATT CCC CTC CAT CG	60°C
	Reverse	CCA GTT GGT AAC AAT GCC ATG T	
Tbet	Forward	AAC CGC TTA TAT GTC CAC CCA	
	Reverse	CTT GTT GTT GGT GAG CTT TAG C	
RORγT	Forward	CAA GTT TGG CCG AAT GTC C	
	Reverse	CTA TAG ATG CTG TCT CTG C	
IRF4	Forward	GTC TCA CGG GTG CTT TCT GT	
	Reverse	GGC TGG GCA TTC TCA CGA TA	
Pten	Forward	CCT TTT GAA GAC CAT AAC CCA CC	
	Reverse	GAA TTG CTG CAA CAT GAT TGT CA	
NFκB	Forward	ATG GCA GAC GAT GAT CCC TAC	
	Reverse	TGT TGA CAG TGG TAT TTC TGG TG	
IFN-γ	Forward	GCG TCA TTG AAT CAC ACC TG	
	Reverse	GAG CTC ATT GAA TGC TTG GC	
SMAD7	Forward	GCA TTC CTC GGA AGT CAA GAG	
	Reverse	CCA GGG GCC AGA TAA TTC GT	

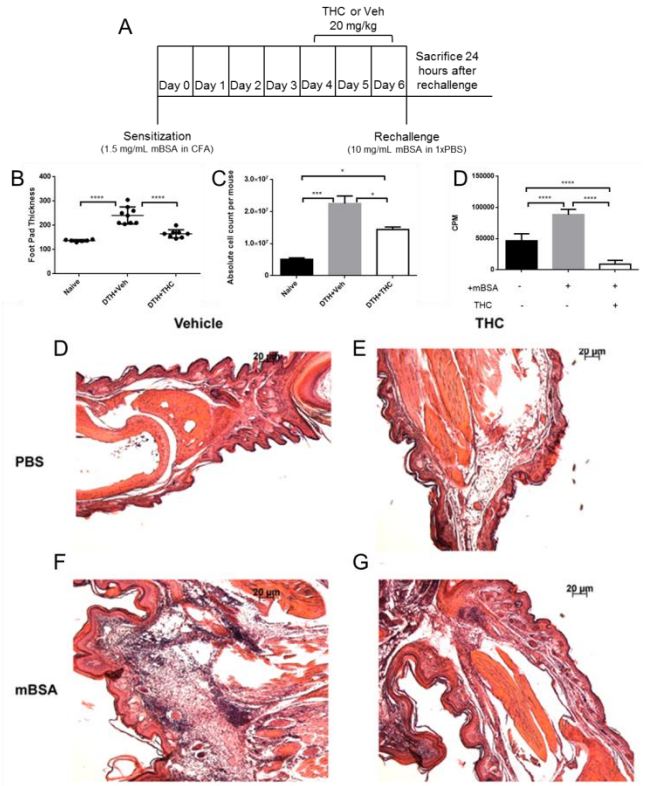

Figure 4.1: THC treatment reduces lymphocyte driven inflammation associated with DTH.

Mice (n=5 per experimental group) were sensitized, subcutaneously 1.5mg/mL of mBSA in CFA. Sensitized mice were treated with THC (20mg/kg) or vehicle, on days 4, 5, and 6 after sensitization. Mice were rechallenged (10mg/mL mBSA) via a foot pad injection on day 6. Swelling was measured as: $\frac{thickness\ of\ mBSA\ footpad - thickness of\ vehicle\ footpad}{Thickness\ of\ vehicle\ footpad} x100\%$. (A) Schematic of model and treatment regimen. (B) Relative percent swelling compared to naïve mouse footpad (for each hind paw foot pad). (C) Absolute cell count of draining lymph nodes (per mouse). Lymphocytes from mBSA-sensitized mice were rechallenged with mBSA, 40 mg/mL, and then cultured for 48 hours. In the last 16 hours of culture, the cells were pulsed with 2µCi of [^{3}H]Thymidine. (D) The cells were harvested and analyzed for Thymidine uptake using a β-Scintillation counter. Histopathological analysis of mBSA rechallenged (DTH) footpad. The footpad was then embedded in paraffin and sectioned into 6µm sections and stained for Hematoxylin and Eosin. Mice were sensitized with mBSA, treated with either vehicle (E&G) or THC (F&H), and rechallenged with either vehicle (E&F) or mBSA (G&H). The footpad was isolated and fixed/decalcified in Cal-Rite. Vertical bars represent Mean+/- SEM. ANOVA/Tukey * $p<0.05$ ** $p<0.01$ ***$p<0.001$ ****$p>0.0001$

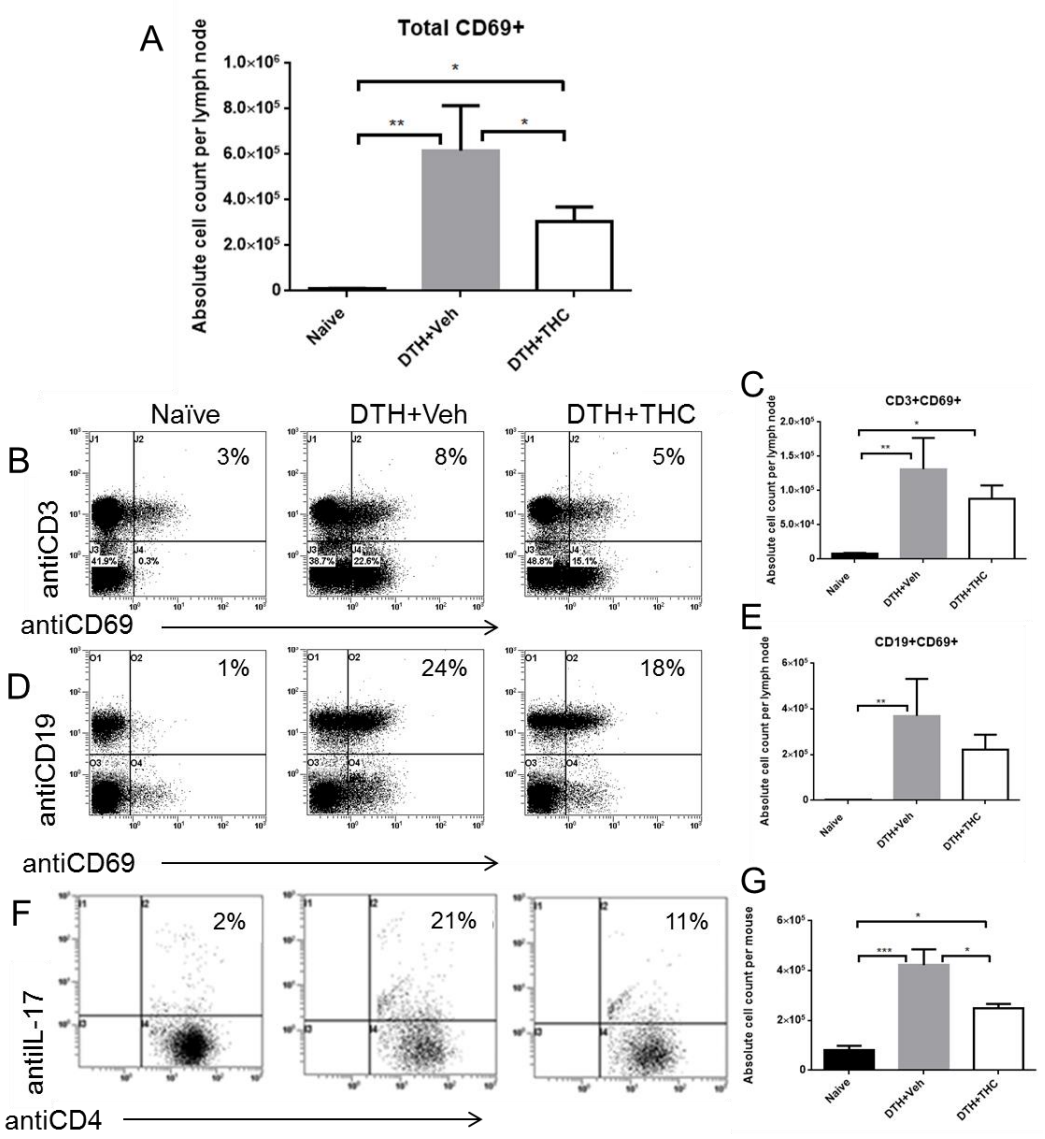

Figure 4.2: THC treatment reduced lymphocyte activation.

DTH-induced mice were treated with THC or vehicle as described in Fig 1 legend. (A) Absolute cell counts CD69+ lymphocytes (per lymph node). (B) Flow cytometry histograms showing CD3+CD69+ T cells and (C) absolute cell counts (per lymph node). (D) Flow cytometry histograms showing CD19+CD69+ B cells and (E) absolute cell counts (per lymph node). Cells from the LN were cultured for 4 hours in the presence of PMA, Ionomycin, and Golgi Plug and stained for IL-17_a secreting cells. (F) Flow cytometry histograms showing CD4+IL17+ T cells and (G) absolute cell counts (per lymph node).Vertical bars represent Mean+/- SEM. ANOVA/Tukey * $p<0.05$ ** $p<0.01$ ***$p<0.001$ ****$p>0.0001$

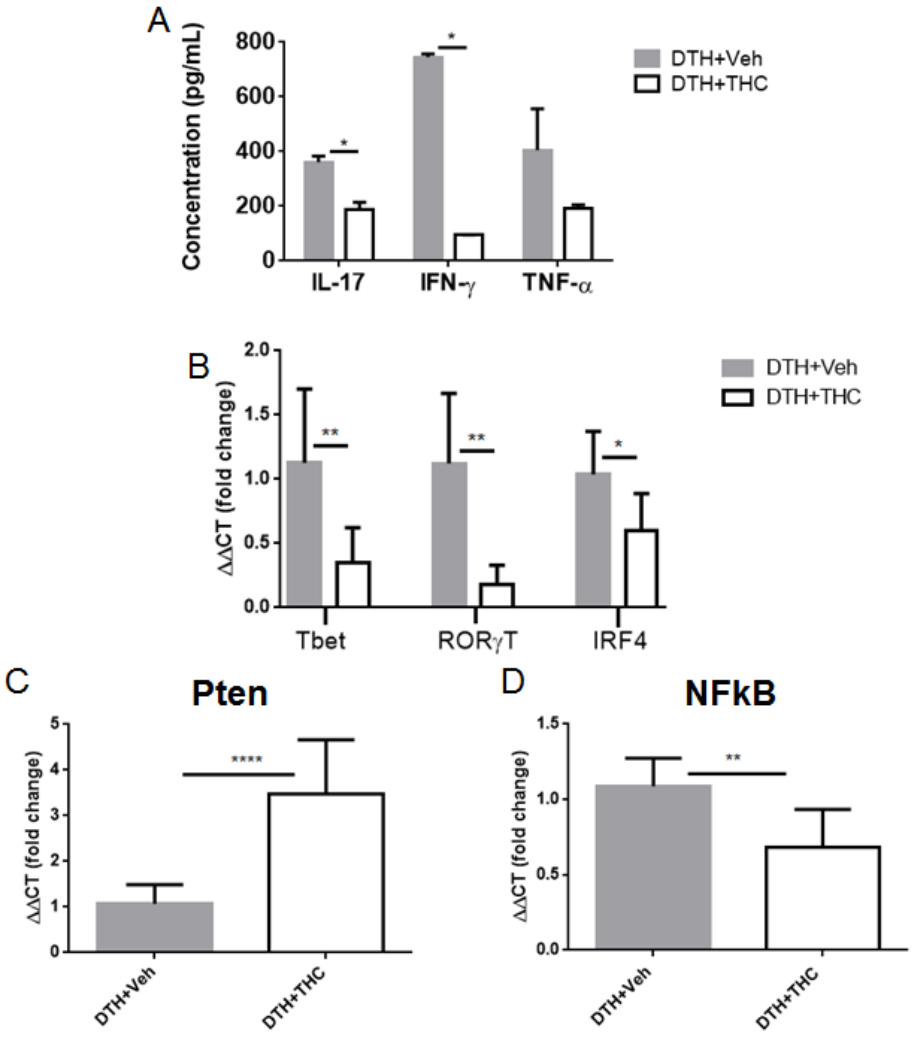

Figure 4.3: THC treatment reduces inflammatory cytokines and transcription factors.

DTH-induced mice were treated with THC or vehicle as described in Fig 1 legend. Cells, mBSA-sensitized *in vivo*, were cultured overnight without mBSA to analyze spontaneous cytokine secretion. (A) Culture supernatants were analyzed for pro-inflammatory cytokines IL-17, IFN-γ, and TNF-α via ELISA MAX kit (Biolegend). (B-D) cDNA was isolated from the PopLN of and analyzed using qPCR. (B) Analysis of pro-inflammatory T cell transcription factors Tbet, RORγT, and IRF4, (C) Analysis for PIK_3/Akt regulator Pten, and (D) Analysis of transcription factor NFκB. Vertical bars represent Mean+/-SEM. Student's t test * $p<0.05$ ** $p<0.01$ ***$p<0.001$ ****$p>0.0001$

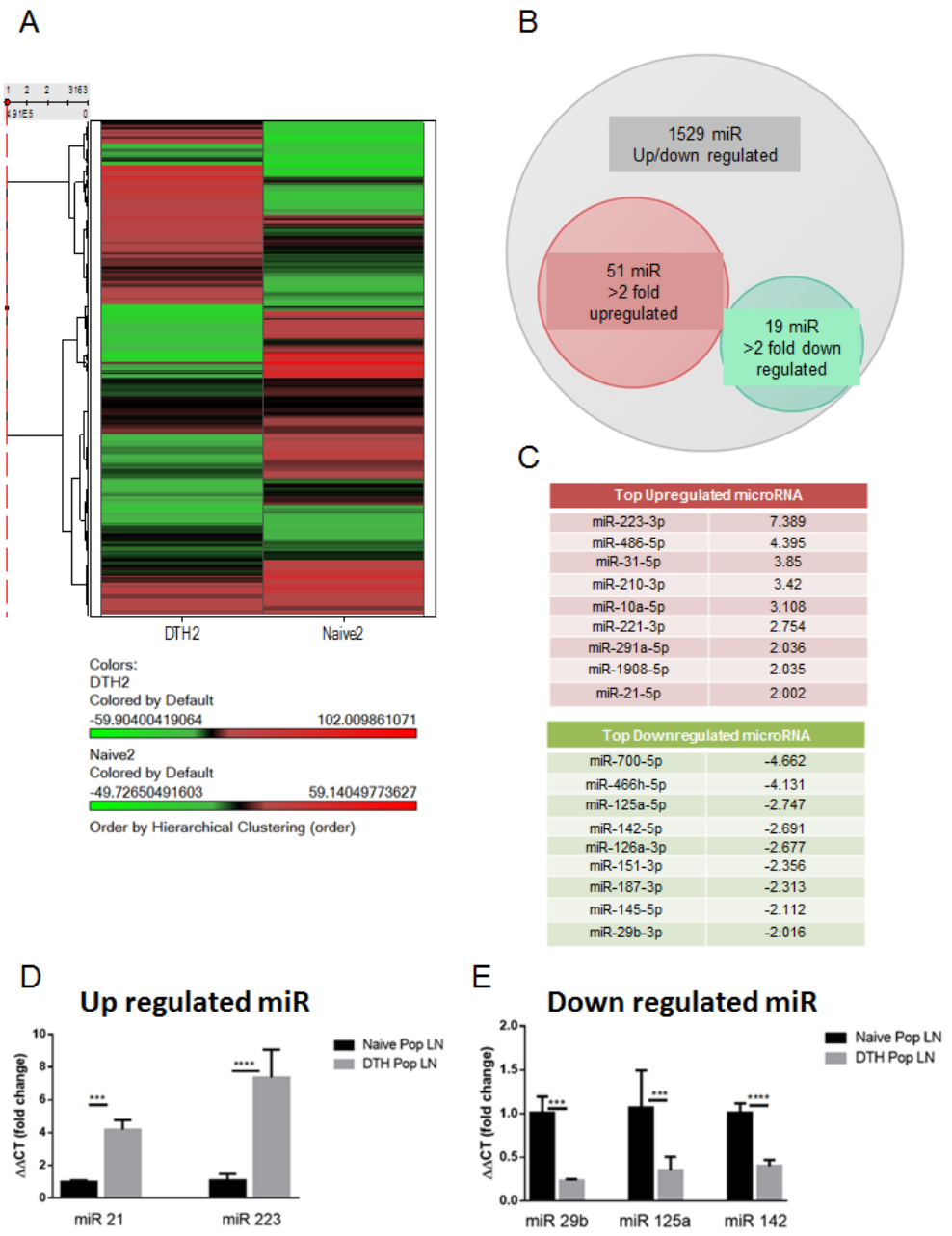

Figure 4.4: DTH reaction causes changes to microRNA expression in immune cells.

Lymphocytes from popliteal lymph nodes (PopLN) of naïve and DTH mice were assessed for miR expression. (A) Heat map highlighting the microRNA dysregulation between naïve and DTH samples (n=5 per experimental group). (B) Venn diagram depicting the up and down regulated microRNA (greater than 2 fold). (C) IPA ingenuity analysis of top up and down regulated microRNA. (D-E) qPCR validation of microRNAs of interest (D) miR-21-5p and miR-223-3p (E) miR-29b-3p, miR-125a-5p, and miR-142-5p. Vertical bars represent Mean+/- SEM. Student's t test * $p<0.05$ ** $p<0.01$ ***$p<0.001$ ****$p>0.0001$

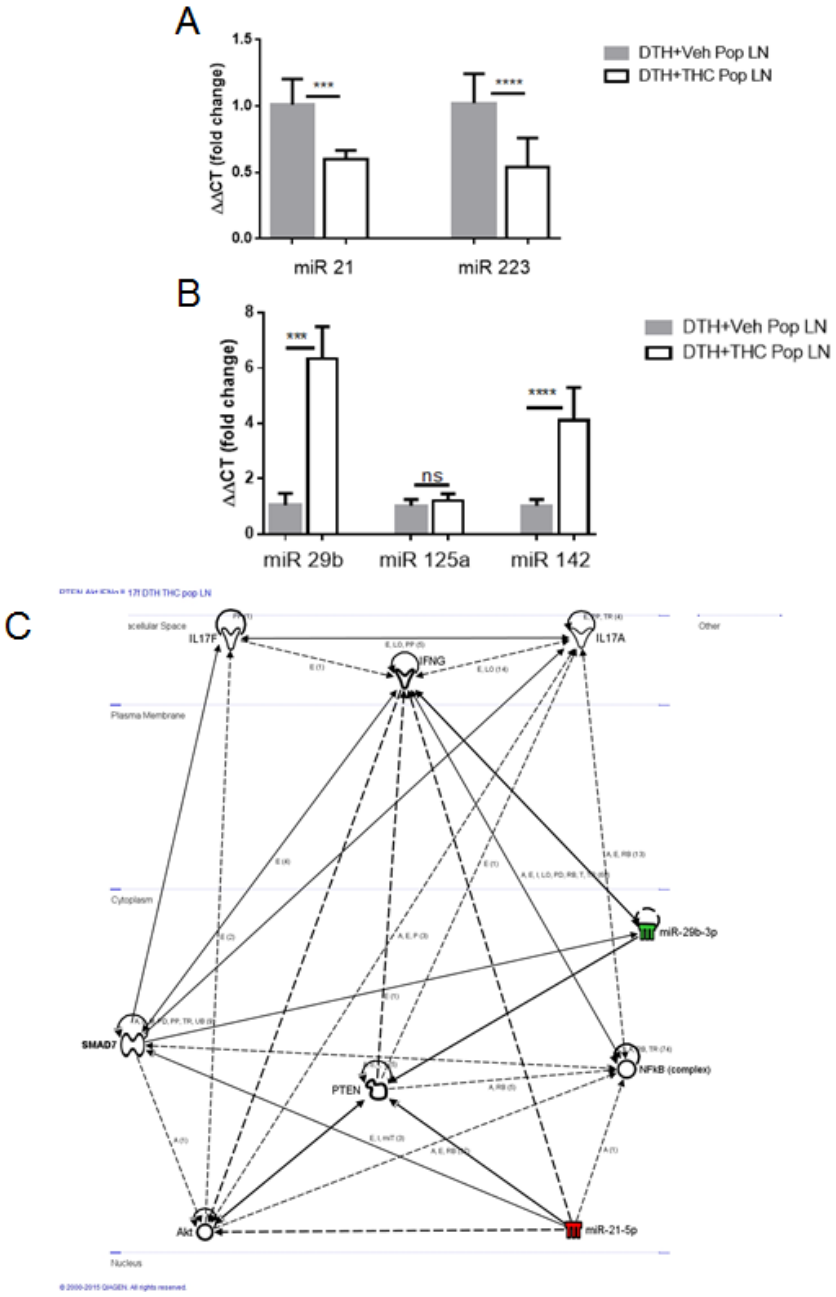

Figure 4.5: THC treatment reverses DTH-mediated alterations in microRNA expression.

DTH-induced mice were treated with THC or vehicle as described in Fig 1 legend. (A-B) cDNA was isolated from DTH+Veh and DTH+THC PopLN for validation of microRNA array using q-PCR (A) Analysis of miR-21-5p and miR-223-3p (B) Analysis of miR-29b-3p, miR-125a-5p, and miR-142-5p. (C) IPA ingenuity software was used to determine interactions between miR-21-5p and miR29b-3p and the pro-inflammatory T cell pathway. Vertical bars represent Mean+/- SEM. Student's t test * $p<0.05$ ** $p<0.01$ ***$p<0.001$ ****$p>0.0001$

A

miR	miRBase Accession	Targets	miR SVR score	miR Walk
mmu-miR-29b-3p	MIMAT0000100	IFNγ	-0.22	5
mmu-miR-21-5p	MIMAT0000530	SMAD-7	-1.26	6

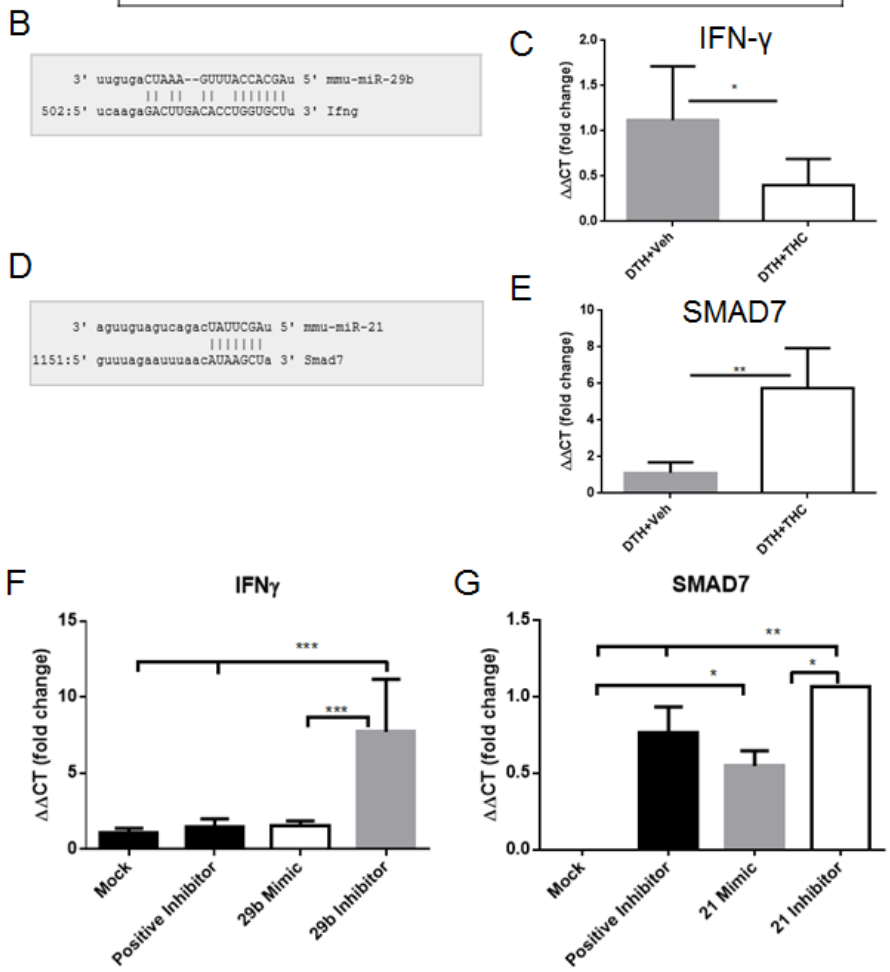

Figure 4.6: THC treatment alters microRNA-specific target gene expression.

DTH-induced mice were treated with THC or vehicle as described in Fig 1 legend. cDNA and protein was isolated from DTH+Veh and DTH+THC PopLN for validation of target gene message using q-PCR. (A) Predicted or experimentally observed miRNA target genes (TargetScan and miRWalk). (B and D) Schematic illustration of differentially regulated miRNA (B) miR-29b and (D) miR-21 targeting the 3'-UTR of potential target genes (microRNA.org). (C and E) q-PCR validation of microRNA target gene message (C) IFN-γ and (D) SMAD7. Draining lymph nodes, from DTH mice, were transfected for 6 hours and then cultured overnight (18 hours). (E-F) Validation of pro-inflammatory T cell gene targets (E) IFN-γ and (F) SMAD7. Vertical bars represent Mean+/- SEM. Student's t test or ANOVA/Tukey * $p<0.05$ ** $p<0.01$ ***$p<0.001$

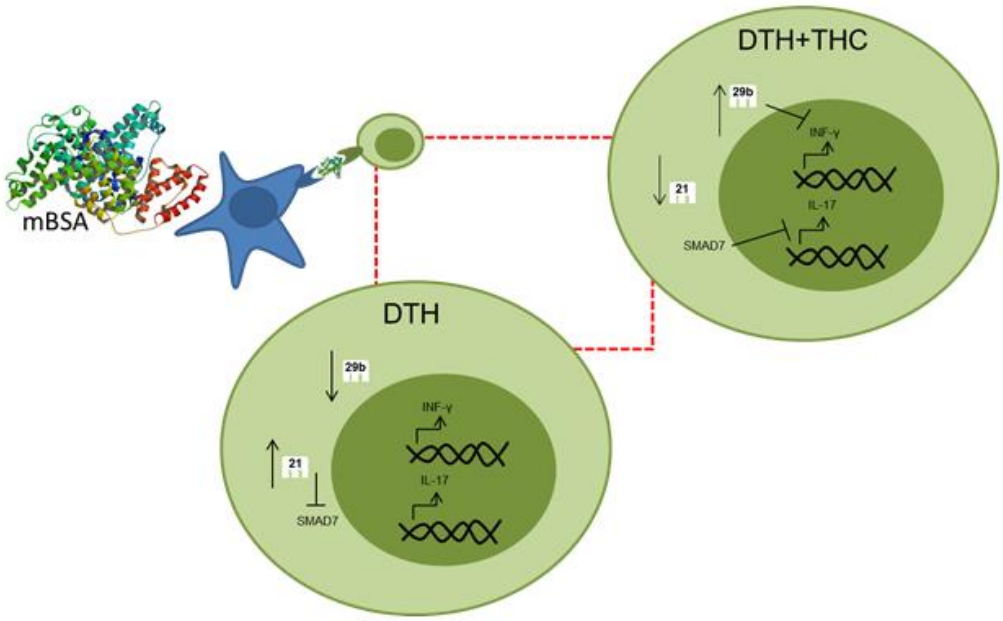

Figure 4.7: Schematic of the role microRNA plays in mBSA induced DTH.

mBSA induced DTH is classically associated with elevated Th1 and Th17 response, and increased expression of miR-21. Th17 differentiation is increased via miR-21 inhibition of SMAD7. THC treatment of DTH mice causes a decrease in the proinflammatory response through microRNA regulation, increasing expression of miR-29b (inhibitory of IFN-γ) and decreasing miR-21 expression. Thus THC treatment reduces IFN-γ production and inhibition of IL-17 regulation via SMAD7 derepression.

CHAPTER V: Endocannabinoid 2-arachidonyl glycerol inhibits inflammation associated with delayed type hypersensitivity via reduced T cell response

5.1 INTRODUCTION

The endocannabinoid (EC) system consists of cannabinoid (CB) receptors (CB1 and CB2) as well as the endogenous ligands for these receptors, called endocannabinoids (EC) (3). Anandamide (AEA) and 2-arachidonyl glycerol (2-AG) the first discovered ECs remain the most widely studied to this day (23); (24). 2-AG has been proposed as the "true natural ligand" for CB receptors for three main reasons: multiple synthesis pathways, elevated tissue expression, and agonist activity at both CB receptors (241). 2-AG can be formed along a degredative pathway from inositol phospholipid hydrolysis via multiple phospholipases (PL) and diacylglycerol lipase (31); (32). Additionally, 2-AG can be synthesized from arachidonic acid-containing phosphatidylcholine via variable PL and phosphatidic acid phosphatase (31). Increased pathways for biosynthesis explains why, unlike AEA which is only present at high levels in the brain and uterus, 2-AG is well expressed in numerous tissues (242); (243); (23); (244); (245); (246). Furthermore, 2-AG exhibits both binding affinity and efficacy for CB1 and CB2 receptors making it a full agonist for the CB receptors (247).

The notion that the EC system plays a role in immune response has long been apparent, with CB2 constitutively expressed on immune cells and the expression of CB1 upregulated upon activation in T cells (13). Type IV hypersensitivity (delayed type

hypersensitivity, DTH) is driven by proinflammatory T helper cell subsets, Th1 and Th17 that produce IFN-γ and IL-17 respectively (69); (52); (248). Moreover, a study using 2,4-dinitroflurobenzene to induce ear dermatitis found increased ear weight to correlate with elevated 2-AG levels (249). Also, mice deficient in CB receptors were found to exhibit increased response to contact hypersensitivity (217). In contrast, mice lacking Fatty Acid Amide Hydrolase (FAAH) that express heightened anandamide levels showed decreased response to contact hypersensitivity (217). These data clearly suggested a role for endocannabinoids in suppressing the DTH response *in vivo*. Nonetheless, there is also evidence to suggest that endocannabinoid levels increase during inflammation or autoimmune disease, a finding that has been used to indicate that endocannabinoids may in fact promote inflammation (217).

There are no studies that have measured the levels of endocannabinoids in immune cells during naïve and activation stage and tried to correlate that with the levels found during an ongoing immune response. In the current study, we investigated the levels of ECs, particularly 2-AG in naïve and activated T and B cells using mBSA as an antigen which triggers not only DTH response mediated by Th1 and Th17 cells but also B cells to produce antibodies. The data suggest that 2-AG is produced at higher levels upon T and B cell activation and systemically during the DTH response but that 2-AG plays a regulatory role in trying suppress inflammation rather than promote it.

Here we demonstrate that exogenous treatment with 2-AG can reduce inflammation seen in DTH via inhibition of T cell activation and proliferation.

5.2 MATERIALS AND METHODS

Mice-

Female C57BL/6 (BL6) mice, aged 6-8 weeks and at an average weight of 20 g, were obtained from Jackson Laboratories and used as naïve controls in each experiment. All mice were housed in pathogen-free conditions and allowed *ad libitum* access to filtered water and Teklad rodent diet 8604 (normal chow) at the Animal Research Facility located at the University of South Carolina School of Medicine. All experiments were conducted under an approved Institutional Animal Care and Use Committee animal protocol.

T and B cell isolation-

Single cell suspension from the spleens of BL6 mice was plated for 1 hour at 37°C, for removal of adherent cells. Cells in suspension were gently aspirated and resuspended in complete RPMI media (1% v/v penicillin/streptomycin, 1% v/v HEPES buffer, 10% v/v heat inactivated FBS, and 0.0002% v/v 2-mercaptoethanol). Nylon wool column, wetted with complete media, was then loaded with single cell suspension and incubated 1 hour at 37°C. T cells were isolated based on nonadherence as elute and wash from nylon wool column (250). B cells adhering to the nylon wool were isolated by compression of incubated nylon wool, using sterile syringe plunger and complete medium. Purity (greater than 90%) was checked using flow cytometer.

Endocannabinoid extraction-

Briefly, endocannabinoids were extracted from sample with internal standards (deuterated endocannabinoids (Cayman Chemical) AEA-d4 (10ng/mL), 2-AG-d5

(20ng/mL), and PEA-d4 (200ng/mL) diluted in 50:50 (methanol:water) and (phenylmethylsulfonyl fluoride) PMSF in acetonitrile. Samples were diluted in 0.1333% TFA ultra purified water, to 20% (v/v) acetonitrile, and ultracentrifugation used to separate out cellular debris. Samples are then cleaned using SPE columns (Bond Elute C8). Briefly, ultracentrifugation supernatant was loaded onto the activated SPE column, the elute was discarded, and then the column was cleaned using 20% acetonitrile, the elute was discarded. The endocannabinoids were eluted using 80% (v/v) acetonitrile in 0.1333% TFA ultra purified water and evaporated to dryness. All samples were stored at -80°C.

Liquid chromatography/Tandem Mass spectrometery -(LC/MS/MS)-

Sample, resuspended in 100uL 80% (v/v) acetonitrile, was injected in a volume of 10 µL on to a C18 reverse phase analytical column (particle size 5 µm 2.1 x 150 mm ES Industries #06601-12-54-45318). Endocannabinoids were eluted using a linear binary gradient flowing at 200 µL/min on a Waters Acquity HPLC system. The gradient solvent composition began at 50% A: 50% B (solvent A: water/acetonitrile (95:5) with 1% ammonium acetate and 0.1% formic acid; solvent B: methanol with 1% ammonium acetate and 0.1% formic acid) and increased to 0%A: 100%B over 28 minutes. The Mass spectrometer (Waters Premier XE triple quadrupole) was operated in multiple reaction monitoring (MRM) mode using positive ion electrospray ionization. The electrospray probe was held at 3 kV.Optimized mass spectrometer operating parameters for quadrupole mass spectrometer with electrospray ionization source in tandem with liquid chromatography (Micromass Quattro-LC, Waters) are listed in Table I. Waters Masslynx software was used for analysis.

Induction of delayed type hypersensitivity (DTH) and 2-AG treatment-

DTH was induced in C57BL/6 mice using a sensitization/rechallenge method (Jackson et al 2014 (83)). Briefly, mice were sensitized with a subcutaneous injection (100 µL/hind flank) of 1.5 mg/mL methylated BSA (mBSA- Sigma Aldrich) emulsified in complete Freunds adjuvant (CFA- Sigma Aldrich). Six days later, the mice were rechallenged with footpad injection (20 µL/footpad) of 10 mg/mL mBSA in 1xPBS. 2-Arachidonoyl glycerol (2-AG- Cayman Chemical) evaporated under a stream of nitrogen was dissolved in ethanol (20mg/mL) and then diluted in 1xPBS to a concentration and used in mice at a concentration of 40mg/kg. 2-AG or vehicle (ethanol diluted in 1xPBS) was administered intraperitoneally (i.p.) at a volume of 0.1 mL/mouse into DTH mice daily Day 4 - Day 6. Percent swelling was measured as [(Thickness(mBSA rechallenged footpad) - Thickness(1xPBS rechallenged footpad)) / Thickness(1xPBS rechallenged footpad)] * 100.

Monoclonal antibodies, reagents, and flow cytometer-

Antibodies used for flow cytometric analysis (BioLegend) included: FC block (93), anti-CD3 (145-2C11), anti-CD19 (6D5), and anti-CD69 (H1.2F3). Popliteal lymph node cells (PopLN- 10^6 cells) from DTH BL6 mice were incubated with FC receptor antibodies (10 min) and incubated with conjugated antibodies (20-30 minutes at 4°C). After incubation, with conjugated antibodies, cells were washed twice with 1xPBS/2% fetal bovine serum buffer. The stained cells were then assessed by flow cytometer (FC500; Beckman Coulter) and the resulting data analyzed by Cytomics CXP software (Beckman Coulter). Three-color flow cytometric analysis was used to profile the lymphocyte activation.

Cytokine analysis in cell culture supernatants-

ELISA MAX sandwich enzyme-linked immunosorbent assay (ELISA) kits (BioLegend) were used to assess the levels of IL-2, IL-6, IL-$17_{a/f}$, IFN-γ, and TNF-α cytokines. Cells were isolated from spleen and draining lymph nodes of DTH mice, plated at $0.8x10^6$ cells/well, cultured 24 hours for cytokine secretion in complete RPMI media (1% v/v penicillin/streptomycin, 1% v/v HEPES buffer, 10% v/v heat inactivated FBS, and 0.0002% v/v 2-mercaptoethanol) with phorbol 12-myristate 13-acetate (PMA) and calcium ionophore ionomycin (50 ng/mL and 10 µg/mL respectively). Cytokine production was quantified from cell supernatants (stored at -20°C). Plasma was assessed for IgG levels using sandwich ELISA (Abcam). Absorbance was measured at 450 nm using a Victor2 1420 Multilable counter (Wallac).

Cell proliferation assays-

Spleen cells from naïve mice were co-cultured in triplicate (0.2 mL/well in a round bottom 96 well plate) with ConA (2.5µg/mL) or LPS (5µg/mL) to stimulate T and B cell proliferation, respectively. Splenocytes from DTH mice rechallenged *in vivo* were assessed for spontaneous proliferation. In some experiments, 2-AG was added at the time of cell seeding at increasing doses (0.9, 1.9, and 2.9 µM). Sixteen hours before collection and analysis, [^{3}H]thymidine (2 µCi/well) was added to the cell cultures. Radioactivity was measured using a liquid scintillation counter (MicroBeta Trilux).

Statistical analysis-

Data were shown as mean ± S.D. Student's t-test was used to compare data between two groups. One-way ANOVA with Tukey post-hoc test was used to compare three or more

groups. Experimental groups were compared to controls, and $p < 0.05$ was considered significant.

5.3 RESULTS

Basal levels of the endocannabinoid, 2-AG increases in lymphocytes upon activation

While endocannabinoid levels have been previously measured in secondary lymphoid organs (245, 246), to the best of our knowledge, the levels in various immune cells during naïve and activation stages have yet to be determined. As such, we isolated naive T and B cells from BL6 mouse spleens, and using LC/MS/MS, quantified basal levels of AEA and 2-AG in these cells (Fig. 5.1A). We found that AEA levels, while detectable were minimal and were significantly lower than 2-AG in both T and B cells (Fig. 5.1B). For this reason, we focused our studies only on 2-AG. In order to quantify changes in 2-AG expression/secretion in activated T and B cells, we activated splenocytes with the mitogens Concanavalin A (ConA) or the endotoxin lipopolysaccharide (LPS), which activate polyclonally, T and B cells respectively, and measured the levels of enocannabinoids within the cells as well as in the culture supernatants. Upon activation, significantly higher levels of 2-AG were found in activated T and B cell supernatants than in the activated cells themselves (Fig. 5.1C-D). Moreover, activated B cell culture supernatants had much higher levels of 2-AG than supernatants from activated T cell cultures.

To ensure that the elevated endocannabinoid levels were biologically relevant, we used methylated bovine serum albumin (mBSA) to induce DTH hypersensitivity, which is associated with proinflammatory T cell response (69); (52); (248). The DTH response

following injection of mBSA into footpads led to significant swelling in the hind footpads of mice (Fig. 5.1E) as well as increased cellularity in the draining popliteal lymph nodes (PopLN) (Fig. 5.1F). Interestingly, when we measured 2-Ag levels in the plasma of the DTH mice, we saw a significant increase in 2-AG levels when compared to naïve mice (Fig. 5.1G), AEA levels remained low although detectable (data not shown). To confirm that the PopLN cells were actually getting activated, we analyzed them for activation markers such as CD69, which was significantly enhanced in mBSA injected T and B cells (Fig. 5.1 H&I).

2-AG treatment reduces inflammation associated with DTH

Because cannabinoids are immunosuppressive, the increase in endocannabinoids following activation of immune cells suggested a negative feedback loop aimed controlling the hypersensitivity response. To that end, we tested if exogenous treatment with this endocannabinoid could inhibit inflammation in higher concentrations would suppress DTH response. As such, DTH mice were treated with 2-AG (40mg/kg i.p.) once daily on days 4-6 (Fig. 5.2A). Interestingly, we found that 2-AG treatment was able to significantly decrease footpad swelling (Fig. 5.2B). Also, the total number of activated T cells (CD3+CD69+) and B cells (CD19+CD69+) in the PopLN were significantly decreased in 2-AG treated mice compared to vehicle controls (Fig. 5.2 C). In order to more fully elucidate how 2-AG was reducing the mBSA induced hypersensitivity we next looked at spontaneous cytokine secretion of PopLN cells of DTH mice. We assessed classical Th17 and Th1 proinflammtory cytokines triggered by mBSA antigen during the DTH response. Cytokines associated with Th17 activation, IL-$17_{a/f}$ (Fig. 5.2E), and differentiation, IL-6 (Fig. 5.2H), were significantly decreased in DTH+2-AG treated mice

compared to DTH+Veh mice. Furthermore, Th1 secreted cytokines including IFN-γ (Fig. 5.2F) and TNF-α (Fig. 5.2G) were also significantly reduced in DTH+2-AG mice, compared to controls. Additionally, we saw IL-2 levels significantly decrease with 2-AG treatment indicative of reduced T cell activation and proliferation in the draining lymph nodes (Fig 5.2I). Because mBSA, can also trigger Ab response (248), we measured IgG levels in the plasma and found that treatment with 2-AG caused significant decrease in IgG levels when compared to vehicle controls (Fig. 5.2J)

2-AG modulates DTH disease parameters via inhibition of T cell proliferation

We next determined if 2-AG acts directly on T and B cells. To that end, we cultured the PopLN cells from mBSA immunized mice in the presence of 2-AG or vehicle. We observed a dose- dependent suppression of spontaneous lymphocyte proliferation of antigen-activated cells as well as Con-A activated T cells and LPS activated B cells in the presence of 2-AG when compared to vehicle controls (Fig. 5.2K-M). These data suggested that 2-AG was acting directly on activated T and B cells to suppress lymphocyte activation and proliferation.

5.4 DISCUSSION

Recently, we hypothesized that endocannabinoids may play a critical role in the regulation of inflammation associated with autoimmune diseases (251). Our laboratory and others have found that exogenous treatment of autoimmune inflammation with AEA can attenuate inflammatory disease (252); (253); (76); (254); (83). However, research on 2-AG in inflammatory models is mostly limited to increasing basal levels via inhibition of the 2-AG degredative enzyme, MAGL (255); (256). One exception being a study

which found that exogenous 2-AG increased the neuroprotection and decreased the mortality in mice bearing experimental autoimmune encephalomyelitis (257). However, there are no studies that have investigated the levels of 2-AG in naïve and activated immune cells and correlated that with inflammation. As such, we set out to test the levels of endocannabinoids during inflammation. We chose mBSA as an antigen because it triggers DTH reaction that can be measure clinically as footpad swelling as well as lymph node activation. In addition, this antigen has been shown to activate not only both Th1 and Th17 cells but also antibodies (258); (83).

The EC system has been associated with immune response due to the fact that cannabinoid receptors are expressed on immune cells and that measurable EC levels have been detected in secondary immune organs (246); (245). Our findings show that basal levels of AEA and 2-AG can also be found in naive T and B cells. Traditionally endocannabinoids are considered to be synthesized as needed, from the lipid membranes, rather than stored (28). However, EC binding of the cannabinoid receptors has been associated with release of signal molecules such as ceramide, a bioactive lipid, which regulates cellular differentiation, proliferation, and apoptosis (74). This suggests that basal levels of endocannabinoids may be necessary for regulation of basic cell function. Furthermore, we found that 2-AG levels were significantly elevated in cell supernatants of activated T and B cells, and in the plasma of DTH mice. These findings suggest that 2-AG may be synthesized upon activation by T and B cells, and are consistent with other studies demonstrating elevated systemic 2-AG levels in various disease models associated with inflammation, including hepatic ischemia-reperfusion injury, obesity, and post-traumatic stress disorder (259); (260); (261).

While Mimura et al. recently observed that 2-AG levels correlated with ear weight gain, due to dermatitis, in a CB2 dependent manner (249), we found that not only does the 2-AG levels increase during DT H *in vivo* but also, exogenous administration of 2-AG was able to suppress the inflammation associated with the DTH response. Exogenous 2-AG has been shown to inhibit the proliferation of T cells, *in vitro*, to anti-CD3 mAb stimulation (89). Furthermore, activated *Jurkat* T cell, as well as primary splenocyte secretion of IL-2 was suppressed *in vitro* upon co-culture with 2-AG (90); (91). The role of 2-AG in regards to B cells is more complicated due to the fact that 2-AG, at nM concentrations, can stimulate chemotaxis and chemokinesis in B220+CD19+IgD+IgM+ spleen cells via CB2 receptor binding (262). However, in LPS activation of B cells, *in vitro*, 2-AG caused decreased proliferation at µM concentrations (89). This evidence supports our claim that exogenous 2-AG treatment can be inhibitory to inflammation associated with type IV hypersensitivity.

The conflicting data surrounding the effect of 2-AG on immune regulation suggests that 2-AG concentration is vital for eliciting an anti-inflammatory response. Our findings highlight the concept that anti-inflammatory properties of 2-AG are dose or threshold-dependent as shown in our proliferation studies. We observed that 2-AG at the lowest dose caused minor or nonsignificant (NS) suppression of lymphocyte proliferation while higher doses ablated DTH and ConA induced T cell proliferation. It should also be noted that in vivo, 2-AG levels are regulated by a serine hydrolase, monoacylglycerol lipase (MAGL), which is the main enzyme responsible for inactivating 2-AG *in vivo* (256). This may account for the fact that to induce significant anti-inflammatory effects, it is necessary to administer higher concentrations of exogenous 2-AG.

Together, the current study suggested that endocannabinoids such as 2-AG may play a critical role in the regulation of immune response. Also, treatment with 2-AG can be used to decrease T and B cell-dependent immune response. The use of 2-AG to suppress DTH may be useful to against contact dermatitis. Additionally, these findings also suggest that 2-AG can be used therapeutically to treat various models of Th1 or Th17 driven inflammation, as seen in a number of autoimmune diseases.

Table 5.I. Optimized MRM tuning parameters.

	MRM Transitions	Cone Voltage (V)	Collision Energies (eV)	Dwell (sec)
AEA	348 > 62	30	18	60
AEA-d4	352 > 66	30	18	
2-AG	396 > 379	15	20	
2-AG-d5	401 > 384	15	20	
O-AEA (loading control)	348 > 62	30	18	
PEA-d4 (extraction control)	304 > 62	30	18	

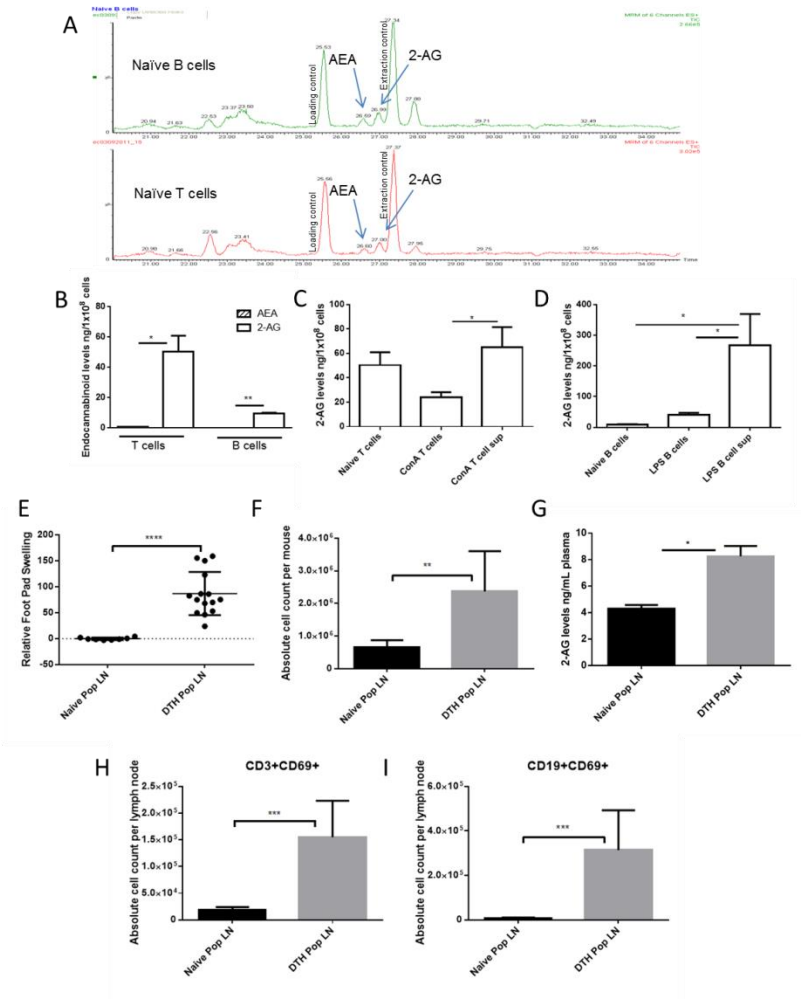

Figure 5.1: Lymphocyte activation both *in vitro* and *in vivo* causes dysregulation of endocannabinoid levels.

T and B cells isolated from naïve C57BL/6 spleens (n=2) using nylon wool column separation after adherent cell exclusion (purity determined using anti-CD3 and anti-CD19 labels by flow cytometry. (A) Raw chromatogram for naïve T and B cells after LC/MS/MS detection. (B) Quantified AEA and 2-AG levels in naive lymphocytes. (C-D) Spleens were collected from naïve C57BL/6 mice (n=4) and activated with ConA (2.5µg/mL) or LPS (5µg/mL) then plated at a density of $1.5x10^6$/mL. Endocannabinoid 2-AG levels quantified, after (C) ConA activation and (D) LPS activation using LC/MS/MS detection. Delayed type hypersensitivity (DTH) induction, 24 hours after rechallenge, was determined using disease parameters including footpad swelling and lymphocyte activation. Plasma was collected and assessed for EC levels (n=5 per treatment group). (E) Relative percent swelling compared to naïve mouse footpad (for each hind paw foot pad). (F) Popliteal lymph node absolute cell counts (per mouse). (G) Circulating 2-AG levels in plasma. (H-I) Absolute cell counts (H) CD3+CD69+ activated T cells and (I) CD19+CD69+ activated B cells. Representative data from replicate experiments; Student's T test or ANOVA/Tukey * $p<0.05$ ** $p<0.01$ ***$p<0.001$ ****$p>0.0001$

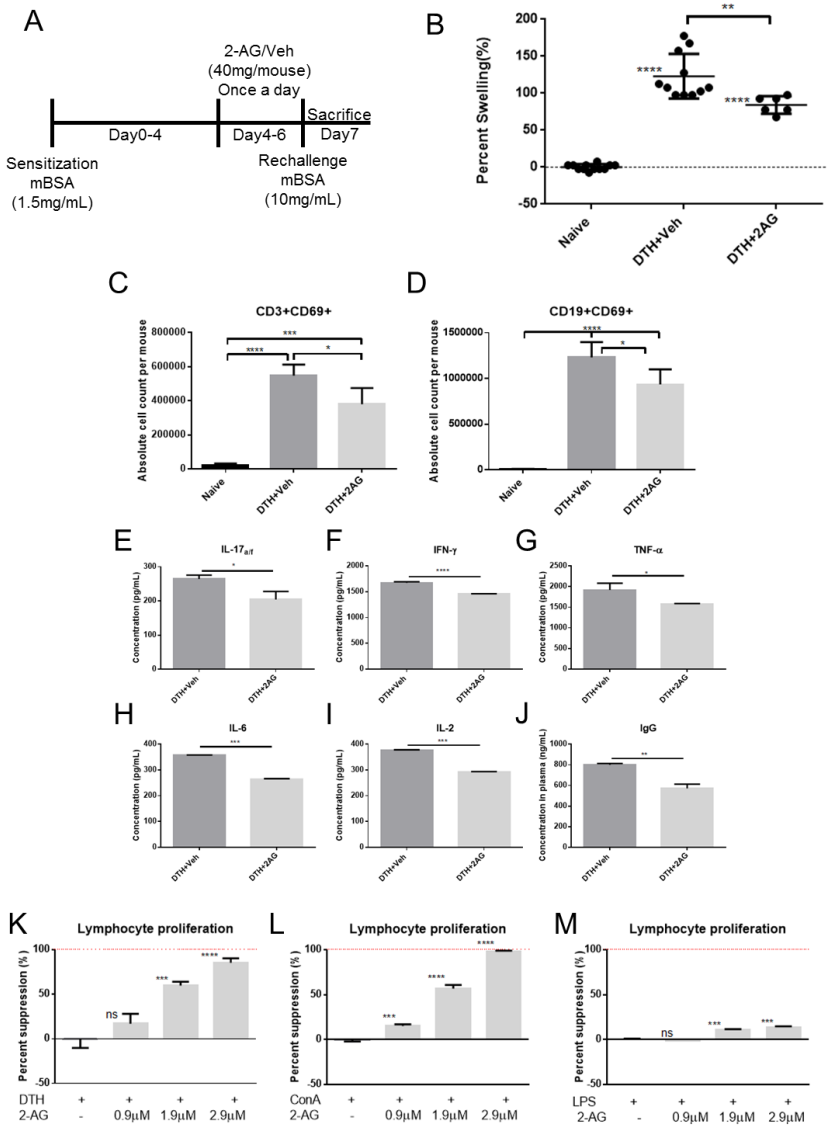

Figure 5.2: Endocannabinoid 2-AG reduces lymphocyte driven inflammation.

2-AG treatment (40 mg/kg) or vehicle (ethanol diluted in 1xPBS) was given on days 4-6 after sensitization. Disease parameters, as described previously, were assessed (n=4 per treatment group). (A) Schematic of model and treatment regimen. (B) Relative percent swelling compared to naïve mouse footpad. (C-D) Absolute cell counts (C) CD3+CD69+ T cell activation and (D) CD19+CD69+ B cell activation. Cytokine secretion was assessed by plating splenocytes with PMA and Ca Ionomycin. (E-I) Secreted levels of (E) IL-$17_{a/f}$, (F) IFN-γ, (G) TNF-α, (H) IL-6, and (I) IL-2. (J) Plasma collected 24 hours after mBSA rechallenge and assessed for IgG levels. (K-M) Splenocytes were stimulated with (K) mBSA rechallenge (10 mg/mL *in vivo*), (L) ConA (2.5ug/mL), or (M) LPS (5.0ug/mL), treated with 2-AG, and co-cultured with 2uCi of [^{3}H]thymidine to assess proliferation. Representative data from replicate experiments; Student's T test or ANOVA/Tukey * $p<0.05$ ** $p<0.01$ ***$p<0.001$ ****$p<0.0001$

CHAPTER VI: SUMMARY AND CONCLUSION

In the current study, we examined the ability of THC to act as a regulator of epigenetic modifications. We first focused on immuneregulatory MDSCs. While there have been studies showing that THC treatment can alter miRNA expression in MDSCs, no studies have determined the impact of DNA methylation in these cells (87). We found that while global methylation patterns, when compared to naïve bone marrow resident MDSCs, were not significantly altered in THC-induced MDSCs, methylation at specific loci was. Specifically, methylation was decreased for Arg1 and STAT3 in THC-induced MDSCs indicative of increased suppressive function.

Next, we looked at the impact of THC on epigenetic modifications in T cells. While research on THC-mediated epigenetic modifications in T cells is severely limited what does exist has focused on inhibition of classical, Th1, inflammation (88); (240); (38). As such, we assessed THC-mediated miRNA regulation in the draining lymph nodes of DTH mice which exhibit both Th1 and Th17 proinflammatory signals (69); (52). We found that miRNA dysregulation due to type IV hypersensitivity was regulated back to naive levels with THC treatment. In particular, miRNAs associated with inflammation, such as miR-21, were decreased, and anti-inflammatory miRNAs, including miR-29b, were overexpressed in THC treated DTH mice.

It has been shown that THC can inhibit Th1 driven inflammation, however its ability to attenuate transplant rejection, a well-established model of Th1 inflammation, has not been elucidated (158). We found that THC treatment significantly reduced Th1 proinflammatory cytokines, including IFN-γ and TNF-α. Furthermore, THC treatment increased survival of both cellular and full thickness skin allogenic grafts in a CB1 dependent manner. We determined that CB1 receptor activation by THC resulted in the mobilization highly immune suppressive of MDSCs. Interestingly, THC induction of MDSCs proved necessary for continued allograft survival in our model of HvGD.

The ability of THC to regulate Th17 response has been correlative focusing on THC-mediated Treg induction rather than direct Th17 inhibition (76); (88). As such, we used a type IV hypersensitivity model, which is representative of non-classical Th1/Th17 driven inflammation, to determine if THC can directly inhibit Th17 lineage differentiation. Interestingly, we found that associated cytokines, lineage specific transcription factors, and absolute numbers of Th1 and Th7 subsets were significantly reduced in DTH+THC mice compared to DTH+Veh mice. We showed a direct link between THC treatment and regulation of both Th1 and Th17 differentiation via miRNA regulation. Specifically, THC treatment of DTH mice increased IFN-γ targeting miRNA miR-29b, halting Th1 response. Concurrently, THC treatment reduced miR-21 expression freeing SMAD7, a regulator of TGFβ mediated TH17 differentiation.

The literature shows that endocannabinoids, the endogenous ligands for the cannabinoid receptors, are often elevated in inflammatory models including autoimmunity and hypersensitivity (263); (264); (259); (260); (261); (249). This evidence in the past was associated with the endocannabinoids exacerbating

inflammation, in particular 2-AG. However, this ideology conflicted with the wealth of data surrounding the exogenous cannabinoid THC. To this end we used exogenous 2-AG, a full agonist for both CB1 and CB2 receptors, therapeutically in a DTH model. We found that 2-AG, like THC a partial agonist at CB1 and CB2 receptors, reduced inflammation associated with type IV hypersensitivity. Specifically, we observed that exogenous treatment with 2-AG reduced lymphocyte activation, the secretion of proinflammatory cytokines, and proliferation. Furthermore, we found that the anti-inflammatory properties seen in DTH were closely mirrored in ConA T cell stimulation. Together, these data suggested that 2-AG was inhibiting hypersensitivity in a T cell specific manner.

The current findings suggest that cannabinoids can inhibit a wide range of inflammatory pathways. Additionally, the therapeutic use of CB receptor agonists seem to be particularly useful as an anti-inflammatory treatment due to the ability of the cannabinoid to attenuate inflammation via multiple pathways. Specifically, we have shown that THC inhibits Th1 and/or Th17 driven inflammation through epigenetic modulation, regulation of T helper cell differentiation, and induction of T cell suppressive MDSCs. We have further highlighted the importance of the EC system in immunoregulation through the therapeutic use of 2-AG in DTH. Taken together, our findings suggest that cannabinoid system plays a critical role in the regulation of inflammation, thereby offering unique targeting opportunities to treat a wide array of clinical disorders associated with chronic inflammation.

REFERENCES

1. Abel, E. L. 1980 *Marijuana, The first twelve thousand years.* Plenum Press, New York.
2. Gaoni, Y., Mechoulam, R. 1964. Isolation, structure and partial synthesis of an active constituent of hashish. *Journal of American Chemical Society* 86: 1646-1647.
3. Tanasescu, R., and C. S. Constantinescu. 2010. Cannabinoids and the immune system: an overview. *Immunobiology* 215: 588-597.
4. Matsuda, L. A., S. J. Lolait, M. J. Brownstein, A. C. Young, and T. I. Bonner. 1990. Structure of a cannabinoid receptor and functional expression of the cloned cDNA. *Nature* 346: 561-564.
5. Munro, S., Thomas, K.L., Abu-Shaar, M. 1992. Molecular characterization of a peripheral receptor for cannabinoids. *Nature* 365: 61-65.
6. Zygmunt, P. M., J. Petersson, D. A. Andersson, H. Chuang, M. Sorgard, V. Di Marzo, D. Julius, and E. D. Hogestatt. 1999. Vanilloid receptors on sensory nerves mediate the vasodilator action of anandamide. *Nature* 400: 452-457.
7. Mezey, E., Z. E. Toth, D. N. Cortright, M. K. Arzubi, J. E. Krause, R. Elde, A. Guo, P. M. Blumberg, and A. Szallasi. 2000. Distribution of mRNA for vanilloid receptor subtype 1 (VR1), and VR1-like immunoreactivity, in the central nervous

system of the rat and human. *Proceedings of the National Academy of Sciences of the United States of America* 97: 3655-3660.

8. Saunders, C. I., R. G. Fassett, and D. P. Geraghty. 2009. Up-regulation of TRPV1 in mononuclear cells of end-stage kidney disease patients increases susceptibility to N-arachidonoyl-dopamine (NADA)-induced cell death. *Biochim Biophys Acta* 1792: 1019-1026.

9. Sharir, H., and M. E. Abood. 2010. Pharmacological characterization of GPR55, a putative cannabinoid receptor. *Pharmacol Ther* 126: 301-313.

10. Ryberg, E., N. Larsson, S. Sjogren, S. Hjorth, N. O. Hermansson, J. Leonova, T. Elebring, K. Nilsson, T. Drmota, and P. J. Greasley. 2007. The orphan receptor GPR55 is a novel cannabinoid receptor. *Br J Pharmacol* 152: 1092-1101.

11. Oka, S., K. Nakajima, A. Yamashita, S. Kishimoto, and T. Sugiura. 2007. Identification of GPR55 as a lysophosphatidylinositol receptor. *Biochem Biophys Res Commun* 362: 928-934.

12. Moldrich, G., and T. Wenger. 2000. Localization of the CB1 cannabinoid receptor in the rat brain. An immunohistochemical study. *Peptides* 21: 1735-1742.

13. Parolaro, D. 1999. Presence and functional regulation of cannabinoid receptors in immune cells. *Life Sci* 65: 637-644.

14. Onaivi, E. S., H. Ishiguro, J. P. Gong, S. Patel, A. Perchuk, P. A. Meozzi, L. Myers, Z. Mora, P. Tagliaferro, E. Gardner, A. Brusco, B. E. Akinshola, Q. R. Liu, B. Hope, S. Iwasaki, T. Arinami, L. Teasenfitz, and G. R. Uhl. 2006. Discovery of the presence and functional expression of cannabinoid CB2 receptors in brain. *Annals of the New York Academy of Sciences* 1074: 514-536.

15. Barnett-Norris, J., D. P. Hurst, D. L. Lynch, F. Guarnieri, A. Makriyannis, and P. H. Reggio. 2002. Conformational memories and the endocannabinoid binding site at the cannabinoid CB1 receptor. *Journal of medicinal chemistry* 45: 3649-3659.

16. Song, Z. H., and T. I. Bonner. 1996. A lysine residue of the cannabinoid receptor is critical for receptor recognition by several agonists but not WIN55212-2. *Mol Pharmacol* 49: 891-896.

17. Bouaboula, M., D. Dussossoy, and P. Casellas. 1999. Regulation of peripheral cannabinoid receptor CB2 phosphorylation by the inverse agonist SR 144528. Implications for receptor biological responses. *J Biol Chem* 274: 20397-20405.

18. Song, Z. H., C. A. Slowey, D. P. Hurst, and P. H. Reggio. 1999. The difference between the CB(1) and CB(2) cannabinoid receptors at position 5.46 is crucial for the selectivity of WIN55212-2 for CB(2). *Mol Pharmacol* 56: 834-840.

19. Feng, W., and Z. H. Song. 2003. Effects of D3.49A, R3.50A, and A6.34E mutations on ligand binding and activation of the cannabinoid-2 (CB2) receptor. *Biochem Pharmacol* 65: 1077-1085.

20. McAllister, S. D., G. Rizvi, S. Anavi-Goffer, D. P. Hurst, J. Barnett-Norris, D. L. Lynch, P. H. Reggio, and M. E. Abood. 2003. An aromatic microdomain at the cannabinoid CB(1) receptor constitutes an agonist/inverse agonist binding region. *Journal of medicinal chemistry* 46: 5139-5152.

21. Rossi, S., G. Bernardi, and D. Centonze. 2010. The endocannabinoid system in the inflammatory and neurodegenerative processes of multiple sclerosis and of amyotrophic lateral sclerosis. *Exp Neurol* 224: 92-102.

22. Devane, W. A., L. Hanus, A. Breuer, R. G. Pertwee, L. A. Stevenson, G. Griffin, D. Gibson, A. Mandelbaum, A. Etinger, and R. Mechoulam. 1992. Isolation and structure of a brain constituent that binds to the cannabinoid receptor. *Science* 258: 1946-1949.

23. Mechoulam, R., S. Ben-Shabat, L. Hanus, M. Ligumsky, N. E. Kaminski, A. R. Schatz, A. Gopher, S. Almog, B. R. Martin, D. R. Compton, and et al. 1995. Identification of an endogenous 2-monoglyceride, present in canine gut, that binds to cannabinoid receptors. *Biochem Pharmacol* 50: 83-90.

24. Sugiura, T., S. Kondo, A. Sukagawa, S. Nakane, A. Shinoda, K. Itoh, A. Yamashita, and K. Waku. 1995. 2-Arachidonoylglycerol: a possible endogenous cannabinoid receptor ligand in brain. *Biochem Biophys Res Commun* 215: 89-97.

25. Cravatt, B. F., and A. H. Lichtman. 2004. The endogenous cannabinoid system and its role in nociceptive behavior. *J Neurobiol* 61: 149-160.

26. Ueda, N. 2002. Endocannabinoid hydrolases. *Prostaglandins & other lipid mediators* 68-69: 521-534.

27. Dinh, T. P., T. F. Freund, and D. Piomelli. 2002. A role for monoglyceride lipase in 2-arachidonoylglycerol inactivation. *Chemistry and physics of lipids* 121: 149-158.

28. Pandey, R., V. L. Hegde, N. P. Singh, L. Hofseth, U. Singh, S. Ray, M. Nagarkatti, and P. S. Nagarkatti. 2009. Use of cannabinoids as a novel therapeutic modality against autoimmune hepatitis. *Vitam Horm* 81: 487-504.

29. Di Marzo, V., De Petrocellis, L., Bisogno, T. . 2005. The biosynthesis, fate and pharmacological properties of endocannabinoids. *The Handbook of Experimental Pharmacology* 168: 147-185.

30. Liu, J., L. Wang, J. Harvey-White, D. Osei-Hyiaman, R. Razdan, Q. Gong, A. C. Chan, Z. Zhou, B. X. Huang, H. Y. Kim, and G. Kunos. 2006. A biosynthetic pathway for anandamide. *Proceedings of the National Academy of Sciences of the United States of America* 103: 13345-13350.

31. Sugiura, T., Y. Kobayashi, S. Oka, and K. Waku. 2002. Biosynthesis and degradation of anandamide and 2-arachidonoylglycerol and their possible physiological significance. *Prostaglandins, leukotrienes, and essential fatty acids* 66: 173-192.

32. Prescott, S. M., and P. W. Majerus. 1983. Characterization of 1,2-diacylglycerol hydrolysis in human platelets. Demonstration of an arachidonoyl-monoacylglycerol intermediate. *J Biol Chem* 258: 764-769.

33. Fowler, C. J. 2007. The pharmacology of the cannabinoid system--a question of efficacy and selectivity. *Mol Neurobiol* 36: 15-25.

34. Borner, C., V. Hollt, and J. Kraus. 2007. Activation of human T cells induces upregulation of cannabinoid receptor type 1 transcription. *Neuroimmunomodulation* 14: 281-286.

35. Jiang, C., and B. F. Pugh. 2009. Nucleosome positioning and gene regulation: advances through genomics. *Nature reviews. Genetics* 10: 161-172.

36. Zhou, V. W., A. Goren, and B. E. Bernstein. 2011. Charting histone modifications and the functional organization of mammalian genomes. *Nature reviews. Genetics* 12: 7-18.

37. Chen, H. P., Y. T. Zhao, and T. C. Zhao. 2015. Histone deacetylases and mechanisms of regulation of gene expression. *Critical reviews in oncogenesis* 20: 35-47.

38. Yang, X., V. L. Hegde, R. Rao, J. Zhang, P. S. Nagarkatti, and M. Nagarkatti. 2014. Histone modifications are associated with Delta(9)-tetrahydrocannabinol-mediated alterations in antigen-specific T cell responses. *J Biol Chem*.

39. Jeltsch, A. 2006. On the enzymatic properties of Dnmt1: specificity, processivity, mechanism of linear diffusion and allosteric regulation of the enzyme. *Epigenetics : official journal of the DNA Methylation Society* 1: 63-66.

40. Bartel, D. P. 2009. MicroRNAs: target recognition and regulatory functions. *Cell* 136: 215-233.

41. Jeltsch, A. 2006. Molecular enzymology of mammalian DNA methyltransferases. *Current topics in microbiology and immunology* 301: 203-225.

42. Robertson, K. D. 2005. DNA methylation and human disease. *Nature reviews. Genetics* 6: 597-610.

43. Feinberg, A. P., C. W. Gehrke, K. C. Kuo, and M. Ehrlich. 1988. Reduced genomic 5-methylcytosine content in human colonic neoplasia. *Cancer research* 48: 1159-1161.

44. Baylin, S. B., and J. G. Herman. 2000. DNA hypermethylation in tumorigenesis: epigenetics joins genetics. *Trends in genetics : TIG* 16: 168-174.

45. Hamerman, J. A., S. T. Page, and A. M. Pullen. 1997. Distinct methylation states of the CD8 beta gene in peripheral T cells and intraepithelial lymphocytes. *J Immunol* 159: 1240-1246.

46. Fitzpatrick, D. R., K. M. Shirley, L. E. McDonald, H. Bielefeldt-Ohmann, G. F. Kay, and A. Kelso. 1998. Distinct methylation of the interferon gamma (IFN-gamma) and interleukin 3 (IL-3) genes in newly activated primary CD8+ T lymphocytes: regional IFN-gamma promoter demethylation and mRNA expression are heritable in CD44(high)CD8+ T cells. *The Journal of experimental medicine* 188: 103-117.

47. Cedar, H., and Y. Bergman. 1999. Developmental regulation of immune system gene rearrangement. *Current opinion in immunology* 11: 64-69.

48. Lee, R. C., R. L. Feinbaum, and V. Ambros. 1993. The C. elegans heterochronic gene lin-4 encodes small RNAs with antisense complementarity to lin-14. *Cell* 75: 843-854.

49. Oestreich, K. J., and A. S. Weinmann. 2012. Encoding stability versus flexibility: lessons learned from examining epigenetics in T helper cell differentiation. *Current topics in microbiology and immunology* 356: 145-164.

50. Hirahara, K., G. Vahedi, K. Ghoreschi, X. P. Yang, S. Nakayamada, Y. Kanno, J. J. O'Shea, and A. Laurence. 2011. Helper T-cell differentiation and plasticity: insights from epigenetics. *Immunology* 134: 235-245.

51. Leung, S., X. Liu, L. Fang, X. Chen, T. Guo, and J. Zhang. 2010. The cytokine milieu in the interplay of pathogenic Th1/Th17 cells and regulatory T cells in autoimmune disease. *Cellular & molecular immunology* 7: 182-189.

52. Nakae, S., Y. Komiyama, A. Nambu, K. Sudo, M. Iwase, I. Homma, K. Sekikawa, M. Asano, and Y. Iwakura. 2002. Antigen-specific T cell sensitization is impaired in IL-17-deficient mice, causing suppression of allergic cellular and humoral responses. *Immunity* 17: 375-387.

53. Yin, B., G. Ma, C. Y. Yen, Z. Zhou, G. X. Wang, C. M. Divino, S. Casares, S. H. Chen, W. C. Yang, and P. Y. Pan. 2010. Myeloid-derived suppressor cells prevent type 1 diabetes in murine models. *J Immunol* 185: 5828-5834.

54. Ugel, S., F. Delpozzo, G. Desantis, F. Papalini, F. Simonato, N. Sonda, S. Zilio, and V. Bronte. 2009. Therapeutic targeting of myeloid-derived suppressor cells. *Current opinion in pharmacology* 9: 470-481.

55. Cripps, J. G., and J. D. Gorham. 2011. MDSC in autoimmunity. *Int Immunopharmacol* 11: 789-793.

56. Guan, H., N. P. Singh, U. P. Singh, P. S. Nagarkatti, and M. Nagarkatti. 2012. Resveratrol prevents endothelial cells injury in high-dose interleukin-2 therapy against melanoma. *PloS one* 7: e35650.

57. Gabrilovich, D. I., and S. Nagaraj. 2009. Myeloid-derived suppressor cells as regulators of the immune system. *Nature reviews. Immunology* 9: 162-174.

58. Kusmartsev, S., Y. Nefedova, D. Yoder, and D. I. Gabrilovich. 2004. Antigen-specific inhibition of CD8+ T cell response by immature myeloid cells in cancer is mediated by reactive oxygen species. *J Immunol* 172: 989-999.

59. Zhao, X., O. Boenisch, M. Yeung, B. Mfarrej, S. Yang, L. A. Turka, M. H. Sayegh, J. Iacomini, and X. Yuan. 2012. Critical role of proinflammatory cytokine IL-6 in allograft rejection and tolerance. *American journal of*

transplantation : official journal of the American Society of Transplantation and the American Society of Transplant Surgeons 12: 90-101.

60. De Wilde, V., N. Van Rompaey, M. Hill, J. F. Lebrun, P. Lemaitre, F. Lhomme, C. Kubjak, B. Vokaer, G. Oldenhove, L. M. Charbonnier, M. C. Cuturi, M. Goldman, and A. Le Moine. 2009. Endotoxin-induced myeloid-derived suppressor cells inhibit alloimmune responses via heme oxygenase-1. *American journal of transplantation : official journal of the American Society of Transplantation and the American Society of Transplant Surgeons* 9: 2034-2047.

61. Tedesco, D., and L. Haragsim. 2012. Cyclosporine: a review. *Journal of transplantation* 2012: 230386.

62. Powell, J. D., C. G. Lerner, G. R. Ewoldt, and R. H. Schwartz. 1999. The -180 site of the IL-2 promoter is the target of CREB/CREM binding in T cell anergy. *J Immunol* 163: 6631-6639.

63. Campara, M., I. G. Tzvetanov, and J. Oberholzer. 2010. Interleukin-2 receptor blockade with humanized monoclonal antibody for solid organ transplantation. *Expert opinion on biological therapy* 10: 959-969.

64. Villarroel, M. C., M. Hidalgo, and A. Jimeno. 2009. Mycophenolate mofetil: An update. *Drugs of today* 45: 521-532.

65. Grenda, R., and N. J. Webb. 2010. Steroid minimization in pediatric renal transplantation: Early withdrawal or avoidance? *Pediatric transplantation* 14: 961-967.

66. Van den Hof, W. F., A. Van Summeren, A. Lommen, M. L. Coonen, K. Brauers, M. van Herwijnen, W. K. Wodzig, and J. C. Kleinjans. 2014. Integrative cross-

omics analysis in primary mouse hepatocytes unravels mechanisms of cyclosporin A-induced hepatotoxicity. *Toxicology* 324: 18-26.

67. Engels, E. A., R. M. Pfeiffer, J. F. Fraumeni, Jr., B. L. Kasiske, A. K. Israni, J. J. Snyder, R. A. Wolfe, N. P. Goodrich, A. R. Bayakly, C. A. Clarke, G. Copeland, J. L. Finch, M. L. Fleissner, M. T. Goodman, A. Kahn, L. Koch, C. F. Lynch, M. M. Madeleine, K. Pawlish, C. Rao, M. A. Williams, D. Castenson, M. Curry, R. Parsons, G. Fant, and M. Lin. 2011. Spectrum of cancer risk among US solid organ transplant recipients. *Jama* 306: 1891-1901.

68. Ghaziani, T., H. Sendi, S. Shahraz, P. Zamor, and H. L. Bonkovsky. 2014. Hepatitis B and liver transplantation: Molecular and clinical features that influence recurrence and outcome. *World journal of gastroenterology : WJG* 20: 14142-14155.

69. Fong, T. A., and T. R. Mosmann. 1989. The role of IFN-gamma in delayed-type hypersensitivity mediated by Th1 clones. *J Immunol* 143: 2887-2893.

70. Esser, P. R., U. Wolfle, C. Durr, F. D. von Loewenich, C. M. Schempp, M. A. Freudenberg, T. Jakob, and S. F. Martin. 2012. Contact sensitizers induce skin inflammation via ROS production and hyaluronic acid degradation. *PloS one* 7: e41340.

71. McFadden, J. P., R. J. Dearman, J. M. White, D. A. Basketter, and I. Kimber. 2011. The Hapten-Atopy hypothesis II: the 'cutaneous hapten paradox'. *Clinical and experimental allergy : journal of the British Society for Allergy and Clinical Immunology* 41: 327-337.

72. McFadden, J. P., D. A. Basketter, R. J. Dearman, and I. R. Kimber. 2011. Extra domain A-positive fibronectin-positive feedback loops and their association with cutaneous inflammatory disease. *Clinics in dermatology* 29: 257-265.

73. Howlett, A. C., and S. Mukhopadhyay. 2000. Cellular signal transduction by anandamide and 2-arachidonoylglycerol. *Chemistry and physics of lipids* 108: 53-70.

74. Galve-Roperh, I., C. Sanchez, M. L. Cortes, T. Gomez del Pulgar, M. Izquierdo, and M. Guzman. 2000. Anti-tumoral action of cannabinoids: involvement of sustained ceramide accumulation and extracellular signal-regulated kinase activation. *Nat Med* 6: 313-319.

75. Jackson, A. R., V. L. Hegde, P. S. Nagarkatti, and M. Nagarkatti. 2014. Characterization of endocannabinoid-mediated induction of myeloid-derived suppressor cells involving mast cells and MCP-1. *Journal of leukocyte biology* 95: 609-619.

76. Hegde, V. L., S. Hegde, B. F. Cravatt, L. J. Hofseth, M. Nagarkatti, and P. S. Nagarkatti. 2008. Attenuation of experimental autoimmune hepatitis by exogenous and endogenous cannabinoids: involvement of regulatory T cells. *Molecular pharmacology* 74: 20-33.

77. Nagarkatti, P., R. Pandey, S. A. Rieder, V. L. Hegde, and M. Nagarkatti. 2009. Cannabinoids as novel anti-inflammatory drugs. *Future medicinal chemistry* 1: 1333-1349.

78. Pandey, R., V. L. Hegde, M. Nagarkatti, and P. S. Nagarkatti. 2011. Targeting cannabinoid receptors as a novel approach in the treatment of graft-versus-host

disease: evidence from an experimental murine model. *The Journal of pharmacology and experimental therapeutics* 338: 819-828.

79. Klein, T. W., H. Friedman, and S. Specter. 1998. Marijuana, immunity and infection. *Journal of neuroimmunology* 83: 102-115.

80. McKallip, R. J., C. Lombard, B. R. Martin, M. Nagarkatti, and P. S. Nagarkatti. 2002. Delta(9)-tetrahydrocannabinol-induced apoptosis in the thymus and spleen as a mechanism of immunosuppression in vitro and in vivo. *J Pharmacol Exp Ther* 302: 451-465.

81. Do, Y., R. J. McKallip, M. Nagarkatti, and P. S. Nagarkatti. 2004. Activation through cannabinoid receptors 1 and 2 on dendritic cells triggers NF-kappaB-dependent apoptosis: novel role for endogenous and exogenous cannabinoids in immunoregulation. *J Immunol* 173: 2373-2382.

82. Zhu, W., H. Friedman, and T. W. Klein. 1998. Delta9-tetrahydrocannabinol induces apoptosis in macrophages and lymphocytes: involvement of Bcl-2 and caspase-1. *J Pharmacol Exp Ther* 286: 1103-1109.

83. Jackson, A. R., P. Nagarkatti, and M. Nagarkatti. 2014. Anandamide attenuates Th-17 cell-mediated delayed-type hypersensitivity response by triggering IL-10 production and consequent microRNA induction. *PloS one* 9: e93954.

84. McKallip, R. J., M. Nagarkatti, and P. S. Nagarkatti. 2005. Delta-9-tetrahydrocannabinol enhances breast cancer growth and metastasis by suppression of the antitumor immune response. *J Immunol* 174: 3281-3289.

85. Zhu, L. X., S. Sharma, M. Stolina, B. Gardner, M. D. Roth, D. P. Tashkin, and S. M. Dubinett. 2000. Delta-9-tetrahydrocannabinol inhibits antitumor immunity by a CB2 receptor-mediated, cytokine-dependent pathway. *J Immunol* 165: 373-380.

86. Hegde, V. L., M. Nagarkatti, and P. S. Nagarkatti. 2010. Cannabinoid receptor activation leads to massive mobilization of myeloid-derived suppressor cells with potent immunosuppressive properties. *European journal of immunology* 40: 3358-3371.

87. Hegde, V. L., S. Tomar, A. Jackson, R. Rao, X. Yang, U. P. Singh, N. P. Singh, P. S. Nagarkatti, and M. Nagarkatti. 2013. Distinct microRNA expression profile and targeted biological pathways in functional myeloid-derived suppressor cells induced by Delta9-tetrahydrocannabinol in vivo: regulation of CCAAT/enhancer-binding protein alpha by microRNA-690. *J Biol Chem* 288: 36810-36826.

88. Rao, R., P. S. Nagarkatti, and M. Nagarkatti. 2014. Delta Tetrahydrocannabinol attenuates Staphylococcal enterotoxin B-induced inflammatory lung injury and prevents mortality in mice by modulation of miR-17-92 cluster and induction of T-regulatory cells. *Br J Pharmacol*.

89. Lee, M., K. H. Yang, and N. E. Kaminski. 1995. Effects of putative cannabinoid receptor ligands, anandamide and 2-arachidonyl-glycerol, on immune function in B6C3F1 mouse splenocytes. *J Pharmacol Exp Ther* 275: 529-536.

90. Rockwell, C. E., P. Raman, B. L. Kaplan, and N. E. Kaminski. 2008. A COX-2 metabolite of the endogenous cannabinoid, 2-arachidonyl glycerol, mediates suppression of IL-2 secretion in activated Jurkat T cells. *Biochem Pharmacol* 76: 353-361.

91. Ouyang, Y., S. G. Hwang, S. H. Han, and N. E. Kaminski. 1998. Suppression of interleukin-2 by the putative endogenous cannabinoid 2-arachidonyl-glycerol is mediated through down-regulation of the nuclear factor of activated T cells. *Mol Pharmacol* 53: 676-683.

92. Schwarz, H., F. J. Blanco, and M. Lotz. 1994. Anadamide, an endogenous cannabinoid receptor agonist inhibits lymphocyte proliferation and induces apoptosis. *Journal of neuroimmunology* 55: 107-115.

93. Ribeiro, A., V. Ferraz-de-Paula, M. L. Pinheiro, M. Sakai, F. A. Costa-Pinto, and J. Palermo-Neto. 2010. Anandamide prior to sensitization increases cell-mediated immunity in mice. *Int Immunopharmacol* 10: 431-439.

94. Wesolowski, R., J. Markowitz, and W. E. Carson, 3rd. 2013. Myeloid derived suppressor cells - a new therapeutic target in the treatment of cancer. *Journal for immunotherapy of cancer* 1: 10.

95. Keskinov, A. A., and M. R. Shurin. 2014. Myeloid regulatory cells in tumor spreading and metastasis. *Immunobiology*.

96. Hestdal, K., F. W. Ruscetti, J. N. Ihle, S. E. Jacobsen, C. M. Dubois, W. C. Kopp, D. L. Longo, and J. R. Keller. 1991. Characterization and regulation of RB6-8C5 antigen expression on murine bone marrow cells. *J Immunol* 147: 22-28.

97. Movahedi, K., M. Guilliams, J. Van den Bossche, R. Van den Bergh, C. Gysemans, A. Beschin, P. De Baetselier, and J. A. Van Ginderachter. 2008. Identification of discrete tumor-induced myeloid-derived suppressor cell subpopulations with distinct T cell-suppressive activity. *Blood* 111: 4233-4244.

98. Dugast, A. S., T. Haudebourg, F. Coulon, M. Heslan, F. Haspot, N. Poirier, R. Vuillefroy de Silly, C. Usal, H. Smit, B. Martinet, P. Thebault, K. Renaudin, and B. Vanhove. 2008. Myeloid-derived suppressor cells accumulate in kidney allograft tolerance and specifically suppress effector T cell expansion. *J Immunol* 180: 7898-7906.

99. Nagaraj, S., and D. I. Gabrilovich. 2012. Regulation of suppressive function of myeloid-derived suppressor cells by CD4+ T cells. *Seminars in cancer biology* 22: 282-288.

100. Young, H. A., P. Ghosh, J. Ye, J. Lederer, A. Lichtman, J. R. Gerard, L. Penix, C. B. Wilson, A. J. Melvin, M. E. McGurn, and et al. 1994. Differentiation of the T helper phenotypes by analysis of the methylation state of the IFN-gamma gene. *J Immunol* 153: 3603-3610.

101. Gamper, C. J., A. T. Agoston, W. G. Nelson, and J. D. Powell. 2009. Identification of DNA methyltransferase 3a as a T cell receptor-induced regulator of Th1 and Th2 differentiation. *J Immunol* 183: 2267-2276.

102. Guan, H., P. S. Nagarkatti, and M. Nagarkatti. 2011. CD44 Reciprocally regulates the differentiation of encephalitogenic Th1/Th17 and Th2/regulatory T cells through epigenetic modulation involving DNA methylation of cytokine gene promoters, thereby controlling the development of experimental autoimmune encephalomyelitis. *J Immunol* 186: 6955-6964.

103. Chuchawankul, S., M. Shima, N. E. Buckley, C. B. Hartmann, and K. L. McCoy. 2004. Role of cannabinoid receptors in inhibiting macrophage costimulatory activity. *Int Immunopharmacol* 4: 265-278.

104. Sahakian, E., J. J. Powers, J. Chen, S. L. Deng, F. Cheng, A. Distler, D. M. Woods, J. Rock-Klotz, A. L. Sodre, J. I. Youn, K. V. Woan, A. Villagra, D. Gabrilovich, E. M. Sotomayor, and J. Pinilla-Ibarz. 2014. Histone deacetylase 11: A novel epigenetic regulator of myeloid derived suppressor cell expansion and function. *Molecular immunology*.

105. Guan, H., P. S. Nagarkatti, and M. Nagarkatti. 2009. Role of CD44 in the differentiation of Th1 and Th2 cells: CD44-deficiency enhances the development of Th2 effectors in response to sheep RBC and chicken ovalbumin. *J Immunol* 183: 172-180.

106. Langmead, B., C. Trapnell, M. Pop, and S. L. Salzberg. 2009. Ultrafast and memory-efficient alignment of short DNA sequences to the human genome. *Genome biology* 10: R25.

107. Lienhard, M., C. Grimm, M. Morkel, R. Herwig, and L. Chavez. 2014. MEDIPS: genome-wide differential coverage analysis of sequencing data derived from DNA enrichment experiments. *Bioinformatics* 30: 284-286.

108. Shin, H., T. Liu, A. K. Manrai, and X. S. Liu. 2009. CEAS: cis-regulatory element annotation system. *Bioinformatics* 25: 2605-2606.

109. Rouse, M., R. Rao, M. Nagarkatti, and P. S. Nagarkatti. 2014. 3,3'-diindolylmethane ameliorates experimental autoimmune encephalomyelitis by promoting cell cycle arrest and apoptosis in activated T cells through microRNA signaling pathways. *J Pharmacol Exp Ther* 350: 341-352.

110. Abramoff, M. D., Magalhaes, P.J., Ram, S.J. . 2004. Image processing with ImageJ. *Biophotonics International* 11: 36-42.

111. Dietlin, T. A., F. M. Hofman, B. T. Lund, W. Gilmore, S. A. Stohlman, and R. C. van der Veen. 2007. Mycobacteria-induced Gr-1+ subsets from distinct myeloid lineages have opposite effects on T cell expansion. *Journal of leukocyte biology* 81: 1205-1212.

112. Zhu, B., Y. Bando, S. Xiao, K. Yang, A. C. Anderson, V. K. Kuchroo, and S. J. Khoury. 2007. CD11b+Ly-6C(hi) suppressive monocytes in experimental autoimmune encephalomyelitis. *J Immunol* 179: 5228-5237.

113. Kusmartsev, S., and D. I. Gabrilovich. 2005. STAT1 signaling regulates tumor-associated macrophage-mediated T cell deletion. *J Immunol* 174: 4880-4891.

114. Sinha, P., C. Okoro, D. Foell, H. H. Freeze, S. Ostrand-Rosenberg, and G. Srikrishna. 2008. Proinflammatory S100 proteins regulate the accumulation of myeloid-derived suppressor cells. *J Immunol* 181: 4666-4675.

115. Trikha, P., and W. E. Carson, 3rd. 2014. Signaling pathways involved in MDSC regulation. *Biochim Biophys Acta* 1846: 55-65.

116. Wu, L., H. Du, Y. Li, P. Qu, and C. Yan. 2011. Signal transducer and activator of transcription 3 (Stat3C) promotes myeloid-derived suppressor cell expansion and immune suppression during lung tumorigenesis. *The American journal of pathology* 179: 2131-2141.

117. Lozovan, M. G., L. A. Pichugina, L. D. Nikitenko, L. M. Bobrik, and M. G. Stratanovich. 1990. [Association of Wegener's granulomatosis and tumor process]. *Problemy tuberkuleza*: 73-75.

118. Vasquez-Dunddel, D., F. Pan, Q. Zeng, M. Gorbounov, E. Albesiano, J. Fu, R. L. Blosser, A. J. Tam, T. Bruno, H. Zhang, D. Pardoll, and Y. Kim. 2013. STAT3

regulates arginase-I in myeloid-derived suppressor cells from cancer patients. *The Journal of clinical investigation* 123: 1580-1589.

119. Cheng, P., C. A. Corzo, N. Luetteke, B. Yu, S. Nagaraj, M. M. Bui, M. Ortiz, W. Nacken, C. Sorg, T. Vogl, J. Roth, and D. I. Gabrilovich. 2008. Inhibition of dendritic cell differentiation and accumulation of myeloid-derived suppressor cells in cancer is regulated by S100A9 protein. *The Journal of experimental medicine* 205: 2235-2249.

120. Compton, D. R., L. H. Gold, S. J. Ward, R. L. Balster, and B. R. Martin. 1992. Aminoalkylindole analogs: cannabimimetic activity of a class of compounds structurally distinct from delta 9-tetrahydrocannabinol. *J Pharmacol Exp Ther* 263: 1118-1126.

121. Okano, M., S. Xie, and E. Li. 1998. Cloning and characterization of a family of novel mammalian DNA (cytosine-5) methyltransferases. *Nature genetics* 19: 219-220.

122. Hoechst, B., J. Gamrekelashvili, M. P. Manns, T. F. Greten, and F. Korangy. 2011. Plasticity of human Th17 cells and iTregs is orchestrated by different subsets of myeloid cells. *Blood* 117: 6532-6541.

123. Pelaez, B., J. A. Campillo, J. A. Lopez-Asenjo, and J. L. Subiza. 2001. Cyclophosphamide induces the development of early myeloid cells suppressing tumor cell growth by a nitric oxide-dependent mechanism. *J Immunol* 166: 6608-6615.

124. Bonnin, A., R. de Miguel, M. L. Hernandez, J. A. Ramos, and J. J. Fernandez-Ruiz. 1995. The prenatal exposure to delta 9-tetrahydrocannabinol affects the

gene expression and the activity of tyrosine hydroxylase during early brain development. *Life Sci* 56: 2177-2184.

125. Hernandez, M. L., L. Garcia-Gil, F. Berrendero, J. A. Ramos, and J. J. Fernandez-Ruiz. 1997. delta 9-Tetrahydrocannabinol increases activity of tyrosine hydroxylase in cultured fetal mesencephalic neurons. *Journal of molecular neuroscience : MN* 8: 83-91.

126. Perez-Rosado, A., J. Manzanares, J. Fernandez-Ruiz, and J. A. Ramos. 2000. Prenatal Delta(9)-tetrahydrocannabinol exposure modifies proenkephalin gene expression in the fetal rat brain: sex-dependent differences. *Brain research. Developmental brain research* 120: 77-81.

127. Gomez, M., M. Hernandez, B. Johansson, R. de Miguel, J. A. Ramos, and J. Fernandez-Ruiz. 2003. Prenatal cannabinoid and gene expression for neural adhesion molecule L1 in the fetal rat brain. *Brain research. Developmental brain research* 147: 201-207.

128. Maccarrone, M., and A. Finazzi-Agro. 2003. The endocannabinoid system, anandamide and the regulation of mammalian cell apoptosis. *Cell death and differentiation* 10: 946-955.

129. Molina, P. E., A. Amedee, N. J. LeCapitaine, J. Zabaleta, M. Mohan, P. Winsauer, and C. Vande Stouwe. 2011. Cannabinoid neuroimmune modulation of SIV disease. *Journal of neuroimmune pharmacology : the official journal of the Society on NeuroImmune Pharmacology* 6: 516-527.

130. Paradisi, A., N. Pasquariello, D. Barcaroli, and M. Maccarrone. 2008. Anandamide regulates keratinocyte differentiation by inducing DNA methylation in a CB1 receptor-dependent manner. *J Biol Chem* 283: 6005-6012.

131. Nelson, E. D., E. T. Kavalali, and L. M. Monteggia. 2008. Activity-dependent suppression of miniature neurotransmission through the regulation of DNA methylation. *The Journal of neuroscience : the official journal of the Society for Neuroscience* 28: 395-406.

132. Delano, M. J., P. O. Scumpia, J. S. Weinstein, D. Coco, S. Nagaraj, K. M. Kelly-Scumpia, K. A. O'Malley, J. L. Wynn, S. Antonenko, S. Z. Al-Quran, R. Swan, C. S. Chung, M. A. Atkinson, R. Ramphal, D. I. Gabrilovich, W. H. Reeves, A. Ayala, J. Phillips, D. Laface, P. G. Heyworth, M. Clare-Salzler, and L. L. Moldawer. 2007. MyD88-dependent expansion of an immature GR-1(+)CD11b(+) population induces T cell suppression and Th2 polarization in sepsis. *The Journal of experimental medicine* 204: 1463-1474.

133. Lee, I. T., C. C. Lin, C. H. Wang, W. J. Cherng, J. S. Wang, and C. M. Yang. 2013. ATP stimulates PGE(2)/cyclin D1-dependent VSMCs proliferation via STAT3 activation: role of PKCs-dependent NADPH oxidase/ROS generation. *Biochem Pharmacol* 85: 954-964.

134. Hegde, V. L., P. S. Nagarkatti, and M. Nagarkatti. 2011. Role of myeloid-derived suppressor cells in amelioration of experimental autoimmune hepatitis following activation of TRPV1 receptors by cannabidiol. *PloS one* 6: e18281.

135. Rodriguez, P. C., D. G. Quiceno, and A. C. Ochoa. 2007. L-arginine availability regulates T-lymphocyte cell-cycle progression. *Blood* 109: 1568-1573.

136. Pan, P. Y., G. Ma, K. J. Weber, J. Ozao-Choy, G. Wang, B. Yin, C. M. Divino, and S. H. Chen. 2010. Immune stimulatory receptor CD40 is required for T-cell suppression and T regulatory cell activation mediated by myeloid-derived suppressor cells in cancer. *Cancer research* 70: 99-108.

137. Srivastava, M. K., P. Sinha, V. K. Clements, P. Rodriguez, and S. Ostrand-Rosenberg. 2010. Myeloid-derived suppressor cells inhibit T-cell activation by depleting cystine and cysteine. *Cancer research* 70: 68-77.

138. Howlett, A. C., L. C. Blume, and G. D. Dalton. 2010. CB(1) cannabinoid receptors and their associated proteins. *Current medicinal chemistry* 17: 1382-1393.

139. Jeon, Y. J., K. H. Yang, J. T. Pulaski, and N. E. Kaminski. 1996. Attenuation of inducible nitric oxide synthase gene expression by delta 9-tetrahydrocannabinol is mediated through the inhibition of nuclear factor- kappa B/Rel activation. *Mol Pharmacol* 50: 334-341.

140. Ichikawa, M., R. Williams, L. Wang, T. Vogl, and G. Srikrishna. 2011. S100A8/A9 activate key genes and pathways in colon tumor progression. *Molecular cancer research : MCR* 9: 133-148.

141. Hiroshima, Y., K. Hsu, N. Tedla, Y. M. Chung, S. Chow, C. Herbert, and C. L. Geczy. 2014. S100A8 induces IL-10 and protects against acute lung injury. *J Immunol* 192: 2800-2811.

142. Simard, J. C., A. Cesaro, J. Chapeton-Montes, M. Tardif, F. Antoine, D. Girard, and P. A. Tessier. 2013. S100A8 and S100A9 induce cytokine expression and

regulate the NLRP3 inflammasome via ROS-dependent activation of NF-kappaB(1.). *PloS one* 8: e72138.

143. Goyette, J., and C. L. Geczy. 2011. Inflammation-associated S100 proteins: new mechanisms that regulate function. *Amino acids* 41: 821-842.

144. Munder, M., K. Eichmann, J. M. Moran, F. Centeno, G. Soler, and M. Modolell. 1999. Th1/Th2-regulated expression of arginase isoforms in murine macrophages and dendritic cells. *J Immunol* 163: 3771-3777.

145. El Kasmi, K. C., J. E. Qualls, J. T. Pesce, A. M. Smith, R. W. Thompson, M. Henao-Tamayo, R. J. Basaraba, T. Konig, U. Schleicher, M. S. Koo, G. Kaplan, K. A. Fitzgerald, E. I. Tuomanen, I. M. Orme, T. D. Kanneganti, C. Bogdan, T. A. Wynn, and P. J. Murray. 2008. Toll-like receptor-induced arginase 1 in macrophages thwarts effective immunity against intracellular pathogens. *Nature immunology* 9: 1399-1406.

146. Vogl, T., K. Tenbrock, S. Ludwig, N. Leukert, C. Ehrhardt, M. A. van Zoelen, W. Nacken, D. Foell, T. van der Poll, C. Sorg, and J. Roth. 2007. Mrp8 and Mrp14 are endogenous activators of Toll-like receptor 4, promoting lethal, endotoxin-induced shock. *Nat Med* 13: 1042-1049.

147. van Lent, P. L., L. C. Grevers, R. Schelbergen, A. Blom, J. Geurts, A. Sloetjes, T. Vogl, J. Roth, and W. B. van den Berg. 2010. S100A8 causes a shift toward expression of activatory Fcgamma receptors on macrophages via toll-like receptor 4 and regulates Fcgamma receptor expression in synovium during chronic experimental arthritis. *Arthritis and rheumatism* 62: 3353-3364.

148. Klempt, M., H. Melkonyan, H. A. Hofmann, I. Eue, and C. Sorg. 1998. The transcription factors c-myb and C/EBP alpha regulate the monocytic/myeloic gene MRP14. *Immunobiology* 199: 148-151.

149. Gaoni, Y., and R. Mechoulam. 1964. Isolation, Structure, and Partial Synthesis of an Active Constituent of Hashish. *J Am Chem Soc* 86: 1646-1647.

150. Munro, S., K. L. Thomas, and M. Abu-Shaar. 1993. Molecular characterization of a peripheral receptor for cannabinoids. *Nature* 365: 61-65.

151. Glass, M., and J. K. Northup. 1999. Agonist selective regulation of G proteins by cannabinoid CB(1) and CB(2) receptors. *Mol Pharmacol* 56: 1362-1369.

152. Felder, C. C., K. E. Joyce, E. M. Briley, J. Mansouri, K. Mackie, O. Blond, Y. Lai, A. L. Ma, and R. L. Mitchell. 1995. Comparison of the pharmacology and signal transduction of the human cannabinoid CB1 and CB2 receptors. *Mol Pharmacol* 48: 443-450.

153. Agudelo, M., C. Newton, R. Widen, T. Sherwood, L. Nong, H. Friedman, and T. W. Klein. 2008. Cannabinoid receptor 2 (CB2) mediates immunoglobulin class switching from IgM to IgE in cultures of murine-purified B lymphocytes. *Journal of neuroimmune pharmacology : the official journal of the Society on NeuroImmune Pharmacology* 3: 35-42.

154. Newton, C. A., P. J. Chou, I. Perkins, and T. W. Klein. 2009. CB(1) and CB(2) cannabinoid receptors mediate different aspects of delta-9-tetrahydrocannabinol (THC)-induced T helper cell shift following immune activation by Legionella pneumophila infection. *Journal of neuroimmune pharmacology : the official journal of the Society on NeuroImmune Pharmacology* 4: 92-102.

155. Klein, T. W., C. Newton, K. Larsen, L. Lu, I. Perkins, L. Nong, and H. Friedman. 2003. The cannabinoid system and immune modulation. *Journal of leukocyte biology* 74: 486-496.

156. Grotenhermen, F. 2004. Pharmacology of cannabinoids. *Neuro endocrinology letters* 25: 14-23.

157. Borgelt, L. M., K. L. Franson, A. M. Nussbaum, and G. S. Wang. 2013. The pharmacologic and clinical effects of medical cannabis. *Pharmacotherapy* 33: 195-209.

158. Nagarkatti, M., S. A. Rieder, V. L. Hegde, S. Kanada, and P. Nagarkatti. 2010. Do cannabinoids have a therapeutic role in transplantation? *Trends in pharmacological sciences* 31: 345-350.

159. Pereira, G. M., J. F. Miller, and E. M. Shevach. 1990. Mechanism of action of cyclosporine A in vivo. II. T cell priming in vivo to alloantigen can be mediated by an IL-2-independent cyclosporine A-resistant pathway. *J Immunol* 144: 2109-2116.

160. Schorlemmer, H. U., E. Ruuth, and R. Kurrle. 1998. Regulation of alloreactivity in the popliteal lymph node assay by the new immunosuppressants: malononitrilamides. *Transplant international : official journal of the European Society for Organ Transplantation* 11 Suppl 1: S448-451.

161. Chaudhuri, S., S. Chaudhuri, R. Barfoot, S. Denham, and J. G. Hall. 1993. The stimulation by dendritic cells of host-versus-graft reactivity in vivo. *Immunology and cell biology* 71 (Pt 6): 527-533.

162. Koch, E. 1990. Reduction in popliteal lymph node graft-versus-host reactivity by homologous and heterologous pregnancy serum. *Journal of reproductive immunology* 18: 147-159.

163. Chen, J. C., M. L. Chang, and M. O. Muench. 2003. A kinetic study of the murine mixed lymphocyte reaction by 5,6-carboxyfluorescein diacetate succinimidyl ester labeling. *Journal of immunological methods* 279: 123-133.

164. Jackson, A. R., V. L. Hegde, P. S. Nagarkatti, and M. Nagarkatti. 2013. Characterization of endocannabinoid-mediated induction of myeloid-derived suppressor cells involving mast cells and MCP-1. *Journal of leukocyte biology*.

165. Ma, C., T. Kapanadze, J. Gamrekelashvili, M. P. Manns, F. Korangy, and T. F. Greten. 2012. Anti-Gr-1 antibody depletion fails to eliminate hepatic myeloid-derived suppressor cells in tumor-bearing mice. *Journal of leukocyte biology* 92: 1199-1206.

166. Billingham, R. E., and P. B. Medawar. 1951. The Technique of Free Skin Grafting in Mammals. *J Exp Biol* 28: 385-&.

167. Krupnick, A. S., D. Kreisel, S. H. Popma, K. R. Balsara, W. Y. Szeto, A. M. Krasinskas, M. Riha, A. D. Wells, L. A. Turka, and B. R. Rosengard. 2002. Mechanism of T cell-mediated endothelial apoptosis. *Transplantation* 74: 871-876.

168. Semenov, V. I., and N. P. Reshetnikov. 1990. [The Bristow-Latarjet operation in the treatment of habitual dislocation of the shoulder]. *Ortopediia travmatologiia i protezirovanie*: 46-47.

169. Ostanin, D. V., and D. Bhattacharya. 2013. Myeloid-derived suppressor cells in the inflammatory bowel diseases. *Inflammatory bowel diseases* 19: 2468-2477.

170. Ostrand-Rosenberg, S., P. Sinha, O. Chornoguz, and C. Ecker. 2012. Regulating the suppressors: apoptosis and inflammation govern the survival of tumor-induced myeloid-derived suppressor cells (MDSC). *Cancer immunology, immunotherapy : CII* 61: 1319-1325.

171. Huang, B., Z. Lei, J. Zhao, W. Gong, J. Liu, Z. Chen, Y. Liu, D. Li, Y. Yuan, G. M. Zhang, and Z. H. Feng. 2007. CCL2/CCR2 pathway mediates recruitment of myeloid suppressor cells to cancers. *Cancer letters* 252: 86-92.

172. Adams, I. B., and B. R. Martin. 1996. Cannabis: pharmacology and toxicology in animals and humans. *Addiction* 91: 1585-1614.

173. Croxford, J. L., and T. Yamamura. 2005. Cannabinoids and the immune system: potential for the treatment of inflammatory diseases? *Journal of neuroimmunology* 166: 3-18.

174. Massi, P., A. Vaccani, and D. Parolaro. 2006. Cannabinoids, immune system and cytokine network. *Current pharmaceutical design* 12: 3135-3146.

175. Ashton, J. C. 2007. Cannabinoids for the treatment of inflammation. *Current opinion in investigational drugs* 8: 373-384.

176. Yuan, M., S. M. Kiertscher, Q. Cheng, R. Zoumalan, D. P. Tashkin, and M. D. Roth. 2002. Delta 9-Tetrahydrocannabinol regulates Th1/Th2 cytokine balance in activated human T cells. *Journal of neuroimmunology* 133: 124-131.

177. Lombard, C., V. L. Hegde, M. Nagarkatti, and P. S. Nagarkatti. 2011. Perinatal exposure to Delta9-tetrahydrocannabinol triggers profound defects in T cell

differentiation and function in fetal and postnatal stages of life, including decreased responsiveness to HIV antigens. *J Pharmacol Exp Ther* 339: 607-617.

178. Young, M. R., M. Newby, and H. T. Wepsic. 1987. Hematopoiesis and suppressor bone marrow cells in mice bearing large metastatic Lewis lung carcinoma tumors. *Cancer research* 47: 100-105.

179. Zhang, Y., Y. Bi, H. Yang, X. Chen, H. Liu, Y. Lu, Z. Zhang, J. Liao, S. Yang, Y. Chu, R. Yang, and G. Liu. 2014. mTOR limits the recruitment of CD11b+Gr1+Ly6Chigh myeloid-derived suppressor cells in protecting against murine immunological hepatic injury. *Journal of leukocyte biology* 95: 961-970.

180. Highfill, S. L., P. C. Rodriguez, Q. Zhou, C. A. Goetz, B. H. Koehn, R. Veenstra, P. A. Taylor, A. Panoskaltsis-Mortari, J. S. Serody, D. H. Munn, J. Tolar, A. C. Ochoa, and B. R. Blazar. 2010. Bone marrow myeloid-derived suppressor cells (MDSCs) inhibit graft-versus-host disease (GVHD) via an arginase-1-dependent mechanism that is up-regulated by interleukin-13. *Blood* 116: 5738-5747.

181. Jia, W., V. L. Hegde, N. P. Singh, D. Sisco, S. Grant, M. Nagarkatti, and P. S. Nagarkatti. 2006. Delta9-tetrahydrocannabinol-induced apoptosis in Jurkat leukemia T cells is regulated by translocation of Bad to mitochondria. *Molecular cancer research : MCR* 4: 549-562.

182. Meyer, C., A. Sevko, M. Ramacher, A. V. Bazhin, C. S. Falk, W. Osen, I. Borrello, M. Kato, D. Schadendorf, M. Baniyash, and V. Umansky. 2011. Chronic inflammation promotes myeloid-derived suppressor cell activation blocking antitumor immunity in transgenic mouse melanoma model. *Proceedings*

of the National Academy of Sciences of the United States of America 108: 17111-17116.

183. Robinson, R. H., J. J. Meissler, J. M. Breslow-Deckman, J. Gaughan, M. W. Adler, and T. K. Eisenstein. 2013. Cannabinoids Inhibit T-cells via Cannabinoid Receptor 2 in an In Vitro Assay for Graft Rejection, the Mixed Lymphocyte Reaction. *Journal of neuroimmune pharmacology : the official journal of the Society on NeuroImmune Pharmacology*.

184. Daaka, Y., H. Friedman, and T. W. Klein. 1996. Cannabinoid receptor proteins are increased in Jurkat, human T-cell line after mitogen activation. *J Pharmacol Exp Ther* 276: 776-783.

185. Borner, C., V. Hollt, W. Sebald, and J. Kraus. 2007. Transcriptional regulation of the cannabinoid receptor type 1 gene in T cells by cannabinoids. *Journal of leukocyte biology* 81: 336-343.

186. Massi, P., P. Sacerdote, W. Ponti, D. Fuzio, B. Manfredi, D. Vigano, T. Rubino, M. Bardotti, and D. Parolaro. 1998. Immune function alterations in mice tolerant to delta9-tetrahydrocannabinol: functional and biochemical parameters. *Journal of neuroimmunology* 92: 60-66.

187. Lu, H., B. L. Kaplan, T. Ngaotepprutaram, and N. E. Kaminski. 2009. Suppression of T cell costimulator ICOS by Delta9-tetrahydrocannabinol. *Journal of leukocyte biology* 85: 322-329.

188. Annibaldi, A., A. Sajeva, M. Muscolini, F. Ciccosanti, M. Corazzari, M. Piacentini, and L. Tuosto. 2008. CD28 ligation in the absence of TCR promotes

RelA/NF-kappaB recruitment and trans-activation of the HIV-1 LTR. *European journal of immunology* 38: 1446-1451.

189. Zhou, P., K. W. Hwang, D. A. Palucki, Z. Guo, M. Boothby, K. A. Newell, and M. L. Alegre. 2003. Impaired NF-kappaB activation in T cells permits tolerance to primary heart allografts and to secondary donor skin grafts. *American journal of transplantation : official journal of the American Society of Transplantation and the American Society of Transplant Surgeons* 3: 139-147.

190. Ying, H., H. Fu, M. L. Rose, A. M. McCormack, P. Sarathchandra, K. Okkenhaug, and F. M. Marelli-Berg. 2012. Genetic or pharmaceutical blockade of phosphoinositide 3-kinase p110delta prevents chronic rejection of heart allografts. *PloS one* 7: e32892.

191. Joss, A., M. Akdis, A. Faith, K. Blaser, and C. A. Akdis. 2000. IL-10 directly acts on T cells by specifically altering the CD28 co-stimulation pathway. *European journal of immunology* 30: 1683-1690.

192. Harding, F. A., J. G. McArthur, J. A. Gross, D. H. Raulet, and J. P. Allison. 1992. CD28-mediated signalling co-stimulates murine T cells and prevents induction of anergy in T-cell clones. *Nature* 356: 607-609.

193. Ongradi, J., S. Specter, A. Horvath, and H. Friedman. 1999. [Additive effect of marihuana and retrovirus in the anergy of natural killer cells in mice]. *Orvosi hetilap* 140: 81-84.

194. Noble, A., D. Z. Staynov, and D. M. Kemeny. 1993. Generation of rat Th2-like cells in vitro is interleukin-4-dependent and inhibited by interferon-gamma. *Immunology* 79: 562-567.

195. Fishman, M. A., and A. S. Perelson. 1994. Th1/Th2 cross regulation. *Journal of theoretical biology* 170: 25-56.

196. Romagnani, S., E. Maggi, and G. Del Prete. 1994. An alternative view of the Th1/Th2 switch hypothesis in HIV infection. *AIDS research and human retroviruses* 10: iii-ix.

197. Singh, V. K., S. Mehrotra, and S. S. Agarwal. 1999. The paradigm of Th1 and Th2 cytokines: its relevance to autoimmunity and allergy. *Immunologic research* 20: 147-161.

198. McGuirk, P., and K. H. Mills. 2002. Pathogen-specific regulatory T cells provoke a shift in the Th1/Th2 paradigm in immunity to infectious diseases. *Trends in immunology* 23: 450-455.

199. Romagnani, S. 2004. Immunologic influences on allergy and the TH1/TH2 balance. *The Journal of allergy and clinical immunology* 113: 395-400.

200. Crane, I. J., and J. V. Forrester. 2005. Th1 and Th2 lymphocytes in autoimmune disease. *Critical reviews in immunology* 25: 75-102.

201. Ferber, I. A., S. Brocke, C. Taylor-Edwards, W. Ridgway, C. Dinisco, L. Steinman, D. Dalton, and C. G. Fathman. 1996. Mice with a disrupted IFN-gamma gene are susceptible to the induction of experimental autoimmune encephalomyelitis (EAE). *J Immunol* 156: 5-7.

202. Jones, L. S., L. V. Rizzo, R. K. Agarwal, T. K. Tarrant, C. C. Chan, B. Wiggert, and R. R. Caspi. 1997. IFN-gamma-deficient mice develop experimental autoimmune uveitis in the context of a deviant effector response. *J Immunol* 158: 5997-6005.

203. Luger, D., P. B. Silver, J. Tang, D. Cua, Z. Chen, Y. Iwakura, E. P. Bowman, N. M. Sgambellone, C. C. Chan, and R. R. Caspi. 2008. Either a Th17 or a Th1 effector response can drive autoimmunity: conditions of disease induction affect dominant effector category. *The Journal of experimental medicine* 205: 799-810.

204. Haak, S., A. L. Croxford, K. Kreymborg, F. L. Heppner, S. Pouly, B. Becher, and A. Waisman. 2009. IL-17A and IL-17F do not contribute vitally to autoimmune neuro-inflammation in mice. *The Journal of clinical investigation* 119: 61-69.

205. Lee, Y. K., H. Turner, C. L. Maynard, J. R. Oliver, D. Chen, C. O. Elson, and C. T. Weaver. 2009. Late developmental plasticity in the T helper 17 lineage. *Immunity* 30: 92-107.

206. Shi, G., C. A. Cox, B. P. Vistica, C. Tan, E. F. Wawrousek, and I. Gery. 2008. Phenotype switching by inflammation-inducing polarized Th17 cells, but not by Th1 cells. *J Immunol* 181: 7205-7213.

207. Hirota, K., J. H. Duarte, M. Veldhoen, E. Hornsby, Y. Li, D. J. Cua, H. Ahlfors, C. Wilhelm, M. Tolaini, U. Menzel, A. Garefalaki, A. J. Potocnik, and B. Stockinger. 2011. Fate mapping of IL-17-producing T cells in inflammatory responses. *Nature immunology* 12: 255-263.

208. Annunziato, F., L. Cosmi, F. Liotta, E. Maggi, and S. Romagnani. 2008. The phenotype of human Th17 cells and their precursors, the cytokines that mediate their differentiation and the role of Th17 cells in inflammation. *International immunology* 20: 1361-1368.

209. Cosmi, L., L. Maggi, V. Santarlasci, F. Liotta, and F. Annunziato. 2014. T helper cells plasticity in inflammation. *Cytometry. Part A : the journal of the International Society for Analytical Cytology* 85: 36-42.

210. Morinobu, A., Y. Kanno, and J. J. O'Shea. 2004. Discrete roles for histone acetylation in human T helper 1 cell-specific gene expression. *J Biol Chem* 279: 40640-40646.

211. Lee, G. R., S. T. Kim, C. G. Spilianakis, P. E. Fields, and R. A. Flavell. 2006. T helper cell differentiation: regulation by cis elements and epigenetics. *Immunity* 24: 369-379.

212. Rao, R., S. A. Rieder, P. Nagarkatti, and M. Nagarkatti. 2014. Staphylococcal enterotoxin B-induced microRNA-155 targets SOCS1 to promote acute inflammatory lung injury. *Infection and immunity* 82: 2971-2979.

213. Baumjohann, D., and K. M. Ansel. 2013. MicroRNA-mediated regulation of T helper cell differentiation and plasticity. *Nature reviews. Immunology* 13: 666-678.

214. Sido, J. M., X. Yang, P. S. Nagarkatti, and M. Nagarkatti. 2015. Delta9 Tetrahydrocannabinol-mediated epigenetic modifications elicit myeloid-derived suppressor cell activation via STAT3/S100A8. *Journal of leukocyte biology*.

215. Niedbala, W., A. G. Besnard, H. R. Jiang, J. C. Alves-Filho, S. Y. Fukada, D. Nascimento, A. Mitani, P. Pushparaj, M. H. Alqahtani, and F. Y. Liew. 2013. Nitric oxide-induced regulatory T cells inhibit Th17 but not Th1 cell differentiation and function. *J Immunol* 191: 164-170.

216. Kozela, E., A. Juknat, N. Kaushansky, N. Rimmerman, A. Ben-Nun, and Z. Vogel. 2013. Cannabinoids decrease the th17 inflammatory autoimmune phenotype. *Journal of neuroimmune pharmacology : the official journal of the Society on NeuroImmune Pharmacology* 8: 1265-1276.

217. Karsak, M., E. Gaffal, R. Date, L. Wang-Eckhardt, J. Rehnelt, S. Petrosino, K. Starowicz, R. Steuder, E. Schlicker, B. Cravatt, R. Mechoulam, R. Buettner, S. Werner, V. Di Marzo, T. Tuting, and A. Zimmer. 2007. Attenuation of allergic contact dermatitis through the endocannabinoid system. *Science* 316: 1494-1497.

218. Gaffal, E., M. Cron, N. Glodde, and T. Tuting. 2013. Anti-inflammatory activity of topical THC in DNFB-mediated mouse allergic contact dermatitis independent of CB1 and CB2 receptors. *Allergy* 68: 994-1000.

219. Lee, H. Y., M. Stieger, N. Yawalkar, and M. Kakeda. 2013. Cytokines and chemokines in irritant contact dermatitis. *Mediators of inflammation* 2013: 916497.

220. Fields, P. E., S. T. Kim, and R. A. Flavell. 2002. Cutting edge: changes in histone acetylation at the IL-4 and IFN-gamma loci accompany Th1/Th2 differentiation. *J Immunol* 169: 647-650.

221. Yang, X. O., B. P. Pappu, R. Nurieva, A. Akimzhanov, H. S. Kang, Y. Chung, L. Ma, B. Shah, A. D. Panopoulos, K. S. Schluns, S. S. Watowich, Q. Tian, A. M. Jetten, and C. Dong. 2008. T helper 17 lineage differentiation is programmed by orphan nuclear receptors ROR alpha and ROR gamma. *Immunity* 28: 29-39.

222. Huber, M., A. Brustle, K. Reinhard, A. Guralnik, G. Walter, A. Mahiny, E. von Low, and M. Lohoff. 2008. IRF4 is essential for IL-21-mediated induction,

amplification, and stabilization of the Th17 phenotype. *Proceedings of the National Academy of Sciences of the United States of America* 105: 20846-20851.

223. Harris, S. J., R. V. Parry, J. Westwick, and S. G. Ward. 2008. Phosphoinositide lipid phosphatases: natural regulators of phosphoinositide 3-kinase signaling in T lymphocytes. *J Biol Chem* 283: 2465-2469.

224. Manning, A. M., F. P. Bell, C. L. Rosenbloom, J. G. Chosay, C. A. Simmons, J. L. Northrup, R. J. Shebuski, C. J. Dunn, and D. C. Anderson. 1995. NF-kappa B is activated during acute inflammation in vivo in association with elevated endothelial cell adhesion molecule gene expression and leukocyte recruitment. *Journal of inflammation* 45: 283-296.

225. Vennegaard, M. T., C. M. Bonefeld, P. H. Hagedorn, N. Bangsgaard, M. B. Lovendorf, N. Odum, A. Woetmann, C. Geisler, and L. Skov. 2012. Allergic contact dermatitis induces upregulation of identical microRNAs in humans and mice. *Contact dermatitis* 67: 298-305.

226. Murugaiyan, G., A. P. da Cunha, A. K. Ajay, N. Joller, L. P. Garo, S. Kumaradevan, N. Yosef, V. S. Vaidya, and H. L. Weiner. 2015. MicroRNA-21 promotes Th17 differentiation and mediates experimental autoimmune encephalomyelitis. *The Journal of clinical investigation* 125: 1069-1080.

227. Busbee, P. B., M. Nagarkatti, and P. S. Nagarkatti. 2015. Natural Indoles, Indole-3-Carbinol (I3C) and 3,3'-Diindolylmethane (DIM), Attenuate Staphylococcal Enterotoxin B-Mediated Liver Injury by Downregulating miR-31 Expression and Promoting Caspase-2-Mediated Apoptosis. *PloS one* 10: e0118506.

228. Meza-Sanchez, D., G. Perez-Montesinos, J. Sanchez-Garcia, J. Moreno, and L. C. Bonifaz. 2011. Intradermal immunization in the ear with cholera toxin and its non-toxic beta subunit promotes efficient Th1 and Th17 differentiation dependent on migrating DCs. *European journal of immunology* 41: 2894-2904.

229. Newton, C. A., T. Lu, S. J. Nazian, I. Perkins, H. Friedman, and T. W. Klein. 2004. The THC-induced suppression of Th1 polarization in response to Legionella pneumophila infection is not mediated by increases in corticosterone and PGE2. *Journal of leukocyte biology* 76: 854-861.

230. Kong, W., H. Li, R. F. Tuma, and D. Ganea. 2014. Selective CB2 receptor activation ameliorates EAE by reducing Th17 differentiation and immune cell accumulation in the CNS. *Cellular immunology* 287: 1-17.

231. Ambros, V. 2004. The functions of animal microRNAs. *Nature* 431: 350-355.

232. Chandra, A., A. Ray, S. Senapati, and R. Chatterjee. 2015. Genetic and epigenetic basis of psoriasis pathogenesis. *Molecular immunology* 64: 313-323.

233. Ma, X., J. Zhou, Y. Zhong, L. Jiang, P. Mu, Y. Li, N. Singh, M. Nagarkatti, and P. Nagarkatti. 2014. Expression, regulation and function of microRNAs in multiple sclerosis. *International journal of medical sciences* 11: 810-818.

234. Salehi, E., R. Eftekhari, M. Oraei, A. Gharib, and K. Bidad. 2015. MicroRNAs in rheumatoid arthritis. *Clinical rheumatology*.

235. Dong, L., X. Wang, J. Tan, H. Li, W. Qian, J. Chen, Q. Chen, J. Wang, W. Xu, C. Tao, and S. Wang. 2014. Decreased expression of microRNA-21 correlates with the imbalance of Th17 and Treg cells in patients with rheumatoid arthritis. *Journal of cellular and molecular medicine* 18: 2213-2224.

236. Smith, K. M., M. Guerau-de-Arellano, S. Costinean, J. L. Williams, A. Bottoni, G. Mavrikis Cox, A. R. Satoskar, C. M. Croce, M. K. Racke, A. E. Lovett-Racke, and C. C. Whitacre. 2012. miR-29ab1 deficiency identifies a negative feedback loop controlling Th1 bias that is dysregulated in multiple sclerosis. *J Immunol* 189: 1567-1576.

237. Xing, L. N., H. Wang, P. H. Yin, Y. J. Liu, Y. F. Chi, Y. M. Wang, and W. Peng. 2014. Reduced mir-29b-3p expression up-regulate CDK6 and contributes to IgA nephropathy. *International journal of clinical and experimental medicine* 7: 5275-5281.

238. Huang, C., J. M. Zheng, Q. Cheng, K. K. Yu, Q. X. Ling, M. Q. Chen, and N. Li. 2014. Serum microRNA-29 levels correlate with disease progression in patients with chronic hepatitis B virus infection. *Journal of digestive diseases* 15: 614-621.

239. Ma, F., S. Xu, X. Liu, Q. Zhang, X. Xu, M. Liu, M. Hua, N. Li, H. Yao, and X. Cao. 2011. The microRNA miR-29 controls innate and adaptive immune responses to intracellular bacterial infection by targeting interferon-gamma. *Nature immunology* 12: 861-869.

240. Chandra, L. C., V. Kumar, W. Torben, C. Vande Stouwe, P. Winsauer, A. Amedee, P. E. Molina, and M. Mohan. 2015. Chronic administration of Delta9-tetrahydrocannabinol induces intestinal anti-inflammatory microRNA expression during acute simian immunodeficiency virus infection of rhesus macaques. *Journal of virology* 89: 1168-1181.

241. Sugiura, T., S. Kondo, S. Kishimoto, T. Miyashita, S. Nakane, T. Kodaka, Y. Suhara, H. Takayama, and K. Waku. 2000. Evidence that 2-arachidonoylglycerol but not N-palmitoylethanolamine or anandamide is the physiological ligand for the cannabinoid CB2 receptor. Comparison of the agonistic activities of various cannabinoid receptor ligands in HL-60 cells. *J Biol Chem* 275: 605-612.

242. Maccarrone, M., M. Attina, A. Cartoni, M. Bari, and A. Finazzi-Agro. 2001. Gas chromatography-mass spectrometry analysis of endogenous cannabinoids in healthy and tumoral human brain and human cells in culture. *Journal of neurochemistry* 76: 594-601.

243. Schmid, P. C., T. Kuwae, R. J. Krebsbach, and H. H. Schmid. 1997. Anandamide and other N-acylethanolamines in mouse peritoneal macrophages. *Chemistry and physics of lipids* 87: 103-110.

244. Stella, N., P. Schweitzer, and D. Piomelli. 1997. A second endogenous cannabinoid that modulates long-term potentiation. *Nature* 388: 773-778.

245. Kondo, S., H. Kondo, S. Nakane, T. Kodaka, A. Tokumura, K. Waku, and T. Sugiura. 1998. 2-Arachidonoylglycerol, an endogenous cannabinoid receptor agonist: identification as one of the major species of monoacylglycerols in various rat tissues, and evidence for its generation through CA2+-dependent and -independent mechanisms. *FEBS letters* 429: 152-156.

246. Schmid, P. C., K. D. Schwartz, C. N. Smith, R. J. Krebsbach, E. V. Berdyshev, and H. H. Schmid. 2000. A sensitive endocannabinoid assay. The simultaneous analysis of N-acylethanolamines and 2-monoacylglycerols. *Chemistry and physics of lipids* 104: 185-191.

247. Gonsiorek, W., C. Lunn, X. Fan, S. Narula, D. Lundell, and R. W. Hipkin. 2000. Endocannabinoid 2-arachidonyl glycerol is a full agonist through human type 2 cannabinoid receptor: antagonism by anandamide. *Mol Pharmacol* 57: 1045-1050.

248. Getahun, A., J. Dahlstrom, S. Wernersson, and B. Heyman. 2004. IgG2a-mediated enhancement of antibody and T cell responses and its relation to inhibitory and activating Fc gamma receptors. *J Immunol* 172: 5269-5276.

249. Mimura, T., S. Oka, H. Koshimoto, Y. Ueda, Y. Watanabe, and T. Sugiura. 2012. Involvement of the endogenous cannabinoid 2 ligand 2-arachidonyl glycerol in allergic inflammation. *International archives of allergy and immunology* 159: 149-156.

250. Julius, M. H., E. Simpson, and L. A. Herzenberg. 1973. A rapid method for the isolation of functional thymus-derived murine lymphocytes. *European journal of immunology* 3: 645-649.

251. Sido, J. M., P. S. Nagarkatti, and M. Nagarkatti. 2014. Role of Endocannabinoid Activation of Peripheral CB1 Receptors in the Regulation of Autoimmune Disease. *International reviews of immunology*.

252. Correa, F., M. Hernangomez-Herrero, L. Mestre, F. Loria, F. Docagne, and C. Guaza. 2011. The endocannabinoid anandamide downregulates IL-23 and IL-12 subunits in a viral model of multiple sclerosis: evidence for a cross-talk between IL-12p70/IL-23 axis and IL-10 in microglial cells. *Brain Behav Immun* 25: 736-749.

253. Rossi, S., R. Furlan, V. De Chiara, L. Muzio, A. Musella, C. Motta, V. Studer, F. Cavasinni, G. Bernardi, G. Martino, B. F. Cravatt, B. Lutz, M. Maccarrone, and D. Centonze. 2011. Cannabinoid CB1 receptors regulate neuronal TNF-alpha effects in experimental autoimmune encephalomyelitis. *Brain Behav Immun* 25: 1242-1248.

254. Eros, G., S. Ibrahim, N. Siebert, M. Boros, and B. Vollmar. 2009. Oral phosphatidylcholine pretreatment alleviates the signs of experimental rheumatoid arthritis. *Arthritis research & therapy* 11: R43.

255. Alhouayek, M., D. M. Lambert, N. M. Delzenne, P. D. Cani, and G. G. Muccioli. 2011. Increasing endogenous 2-arachidonoylglycerol levels counteracts colitis and related systemic inflammation. *FASEB journal : official publication of the Federation of American Societies for Experimental Biology* 25: 2711-2721.

256. Costola-de-Souza, C., A. Ribeiro, V. Ferraz-de-Paula, A. S. Calefi, T. P. Aloia, J. A. Gimenes-Junior, V. I. de Almeida, M. L. Pinheiro, and J. Palermo-Neto. 2013. Monoacylglycerol lipase (MAGL) inhibition attenuates acute lung injury in mice. *PloS one* 8: e77706.

257. Lourbopoulos, A., N. Grigoriadis, R. Lagoudaki, O. Touloumi, E. Polyzoidou, I. Mavromatis, N. Tascos, A. Breuer, H. Ovadia, D. Karussis, E. Shohami, R. Mechoulam, and C. Simeonidou. 2011. Administration of 2-arachidonoylglycerol ameliorates both acute and chronic experimental autoimmune encephalomyelitis. *Brain research* 1390: 126-141.

258. Queiroz-Junior, C. M., M. F. Madeira, F. M. Coelho, V. V. Costa, R. L. Bessoni, L. F. Sousa, G. P. Garlet, G. Souza Dda, M. M. Teixeira, and T. A. Silva. 2011.

Experimental arthritis triggers periodontal disease in mice: involvement of TNF-alpha and the oral Microbiota. *J Immunol* 187: 3821-3830.

259. Kurabayashi, M., I. Takeyoshi, D. Yoshinari, K. Matsumoto, I. Maruyama, and Y. Morishita. 2005. 2-Arachidonoylglycerol increases in ischemia-reperfusion injury of the rat liver. *Journal of investigative surgery : the official journal of the Academy of Surgical Research* 18: 25-31.

260. Quercioli, A., Z. Pataky, G. Vincenti, V. Makoundou, V. Di Marzo, F. Montecucco, S. Carballo, A. Thomas, C. Staub, S. Steffens, Y. Seimbille, A. Golay, O. Ratib, E. Harsch, F. Mach, and T. H. Schindler. 2011. Elevated endocannabinoid plasma levels are associated with coronary circulatory dysfunction in obesity. *European heart journal* 32: 1369-1378.

261. Hauer, D., G. Schelling, H. Gola, P. Campolongo, J. Morath, B. Roozendaal, G. Hamuni, A. Karabatsiakis, P. Atsak, M. Vogeser, and I. T. Kolassa. 2013. Plasma concentrations of endocannabinoids and related primary fatty acid amides in patients with post-traumatic stress disorder. *PloS one* 8: e62741.

262. Jorda, M. A., S. E. Verbakel, P. J. Valk, Y. V. Vankan-Berkhoudt, M. Maccarrone, A. Finazzi-Agro, B. Lowenberg, and R. Delwel. 2002. Hematopoietic cells expressing the peripheral cannabinoid receptor migrate in response to the endocannabinoid 2-arachidonoylglycerol. *Blood* 99: 2786-2793.

263. Jean-Gilles, L., S. Feng, C. R. Tench, V. Chapman, D. A. Kendall, D. A. Barrett, and C. S. Constantinescu. 2009. Plasma endocannabinoid levels in multiple sclerosis. *Journal of the neurological sciences* 287: 212-215.

264. Richardson, D., R. G. Pearson, N. Kurian, M. L. Latif, M. J. Garle, D. A. Barrett, D. A. Kendall, B. E. Scammell, A. J. Reeve, and V. Chapman. 2008. Characterisation of the cannabinoid receptor system in synovial tissue and fluid in patients with osteoarthritis and rheumatoid arthritis. *Arthritis research & therapy* 10: R43.